

Development of new packed reactor using TiO₂ pellet for drinking water treatment

Von der Naturwissenschaftlichen Fakultät
der Gottfried Wilhelm Leibniz Universität Hannover

zur Erlangung des Grades
Doktor der Naturwissenschaften
Dr. rer. nat.

genehmigte Dissertation
von

Muftah Al-Ghazali Omer
M. Sc.

Geboren am 14.04.1963 in Darna, Libyen

Hannover, 2012

Referent: Prof. Dr. Thomas Scheper

Korreferent: Prof. Dr. Detlef Bahnemann

Tag der Promotion: 28.08.2012

Erklärung

Ich versichere, dass ich diese Dissertation selbstständig und nur unter Verwendung der angegebenen Hilfsmittel und Quellen durchgeführt habe. Diese Arbeit wurde nicht als Diplomarbeit oder ähnliche Prüfungsarbeit verwendet.

Hannover, May 2012

Acknowledgements

I would like to express my deep thanks to my supervisor ***Prof. Dr. Thomas Scheper***, who supported the topic of this thesis.

Great thanks to ***Prof. Dr. Bahnemann*** for his great help. Through all years, he helped me in so many ways to achieve successfully what I need to accomplish in this thesis work. I feel very proud to have the opportunity to work in his research group. What he taught me will surely benefit me throughout my life. My heartfelt gratitude is expressed to him.

My Sincere thanks are also for ***Dr. Ralf Dillert*** who was a very professional in his following up the steps of producing this work, giving good advices to structure this thesis without him this work not finished in good shape.

I will not forget my good friends ***Dr. Gamil Alhakimi*** and ***Dr. Ralf Vogel, Dr. Tarek Kandiel*** for their valuable advices and their help.

I am really indebted to all members of Institute of Technical Chemistry.

Without love and patience, no work can be done; I got the real love and the strongest support to complete this work from my family; my lovely mother ***Salma***, my great father ***Alghazali***, my lovely wife ***Ea-gila*** and my children ***Taher(Shalabi)***, ***Salma (Kech)***, ***Asma (Pazo)*** ***Monira (Mtera)*** and ***Mahmoud (Zelo)***. They were usually beside me in good times as well as in hard times.

Abstract	4
Kurzfassung	6
1 Introduction	8
1.1 Sources and uses of water in Libya	8
1.2 Catalysis	12
1.3 Photocatalysis	14
1.4 Objectives	17
2 Theoretical background	18
2.1 Initial steps in photocatalysis on semiconductors	18
2.2 Factors affecting photocatalysis.....	25
2.2.1 The concentration of the photocatalyst.....	25
2.2.2 The pollutant concentration	25
2.2.3 The presence of inorganic anions	26
2.2.4 The initial pH.....	27
2.2.5 The oxygen concentration	28
2.2.6 Temperature.....	30
2.2.7 Light intensity.....	30
2.3 Kinetics of photocatalysis.....	31
2.4 Photocatalyst forms and their effect on the degradation of organic pollutants	34
2.4.1 Suspension.....	34
2.4.2 Supported photocatalyst	35
2.4.3 Pellet.....	37
2.5 The model compound (DCA).....	37
2.6 Photocatalytic reactors	39
2.7 Solar photocatalysis technology.....	40
2.8 Solar photocatalysis applications.....	45
2.9 Slurry reactors and immobilized photocatalyst.....	46
3 Material and methods	50
3.1 Materials	50
3.1.1 Photocatalysts	50
3.1.2 Chemicals	52
3.1.3 Spiral glass reactor	52
3.1.4 Preparation of coated spiral glass reactor	53

3.2	<i>Procedures</i>	53
3.2.1	Preparation of DCA stock solution (500 mM)	53
3.2.2	Preparation of TiO ₂ suspensions.....	54
3.2.3	Spiral experimental setup	54
3.2.4	Blank experiments	55
3.2.4.1	Effect of UV light on DCA degradation.....	55
3.2.4.2	Blank experiment (Spiral glass reactor)	56
3.2.5	Pan reactor	56
3.2.6	Flat packed reactor	57
3.2.7	Tubular packed reactor.....	58
3.2.8	Analytical procedure	59
3.3	<i>Real wastewater (Solvay sample)</i>	60
4	Results	61
4.1	<i>The spiral glass reactor</i>	61
4.1.1	Blank experiments	61
4.1.2	The spiral glass reactor with suspended photocatalyst	63
4.1.3	The spiral glass reactor with a photocatalytic coating.....	73
4.1.4	The spiral glass reactor packed with photocatalyst pellets	75
4.2	<i>The pan reactor with photocatalyst pellets</i>	78
4.3	<i>The flat packed reactor with photocatalyst pellets</i>	81
4.4	<i>The tubular reactor packed with photocatalyst pellets</i>	83
5	Discussion	87
5.1	<i>Introductory remarks</i>	87
5.2	<i>The spiral glass reactor</i>	90
5.2.1	The spiral glass reactor with suspended photocatalyst	90
5.2.2	The spiral glass reactor with a photocatalytic coating.....	91
5.2.3	The spiral glass reactor packed with photocatalyst pellets	92
5.3	<i>The pan reactor with photocatalyst pellets</i>	94
5.4	<i>The flat packed reactor with photocatalyst pellets</i>	95
5.5	<i>The tubular reactor packed with photocatalyst pellets</i>	95
5.6	<i>Comparison of the photocatalytic systems</i>	97
6	Conclusion and outlook	104
7	References	108
8	Appendix	122

8.1 *Table of Figures* 122
8.2 *list of tables* 126
8.3 *Curriculum Vitae (CV)*..... 128

Abstract

The photocatalytic degradation of organic pollutants in wastewater using UV or sunlight is a very promising and sustainable technology for wastewater or drinking water purification. However, the application of this technology at a large scale has faced challenges due to the need of efficient catalyst separation from the treated effluent.

The separation of the suspended catalyst from the purified water is energy intensive and cost prohibitive. The major objective of this thesis is primarily to determine the possibility of replacing a suspended TiO_2 photocatalyst by a newly developed photocatalyst having pellet form. A second objective is to investigate different reactor configurations like a spiral glass reactor, a pan reactor, a flat packed reactor, and a tubular packed reactor.

To compare the efficiency of the different photoreactor systems the rate of the photocatalytic oxidation of dichloroacetic acid was studied using artificial UV-A light as well as sun light. Additionally, the photocatalytic oxidation of a highly polluted wastewater received from the chemical company Solvay was studied to proof the applicability of the pellet form for wastewater treatment.

It is shown that organic water pollutants are photocatalytically oxidized in all combinations of photocatalyst type (suspended particles and pellets) and photoreactor type investigated in this work. The most efficient dosage form for the photocatalyst was found to be the suspended form. Initial photonic efficiencies as high as 12% were typically observed, indicating that more than 10% of the photons impinging the transparent surface of the photoreactor are adsorbed by the photocatalyst and used to initiate the mineralisation of the probe molecule. Significantly lower photonic efficiencies were determined for the TiO_2 pellets employed in this study.

Based on some realistic assumptions and on a kinetic parameter determined from the experimental data the light-harvesting reactor area necessary for the reduction of the

pollutant concentration by 98% in 1 m³ water was estimated for the tubular and the pan reactor both filled with TiO₂ pellets. Solar-irradiated areas of 28 m² and 15 to 16 m² are sufficient for this task when a tubular packed reactor and a pan reactor is used.

Therefore, the use of TiO₂ photocatalyst pellets in technically simple photoreactors seems to be a promising alternative to oxidation processes well established in wastewater treatment.

Key words: Photoreactor, Pellet photocatalyst, DCA

Kurzfassung

Der photokatalytische Abbau organischer Schadstoffe in Abwasser mit Hilfe von Ultraviolett- oder Sonnenlicht ist eine vielversprechende und richtungsweisende Technologie zur Trinkwasseraufbereitung der Zukunft. Mit der Anwendung der photokatalytischen Wasseraufbereitung in großem Stil sind allerdings einige Schwierigkeiten bezüglich der Abtrennung des Photokatalysators von dem gereinigten Wasser verbunden. Hochdrucktrennung des (suspendierten) Photokatalysators vom gereinigten Wasser ist energieaufwendig und daher nicht die Methode der Wahl.

Das Hauptziel dieser Arbeit ist in erster Linie die Prüfung der Möglichkeit, suspendierte TiO₂-Photokatalysatoren durch einen neu entwickelten Photokatalysator in Tablettenform zu ersetzen. Daneben wurden auch verschiedene Photoreaktortypen, wie z.B. ein Spiral-, ein Pfannen-, ein Flachbett-, und ein Röhrenreaktor untersucht.

Um die Wirksamkeit der verschiedenen Photoreaktoren mit einander vergleichen zu können, wurde die Geschwindigkeit der photokatalytischen Oxidation von Dichloressigsäure bei Bestrahlung mit dem UV-Licht einer künstlichen Lichtquelle und der Sonne in den verschiedenen Reaktorsystemen ermittelt. Außerdem wurde die photokatalytische Oxidation der Inhaltsstoffe eines hochbelasteten Abwassers der Firma Solvay untersucht, um die Eignung des neu entwickelten Photokatalysators für die Behandlung realer Abwässer zu prüfen.

Es wird gezeigt, dass in allen hier untersuchten Kombinationen von Photokatalysatoren (suspendierte Katalysatoren und Katalysatoren in Tablettenform) und Photoreaktoren organische Wasserinhaltsstoffe photokatalytisch abgebaut werden können. Als die wirksamste Anwendungsform wurde der suspendierte Photokatalysator ermittelt; typischerweise wurde Anfangsphotonen efficiencies von 12% berechnet. Dies bedeutet, dass mehr als 10% der auf die transparente Reaktoroberfläche auftreffenden UV-Photonen vom Photokatalysator adsorbiert und zur Einleitung der photokatalytischen Mineralisationsreaktion genutzt werden. Für die

Photokatalysatoren in Tablettenform wurden jedoch deutlich geringere Photoneneffizienzen berechnet.

Ausgehend von einigen realistischen Annahmen und einem aus den experimentellen Daten ermittelten kinetischen Parameter wurde für zwei Reaktortypen, die mit den Katalysatoren in Tablettenform gefüllt sind, die für eine Schadstoffreduktion um 98% notwendigen Reaktorflächen abgeschätzt. Von der Sonne beschienene, transparente Flächen von 28 m² sind für die Behandlung von einem Kubikmeter Abwasser im Röhrenreaktor notwendig; im Pfannenreaktor beträgt die Fläche 15 bis 16 m².

Die Ergebnisse dieser Arbeit lassen vermuten, dass der Einsatz von Photokatalysatoren in Tablettenform in Kombination mit konstruktiv einfachen Photoreaktoren eine vielversprechende Alternative zu den in der Abwasserbehandlung etablierten Oxidationsverfahren sein könnte.

Schlüsselworte: Photoreaktor, Photokatalysatoren in Tablettenform, DCA

1 Introduction

Most of the conflicts around the world are caused by energy or water. The shortage of water around the world is increasing every day.

The water scarcity is already affecting four out of ten people. 1.1 billion people have already serious problems in accessing clean drinking water. Currently, more than 700 million people in developing countries do not have access to water for irrigation which is needed to produce enough food for their own consumption (WHO, 2007).

The lack of water resources prompted many scientists around the world to think about ways of cleaning polluted water using natural energy sources, like sunlight. In countries enjoying long periods of sunshine, the application of a solar driven photocatalytic process for cleaning polluted water could be an interesting and versatile alternative.

1.1 Sources and uses of water in Libya

Libya is a country situated in North Africa with a semi arid atmosphere and very little rain during winter, except the coast the rest is desert, table (1) shows the sources and uses of water in Libya (Frenken, 2005).

Libya faces one of the severest water scarcity problems in the world. With virtually no rainfall except in the narrow coastal belt, the country has increasingly relied on its groundwater resources. In coastal areas these resources are renewed by rain each year, but the country also has vast non-renewed reserves of water underlying the desert. For a number of years, demand for water has far exceeded supply.

As a consequence, the country has experienced heavy over-drafting and mining of aquifers associated with growing problems of aquifer depletion, quality deterioration and saline water intrusion (IWRM, 2007).

Table 1: Sources and uses of water in Libya

Water: sources and use renewable water resources			
	Year	Quantity	Unit
Average precipitation		56	mm yr ⁻¹
		98.53	10 ⁹ m ³ yr ⁻¹
Internal renewable water resources		0.6	10 ⁹ m ³ yr ⁻¹
Total actual renewable water resources		0.6	10 ⁹ m ³ yr ⁻¹
Dependency ratio		0	%
Total actual renewable water resources per inhabitant	2004	106	m ³ yr ⁻¹
Total dam capacity	2000	385	10 ⁶ m ³
Water withdrawal			
Total water withdrawal	2000	4 268	10 ⁶ m ³ yr ⁻¹
irrigation + livestock	2000	3 544	10 ⁶ m ³ yr ⁻¹
Domestic	2000	600	10 ⁶ m ³ yr ⁻¹
Industry	2000	124	10 ⁶ m ³ yr ⁻¹
per inhabitant	2000	815	m ³ yr ⁻¹
as % of total actual renewable water resources	2000	711	%
Non-conventional sources of water			
Produced wastewater	1999	546	10 ⁶ m ³ yr ⁻¹
Treated wastewater	1999	40	10 ⁶ m ³ yr ⁻¹
Reused treated wastewater	1999	40	10 ⁶ m ³ yr ⁻¹
Desalinated water produced	1998	18	10 ⁶ m ³ yr ⁻¹
Depletion of renewable groundwater resources	1998	600	10 ⁶ m ³ yr ⁻¹
Use of fossil groundwater	1998	708	10 ⁶ m ³ yr ⁻¹

To solve the problem of water deficiency in Libya, the project of Great Man Made River (GMMR) was executed to provide more than three million m³ /day to satisfy the needs of the population. As the project of Great Man Made River has been completed, Libya's need for fresh water increases. Besides that, when the water is transported from the well in the desert to the open reservoirs at the coast it becomes contaminated with bacteria and organic material, due to the direct contact with the environment. The cheapest way to clean the water from the microorganism is to add chlorine. The uses of chlorine as a disinfectant have some disadvantages like:

- Reaction with some of organic compound yielding chlorinated organic (Rook, 1974; Gallard and von Gunten, 2002; Schaffer et al., 2011)
- high cost,
- need of a dosing facility.

Chemical treatment methods known as Advanced Oxidation Processes (AOP's) are also an attractive alternative for the treatment of contaminated ground, surface, and wastewaters containing hardly-biodegradable anthropogenic substances as well as for the purification and disinfection of drinking waters (Legrini et al., 1993; Hoffmann et al., 1995; Bahnemann, 2004; Wang and Xu, 2012). The most efficient AOP's are those that produce free hydroxyl radicals (OH[•]). These radicals have a highly oxidizing power superior to the other usual oxidants.

AOP's may be selective but are slow to moderate in destruction rate, or rapid but not selective, thus generating appreciable reactor or energy costs. Examples of chemical treatment methods include the so-called Advanced Oxidation Processes (AOP's) the latter of which involves the following processes:

- (i) Ozonation (Peyton and Glaze, 1988; Scheminski et al., 2000; Van Geluwe et al., 2011).
- (ii) O₃/UV (Prat et al., 1990; Liu et al., 2012).
- (iii) UV/H₂O₂ (Rosario-Ortiz et al., 2010).

-
- (iii) $O_3/UV/H_2O_2$ (Brunet et al., 1984; Duquet et al., 1989; Vogna et al., 2004; Katsoyiannis et al., 2011).
 - (iv) Free radicals generation by γ -Radiolysis (Tölgyessy, 1988).

These conversion processes are limited by high economic cost, oxidative potential, effluent characteristics or tendency to form harmful disinfection by-products as, for example, the case of formation of trihalomethanes (THM's) when a chlorination procedure is used for drinking water treatment (Rook, 1974; Gallard and von Gunten, 2002; Bekbolet, 2009; Bond et al., 2009).

Although AOP's are cheaper than combustion or wet oxidation technologies, a serious drawback of AOP'S is their relatively high operational costs compared to those of biological treatments. The above-mentioned methods are either insufficient to yield complete mineralization or extremely cost prohibitive (Ollis, 1988).

The AOP's alternative complements well established techniques, like flocculation, precipitation, adsorption on granular activated carbon, air stripping, combustion, and aerobic biological oxidation. Some of the latter techniques transfer pollutants from the aqueous phase to a solid phase, but they do not eliminate the pollutants all together.

An interesting alternative to remove bacteria and to remove the organic compounds present in the water could be the photocatalytic technique.

This approach fits into the sustainability category that every country around the world is trying to achieve in their efforts to resolve the energy and water problems. In some of these countries the abundant availability of sunlight throughout the whole year encourages the development of such new technologies.

1.2 Catalysis

Catalysis (derived from the Greek verb: to annul) in its original sense is the enabling or acceleration of a chemical reaction by means of adding a component, the catalyst, which itself chemically remains unchanged during the course of the reaction. The physical reason of catalysis lays in reducing or eliminating (annulling) the activation energy E_a of a particular chemical reaction with reactants X,Y , with the consequence that less external energy or heat has to be applied in order to facilitate the chemical reaction to product Z. (Fig. 1). This fact is of particular importance in the case of highly exothermic reactions where the net energy balance is positive (ΔG negative) and additional input of heat to the system may not be desired, especially at large industrial scale.

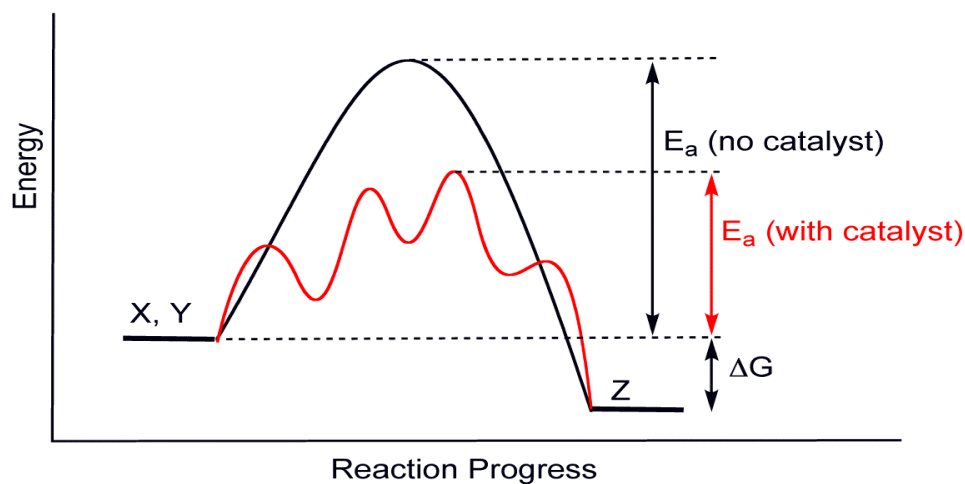


Figure 1: Reaction progress with and without catalysis (source www.wikimedia.org)

In the case of endothermic reactions, with positive ΔG , reducing the activation energy may be also desired for reasons of reactant or product sensitivity to heat, reaction kinetics or material selection for the reactor of an industrial process.

The physical nature of a catalyst can be homogenous, where it remains dissolved in the reaction media as one single phase, or heterogeneous, where the catalyst – reactant system consists of at least two different phases. As a matter of fact, the active sites of

heterogeneous systems are located at the surface boundaries (Hoffmann et al., 1995). Therefore, much effort is spent to increase the surface area of heterogeneous catalysts.

A special case evolves when the surface area to bulk ratio becomes considerable high and particle size of a (solid) catalyst is reduced to nanometer range “Nanocatalyst”. Then the catalyst is able to form a sol with a suitable solvent, virtually resembling a homogeneous system. Nowadays, much effort is spent on the design of new nanocatalytic systems (Hidalgo et al., 2004; Kandiel et al., 2010a; da Costa et al., 2012).

For reasons of easier process design due to separation issues, industrial processes prefer the application of heterogeneous, especially solid catalysts. This also applies to nanocatalysts.

In many cases a catalyst is a very expensive material, which for reasons of process economics shall not be applied at excessive amounts. Therefore, at industrial scale very often the catalyst is applied in small quantities on an inert support material, while R&D catalysts normally are of pure nature in their early stage. Supporting a catalyst also offers an opportunity for developing an initially homogeneous system towards a heterogeneous one by physically or chemically binding the active species on an inert support material, such as SiO₂, Al₂O₃ or a polymer (Zhang et al., 2005; Torres et al., 2007; Kalbasi and Mosaddegh, 2012; Song et al., 2012).

In an ideal world, a catalyst remains unchanged and not affected for a very long time. However, in reality side reactions or impurities coming with the reactants or solvent have a negative effect on the activity of the catalyst. This can be a change of the physical morphology of the catalyst or accumulation of inert material, often called as deactivation, or more drastically a chemical reaction, the “poisoning” of the catalyst.

A special case of catalyst deactivation exists when the catalyst becomes embedded by the reaction product which it catalyzes. For example modern gas phase polyethylene and polypropylene processes using Ziegler- Natta (Cossee, 1964) or metallocene catalysts on support material, “consume” the catalyst by reacting the olefin to

polyolefin around the catalyst micro-particle. However, the catalyst is not consumed (then won't be a catalyst) and remains active, until it becomes deactivated or poisoned by other means, and after the polymerization reaction is completed.

While disposal of deactivated or poisoned catalyst may be one option, the preferred route is to regenerate the material (Dorazio et al., 2008). The issue of catalyst regeneration itself is a very important subject and a science by itself, particularly when it comes to the commercialization of a process. Regeneration can be as simple as washing or burning off the undesired material and then directly re-use of the regenerated catalyst, or a very complex multistep process involving many cycles. It can be a continuous or a batch process. Lifetime of catalysts can be several years, as required for the catalytic converter in light passenger vehicles (Twigg, 2011), or only a few seconds as in some Fluidized Catalytic Cracking (FCC) refinery processes (Bielansky et al., 2010), where the catalyst consists of a rather cheap material, which is continuously regenerated and replenished by fresh catalyst.

1.3 Photocatalysis

Photocatalysis is a special branch of catalysis and if one would strictly apply the original criteria, it may not be quite conform to the definition of catalysis (Valentin et al., 2012). Applying strict criteria, a photocatalyst should be a material, which reduces or eliminates the activation barrier of a reaction by the interaction of photons.

Normally, the photons should not be consumed, just “catalyze” the course of the reaction. However, common understanding and practice in photocatalysis considers the consumption of photons by the catalyst and using them as a source of energy to create chemically available electrons and positive holes in the catalyst molecule (homogeneous) or on the surface of the (heterogeneous) catalytic material.

These electrons and / or positive holes are the reactive species, which trigger a range of reactions, normally referred to photocatalysis. Therefore, and as a matter of fact,

photocatalysis can be regarded as an electrochemical process which uses photons instead of an external voltage (electro-catalysis) to create the required reactive charges in the molecule or on the surface of the catalyst. Thus, a more descriptive term would be “photo-electro-catalysis”. However, for the sake of conformity to common practice, we will continue to use the term photocatalysis.

As a logic consequence of our thoughts so far, a photocatalyst must be a material which owns the following properties (Hidaka, 1998; Herrmann, 1999):

- It must absorb photons (light) in order to generate the electrons and positive holes.
- The electron–hole pair shall have a sufficient long life to carry out the subsequent electrochemical reaction before recombining.
- Once the electron and / or the hole has carried out the desired reaction it must be replenished by other means, e.g. reaction with the solvent
- The photocatalyst shall not deteriorate or react by the action of the generated electrons and holes.
- In case of a solid catalyst, the electron and / or the hole shall be able to migrate towards the surface of the photocatalyst in order to allow the subsequent electrochemical reaction.

One might have observed that the principle of generating electrons and positive holes in a material and then using them for further reactions has much in common with photovoltaic applications. Indeed, a photovoltaic cell uses the same principle with the only difference that electrons and hole are not used for chemical conversion, but separated to generate photovoltage and current.

This work will cover solid photocatalysts, based on TiO_2 , in aqueous solutions with the purpose to oxidize various dissolved organic molecules or contaminants. Chemically, the reaction is a simple and complete oxidation of organic material to CO_2 and water.

The photocatalyst is used to enable a silent burning of the contaminants in the presence of light and oxygen in aqueous solution. The activation energy of this process has been virtually lowered by the action of the light induced formation of electrons and holes on the surface of the photocatalyst, which are transferred to the otherwise inert reactants.

Since 1976, photodetoxification has become a major area of interest, well-discussed in various scientific literatures as an alternative method for the degradation of a wide range of organic compounds polluting water (Carey et al., 1976; Ollis and Turchi, 1990; Ollis and Al-Ekabi, 1993; Bahnemann et al., 1994; Bahnemann, 1999; Chong et al., 2010).

Photodetoxification of wastewater is a novel technique for the complete mineralization of most organic and some inorganic contaminants present in industrial effluent. The technique combines heterogeneous catalysis with solar energy in the presence of oxygen (Fetwell, 1989).

Later, many scientific works consider the use of solar energy for photocatalysis instead of using artificial light source (Pacheco et al., 1990; Ollis and Al-Ekabi, 1993; Goswami, 1997; Dillert et al., 1999a; Sagawe et al., 2003a, b, 2004, 2005). As the solar photocatalysis has been proven to be a good degradation process for organic pollutants in aqueous medium, it leading to total mineralization of a large number of organic compounds (Robert and Malato, 2002; Bahnemann, 2004).

Furthermore, the interest in using photocatalytic methods for water detoxification has grown in the last decade. There are hopes that the use of photocatalytic approaches to clean wastewater will be able to significantly contribute to the public wellbeing (Fernández et al., 2005). This approach is extremely attractive for countries with plenty of sunshine around the year.

1.4 Objectives

In view of the developments in the area of photocatalytic processing of contaminated water and wastewater and access to a high degree of efficiency but it has not been applied to commercial or practical due to the problems associated with the application, such as the problem of filtering and separation of photocatalyst in the case of application or suspension system, or inefficiencies in the application of supported the photocatalyst. It has become necessary to examine other options such as the use of catalyst pellet and to study various types of reactors for the perfect application for this technique.

To study the photocatalytic degradation of the model compound DCA using a new morphology (pellet) of a known photocatalyst and determine its applicability for photocatalytic detoxification of wastewater.

To compare the efficiency of the catalyst suspension and catalyst pellet under similar conditions using DCA as model pollutant.

To study and compare the photocatalytic degradation of DCA using four different reactor configurations, spiral, tubular, flat packed, thin film and pan reactors.

2 Theoretical background

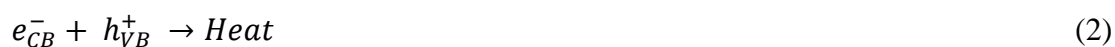
2.1 Initial steps in photocatalysis on semiconductors

In the past decades, oxidative photocatalysis in aqueous media has emerged as a promising process to be used for environmental applications. Nowadays it is playing an increasingly important role in the purification of air and water media. More recently, photocatalysis has become an important area of interest in terms of the development of coated materials.

The mechanism of photocatalysis is based on the use of a semiconductor (Fig. 2) which can generate active oxidizing sites, when it is illuminated with photons whose energy is equal to or higher than the energy corresponding to the band-gap of the semiconductor (eq. 1).



When the photons are absorbed on the surface of the catalyst, and consequently, some electrons (e^-) become excited from the valence to the conduction band. Thus, a positive photohole will be generated in the valence band, and these pairs, named electron/hole pairs, migrate to the surface of the catalyst. In the absence of suitable scavengers, the stored energy is dissipated as thermal energy within a few nanoseconds by recombination (Rothenberger et al., 1985) (Eq. 2).



In some cases, recombination takes place in the form of light emission (fluorescence). When they are not recombined, the electron/hole pairs can react with species adsorbed on the surface of the catalyst. In aqueous systems the water will react with the positive hole to form a hydroxyl radical (Nakamura and Nakato, 2004).

Hydroxyl radicals are strong oxidizing agents and are believed responsible for the ultimate degradation of the organic molecules present in the medium (Herrmann, 1999; Bahnemann, 2004).

While the electrons have the reducing power of the conduction band energy and can react with electron acceptors (A) (Eq.3), the positive holes have the oxidation power of the valence band energy and therefore can react with adsorbed electron donors (D) (Eq. 4)

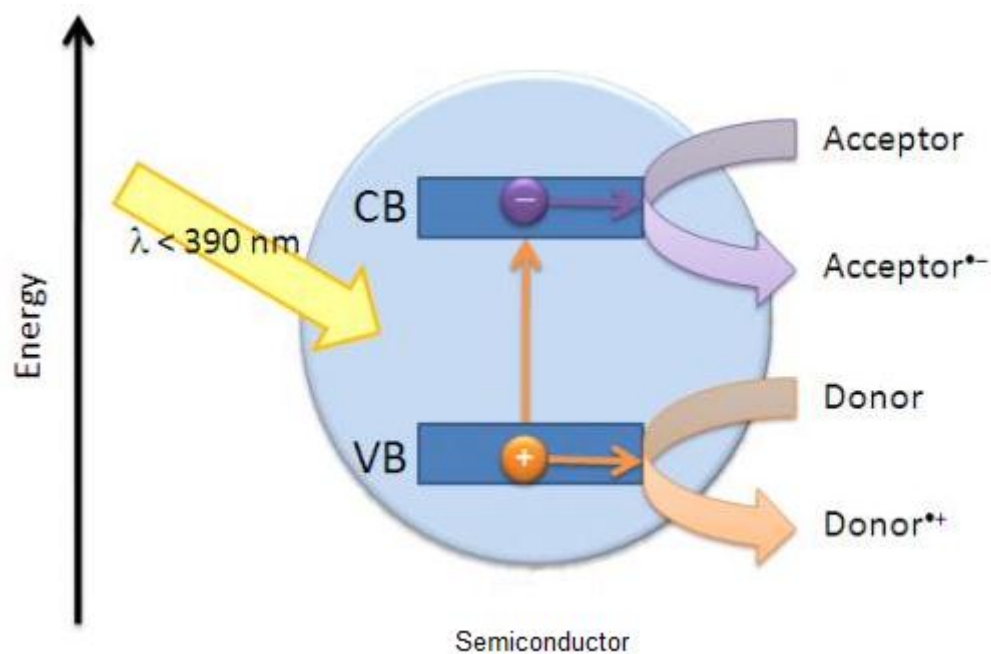
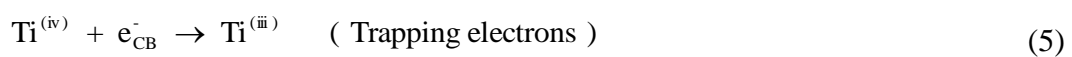


Figure 2: Simple diagram showing the photocatalysis process

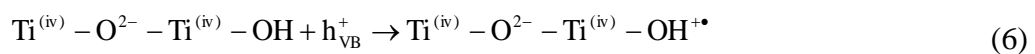
The efficiency of reactions 3 and 4 strongly depends on the efficacy of the suppression of the recombination of the generated electron/hole pairs (Eq. 2). The recombination rate of the charge carriers depends on the purity of the semiconductor, the light intensity and the diffusion length of the charge carriers inside the particle (Memming, 1984)

Electrons and holes have to reach the surface of the semiconductor before they are able to react with adsorbed substrates. This will only be the case, when the transfer time of the charge carriers becomes significantly smaller than the lifetime of the electron/hole pairs, *i.e.* recombination of charge carriers inside the particle can be neglected. Consequently, particles of small diameters are employed for photocatalysis to suppress efficiently the recombination of the electron/hole pairs (Rothenberger et al., 1985).

To prevent recombination of the charge carriers at the surface of the semiconductor, it is necessary to separate the electrons and holes at the particle surface. This is achieved by different reactive centres at the surface, where the electrons and holes are trapped before charge transfer to adsorbed species takes place (Eq. 3 and 4). The higher this rate the more efficiently the recombination of charge carriers (Eq. 2) can be suppressed. It is well known that the conducting band electrons are trapped by titanium (iv) yielding titanium (iii) (Eq. 5) (Martin et al., 1994a; Martin et al., 1994b).



The chemical nature of the trapped holes is still unclear, but there is a wide agreement that they are trapped by hydroxyl groups at the surface of the semiconductor (Eq. 6) (Bahnemann et al., 1994).



A direct experimental proof of such surface adsorbed hydroxyl radicals is still missing because of the short lifetime of such species, but there are several experimental

evidences, that OH radicals are involved in the photocatalytic oxidation process (Matthews, 1986).

Figure 3 shows a scheme exhibits some of the photochemical and photophysical events that might take place on an irradiated semiconductor particle.

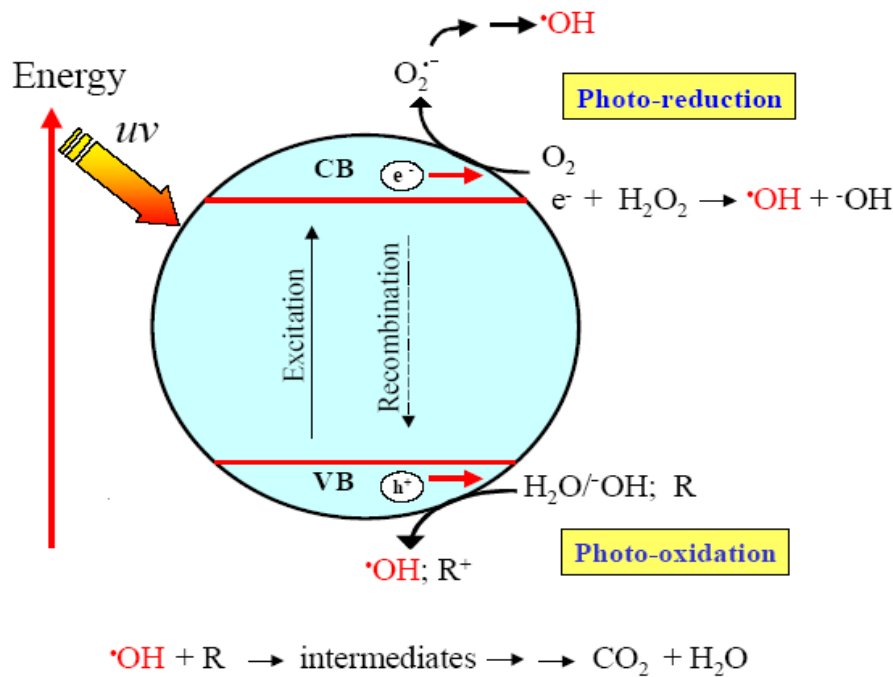


Figure 3: Semiconductor photocatalysis process

Table 2 lists some selected semiconductor materials, which have been used for photocatalytic reactions, together with the VB and CB potentials and the band gap energy and wavelength required to activate the catalyst (Grätzel, 2001).

Among the listed semiconductors, TiO_2 has been found as one of the most suitable photocatalyst for many environmental applications. Titanium dioxide is biologically and chemically inert, it is a photostable metal oxide, *i.e.* not liable to photoanodic corrosion, and therefore can be re-used several times. If regeneration is needed, then

washing the catalyst with pure water and diluted base is usually sufficient (Ahmed and Ollis, 1984).

Table 2: Band positions of some common semiconductor photocatalysts in aqueous solution at pH=1.

Semiconductor	Valence Band (V vs. NHE)	Conductance band (V vs. NHE)	Band gap (eV)	Band gap (nm)
TiO ₂	+ 3.1	- 0.1	3.2	387
SnO ₂	+ 4.1	+ 0.3	3.9	318
ZnO	+ 3.0	- 0.2	3.2	387
ZnS	+ 1.4	- 2.3	3.7	335
WO ₃	+ 3.0	+ 0.2	2.8	443
CdS	+ 2.1	- 0.4	2.5	496
CdSe	+ 1.6	- 0.1	1.7	729
GaAs	+ 1.0	- 0.4	1.4	886
GaP	+ 1.3	- 1.0	2.3	539

Furthermore, TiO₂ is of special interest since it can absorb (solar) UV radiation. This is because TiO₂ has an appropriate energetic gap between its valence and conduction bands, which can be surpassed by the energy of a solar photon.

Titanium dioxide is an inexpensive material and widely used as white paint pigment, as sun blocking material, as cosmetic, abrasive in toothpaste or as neutral filler in medical tablets, among many other uses.

Titanium dioxide exists in three major structures: rutile, brookite and anatase, the latter exhibits the highest photocatalytic efficiency (Augugliaro et al., 1988; Matthews, 1991), which has been explained by faster recombination of charge carriers in rutile compared to anatase (Eq. 2) and also by a considerably lower amount of reactant adsorbed on the surface of a rutile particle.

The bandgap is approximately 3.0 eV for rutile but its band positions are lower compared to anatase. Anatase is thermodynamically unstable as compared with rutile, but its formation is kinetically favoured at lower temperature (<600°C).

Brookite has been rarely used because its preparation is quite difficult. Pure brookite films were deposited from a brookite dispersion obtained by peptizing a mixture brookite–rutile prepared by thermolysis of TiCl_4 in a HCl solution (Di Paola et al., 2007). Zheng et al. synthesized brookite TiO_2 as the major phase by hydrothermal method (Zheng et al., 2000a; Zheng et al., 2000b). Lee and Yang synthesized pure brookite at low temperatures by hydrolysis of TiCl_4 using HNO_3 solution. The presence of HNO_3 was considered to be very important in the formation of pure brookite nanoparticles (Lee and Yang, 2005).

Kandiel et al (Kandiel et al., 2010b) produced high quality brookite TiO_2 nanorods by the thermal hydrolysis of commercially available aqueous solutions of titanium bis(ammonium lactate) dihydroxide in the presence of high concentrations of urea ($\geq 6.0\text{M}$) as an in situ OH^- source. The photocatalytic activity of pure anatase nanoparticles of pure brookite nanorods has been assessed by hydrogen evolution from aqueous methanol solution as well as by the degradation of dichloroacetic acid (DCA) in aqueous solution. The results indicate that the photocatalytic hydrogen evolution activity of pure brookite is higher than that of pure anatase nanoparticles. In case of the photocatalytic degradation of DCA, anatase/brookite mixtures and pure brookite exhibit lower photocatalytic activity than pure anatase nanoparticles. This behaviour correlates well with the surface area of the investigated powders.

Anatase has bandgap of 3.2 eV and thus absorbs light below 400 nm. This implies that nearly 5% of solar energy reaching the surface of the earth can be utilized for photocatalytic degradation.

The conduction band edge (- 0.20 eV vs. Normal Hydrogen Electrode (NHE) at pH= 0) represents the reducing power of the photogenerated electron, and the valence band edge (3.0 eV vs. NHE) represents the oxidizing power of the photogenerated holes (Grätzel and Rotzinger, 1985). Titanium dioxide shows a Nernst behaviour, *e.g.*, the valence and conduction band are shifted to more negative values with increasing pH according to the Nernst law (Eq. 7) (Atkins, 1985):

$$E = E_0 + \frac{RT}{nF} \ln [H^+] \quad (7)$$

with: E : Energy of the valence or conduction band

E₀: Energy of the valence or conduction band at pH = 0

R: General gas constant

T: Temperature

n: Number of involved charge carriers

F: Faraday constant

From equation 7 it becomes obvious that the energy of the valence and conduction band are shifted by - 59 mV for each unit of pH at 25 °C. Thus, the reduction power of electrons increases and the oxidizing power of the holes decreases with rising pH values.

2.2 Factors affecting photocatalysis

2.2.1 The concentration of the photocatalyst

The availability of active sites increases with increasing catalyst loading of the suspension. However, light penetration and hence, the photo-activated volume of the suspension decreases with increasing photocatalytic concentration. As expected for a photocatalytic reaction, the degradation rate should increase linearly with the amount of catalyst up to a level corresponding to complete absorption of the incident light potentially absorbable by TiO₂ (Alsayyed et al., 1991; Sagawe et al., 2010). Such behaviour has been described by a hyperbolic law, and several theoretical models exist which explain such behaviour.

Alhakimi et al. showed in a degradation experiment of potassium hydrogen phthalate as a probe molecule using Degussa P25 as the photocatalyst that the degradation rate is increased linearly by increasing the photocatalyst load up to a certain limit (Alhakimi et al., 2003). They showed that at 3 g L⁻¹ of Degussa P25 a maximum degradation rate was reached.

Further increase of the TiO₂ concentration produced no significant improvement in the degradation rate. This can be explained by the fact that at 3 g L⁻¹ catalyst concentration, the maximum amount of incident light which could be absorbed was reached in the reactor used in this study.

2.2.2 The pollutant concentration

Since the photocatalytic detoxification takes place at the interface of the semiconductor and the aqueous phase, the substrate adsorption plays an important role for oxidation processes. For a given concentration of photocatalyst the degradation rate should increase linearly with increasing pollutant concentration until saturation of the surface active sites is achieved. Higher pollutant concentration does not lead to a further increase in degradation kinetics, *i.e.*, the rate becomes

independent of the pollutant concentration and can be described by pseudo zero order kinetics. Such behaviour has been commonly described by Langmuir-Hinshelwood kinetics, which will be described in more detail in chapter 2.3.

2.2.3 The presence of inorganic anions

Anions present in polluted waters, such as chlorides, phosphates, sulphates, nitrates and nitrites may have an effect on the photocatalytic process, by their competitive reaction with the photoproduced holes. In 1997, Lindner et al. reported the influence of these anions in experiments carried out to compare the efficiency of TiO₂ powder with Sachtleben Hombikat UV 100 (Lindner et al., 1997).

They observed that the photocatalytic degradation of dichloroacetate (DCA) decreased upon addition of various salts e.g. Na₂SO₄, NaCl, etc. Furthermore, as the concentration of these salts increased, the degradation rate of DCA decreased. When 10 mM of KNO₃, NaCl, Na₂SO₄ and Na₃PO₄ were added, the results were as follows:

- * 34% decrease due to KNO₃
- * 50% decrease due to NaCl
- * > 90% reduction in efficiency due to phosphates and sulphates.

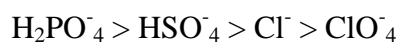
Anions can act as hole scavengers, as shown below



Also, the reaction of DCA with the positive holes as given in equation 10 will compete with the reaction of Cl⁻ or NO₂⁻ which also adsorb on the TiO₂ particle surface.



The adsorption measurements carried out showed the following order of adsorption on the TiO₂ surface at pH values below the isoelectric point of TiO₂ (Bahnemann et al., 1994):



Monovalent anions like nitrates were found to be less effective than multivalent anions such as sulphates or phosphates. The latter showed very effective inhibition of the detoxification process. Washing the catalyst with pure water could solve the activity inhibition by anions. The washing process was sufficient to fully restore the photocatalytic activity when chlorides, nitrates or nitrites were present. Dilute base was required to eliminate the inhibition caused by sulphates or phosphates (Lindner et al., 1997).

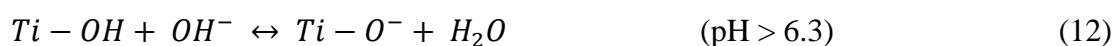
Liang has evaluated the photocatalytic deactivation in the presence of individual anions (NO₃⁻, Cl⁻, SO₄²⁻, and H₂PO₄⁻) (Liang et al., 2008). The inhibition of the photocatalytic degradation of 2,3-dichlorophenol caused by these anions can be ranked from high to low as SO₄²⁻ > Cl⁻ > H₂PO₄⁻ > NO₃⁻.

The observed inhibition effect can be attributed to the competitive adsorption and/or the formation of radicals during the photocatalytic reaction being less reactive than the hydroxyl radical.

2.2.4 The initial pH

Since photocatalytic reactions take place at the interface between the photocatalyst and the aqueous phase, the pH should exercise an important influence on the degradation kinetics of pollutants. The pH influences the energetic position of the valence and conduction band edge, the surface properties of the semiconductor and the adsorption behaviour of pollutants. An isoelectric point of pH 6.3 is widely reported for TiO₂ (Aeroxide P25).

The surface of TiO₂ is composed of amphoteric sites, which can become either positively or negatively charged, depending on the pH of the solution, the surface of the photocatalyst is covered with hydroxyl groups as well as molecular water. Both species show a surface acid-base equilibrium (Eq. 11 and 12) (Tanaka and Saha, 1994).



The pH also influences the dissociation equilibrium of organic acids and basis. Thus, the adsorption properties of a pollutant on a semiconductor depend strongly on the charge of the photocatalyst's surface and of the pollutant itself (Tanaka and Saha, 1994; Bekbölet et al., 1996; Theurich et al., 1996).

The thermodynamic stability of a pollutant is also influenced by the pH, e.g., hydroxyhydroquinone is unstable in acidic media but stable in alkaline media.

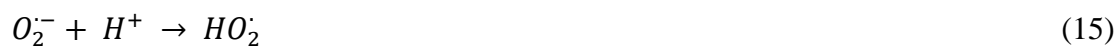
2.2.5 The oxygen concentration

Oxygen acts as an electron acceptor in photocatalytic systems. Furthermore, oxygen is directly involved in the oxidation process of pollutants by the formation of peroxy radicals (Eq. 13) which have been detected as reactive intermediates for the oxidation of several organic compounds (Matthews and McEvoy, 1992).



The adsorbed oxygen is the main electron acceptor and upon reaction gives rise to the formation of the superoxide radical O₂^{•-}





From the experimental results it was also observed that the presence of oxygen is very important to maintain the degradation rate at reasonable values (Zalazar et al., 2005a).

Therefore, the oxygen concentration in the suspension influences the degradation rate (Gerischer and Heller, 1991). This indicates an involvement of molecular oxygen in the rate limiting step of the degradation process. It was found that increasing of the molecular oxygen concentration from air saturated (20% O₂) to oxygen saturated (100% O₂) conditions increases the rate by a factor of ca. 1.7. (Mills et al., 1993).

Zalazar observed that the presence of oxygen is very important to maintain the degradation rate at reasonable values through a kinetic model (Zalazar et al., 2005a; Zalazar et al., 2005b)

Zhang carried out experiments to investigate electron transfer and identify the active species in the photodegradation of phenol in a polymer sensitized TiO₂ system, using charge-trapping species as diagnostic tools (Zhang et al., 2009). Their results showed that electron transfer took place between polymer and TiO₂ under visible light irradiation. The excited polymer reacted with oxygen to generate singlet oxygen (¹O₂), which contributed to the degradation reaction. Hydroxyl radicals (OH[•]) detected using the ESR method were shown to be the predominant active species in the photodegradation of phenol in aqueous suspension. Oxygen played an important role not only in scavenging conduction band electrons (e_{cb}⁻) but also in the formation of active oxygen radicals. In anhydrous solution, singlet oxygen (¹O₂) became the predominant active species.

2.2.6 Temperature

The temperature influences some physical properties of a semiconductor, such as energy of the band gap, conductivity, Fermi-level and the concentration of charge carriers and some physio-chemical properties, such as structure of the surface or adsorption / desorption equilibria of substrates (Atkins, 1985)). Furthermore, the pH, pK-values, solubility of dioxygen, redox potentials and reaction rate are also functions of the temperature.

However, the overall photocatalytic process is not usually found to be very temperature sensitive at least for the aqueous phase. The reported activation energies lie in the range between 5 - 20 kJ mol⁻¹. Increasing the temperature may increase the rate of oxidation of the organic substrate at the interface, but it will also have the effect of lowering the adsorption isotherms associated with the substrate and O₂, and lowering oxygen (Mills et al., 1993).

2.2.7 Light intensity

The photonic nature of the photocatalysis reaction has outlined the dependency of the overall photocatalytic rate on the light source used. Light intensity is one of the few parameters that affect the degree of photocatalytic reaction on organic substrates. Fujishima et al. indicated the initiation of TiO₂ photocatalysis reaction rates is not highly dependent on light intensity, where a few photons of energy (*i.e.* as low as 1 μW cm⁻¹) can sufficiently induce the surface reaction (Fujishima et al., 2000).

The intensity of the absorbed light influences the generation rate of electron/hole pairs in a semiconductor. Consequently, the concentration and generation rate of oxidizing species is also influenced by the light intensity. A square root dependency of the degradation rate on the light intensity (for moderate intensity) is reported (Alsayyed et al., 1991).

For high intensities the rate becomes independent of the light intensity because then the rate limiting step is the diffusion controlled mass transport, while for low intensities a direct relationship between the rate and the light intensity exists (Bahnemann et al., 1991).

Since the electronic structure of the semiconductor's surface is influenced by the light intensity, kinetic parameters and probably the adsorption balances of substrates are also influenced (Kormann et al., 1991).

2.3 Kinetics of photocatalysis

The photocatalytic oxidation of pollutants can be formally described by a hyperbolic kinetic law (Eq. 16) (Nishida and Ohgaki, 1994).

$$r = \frac{k \cdot K \cdot c}{1 + K \cdot c} \quad (16)$$

with: r: the reaction rate

k: the apparent reaction rate constant

K: the adsorption constant

c: the pollutant concentration

If the equation is representative of the reaction, a plot of the reverse reaction rate as a function of the inverse concentration should result in a straight line (Eq.17) from whose intercept $1/K$ and slope $1/kK$ the apparent reaction rate constant and adsorption constant can be calculated

$$\frac{1}{r} = \frac{1}{k \cdot K \cdot c} + \frac{1}{k} \quad (17)$$

Up to now, a hyperbolic kinetic law is the only model which can formally describe the concentration dependence of the photocatalytic oxidation. However, Turchi and

Ollis have demonstrated that such a hyperbolic kinetic law allows no assumption about the mechanism of the degradation reaction because they developed at least four different mechanistic models, all of them leading finally to the same kinetic law (Eq. 16) (Turchi and Ollis, 1989).

The most commonly used model for the interpretation of a photocatalytic degradation of a given model compound is the Langmuir-Hinshelwood adsorption model. Since the photocatalytic oxidation occurs at the interface between the semiconductor and the aqueous phase, adsorption of the reactant on the semiconductor's surface plays an important role in the degradation kinetics.

The Langmuir-Hinshelwood adsorption isotherm is based on the following assumptions (Turchi and Ollis, 1989).

1. All adsorption sites on the semiconductor's surface have the same energy and therefore can be taken as equal.
2. The adsorption enthalpy is independent of the coverage of the semiconductor's surface.
3. Only a monolayer of reactant is adsorbed.

Under the assumption that the concentration of intermediates is small and can be neglected, one can develop the following kinetic law (Eq. 18):

$$r = \zeta \cdot I \cdot \theta_{(Dioxygen)} \cdot \theta_{(Substrate)} \quad (18)$$

with: ζ : the photonic efficiency

I: the light intensity

θ (Substrate) : the coverage degree by the substrate (*function of T, pH,*)

θ (Dioxygen) : the coverage degree by dioxygen (*function of T, pH,*)

Under the conditions of continuous dioxygen purging, the coverage degree of dioxygen can be considered to be constant. Thus, the light intensity, the photonic efficiency and the coverage degree of the dioxygen can be taken as the apparent rate constant k (Eq. 19).

$$k = \zeta \cdot I \cdot \theta_{(Dioxygen)} \quad (19)$$

Resulting in

$$r = k \cdot \theta_{(Substrate)} \quad (20)$$

By definition, the coverage degree is according to the Langmuir adsorption isotherm (Eq. 20).

$$\theta_{(Substrate)} = \frac{K \cdot [Substrate]}{1 + K \cdot [Substrate]} \quad (21)$$

The following kinetic law for the degradation of a given substrate (Eq. 22) can obtain.

$$- \frac{d[Substrate]}{dt} = \frac{k \cdot K \cdot [Substrate]}{1 + K \cdot [Substrate]} \quad (22)$$

Two limiting cases have to be discussed:

For high coverage degrees of the semiconductor's surface, the term $K [Substrate]$ becomes much higher than 1 and equation 22 can be simplified to a zero order kinetic law (Eq. 23)

$$- \frac{d[Substrate]}{dt} = k \quad (23)$$

For low coverage degrees the term $K [Substrate]$ becomes much smaller than 1 and therefore can be neglected and equation 22 can be written as (Eq. 24):

$$- \frac{d[Substrate]}{dt} = k \cdot K \cdot [Substrate] \quad (24)$$

The reaction rate is then a pseudo first order. If the concentrations of intermediates formed during the photocatalytic degradation of a given substrate or the load of

inorganic species are high, they compete with the substrate for free adsorption places on the semiconductor's surface, which will cause a decrease in the reaction rate as a consequence of inhibition of the photocatalyst.

Equation 22 has now to be modified (Eq. 25).

$$-\frac{[Substrate]}{dt} = \frac{k \cdot K \cdot [Substrate]}{1 + K \cdot [Substrate] + \sum_i k_i [intermediate]_i} \quad (25)$$

Cunningham and Sedlak have shown that no correlation exists between the dark adsorption isotherm measured by alternative methods and the kinetic results from detoxification experiments (Cunningham and Sedlak, 1993). Thus, significant photoadsorption could not be ruled out or the Langmuir-Hinshelwood model needs some modification.

2.4 Photocatalyst forms and their effect on the degradation of organic pollutants

2.4.1 Suspension

There are many forms of catalyst that could be used to photo-degrade contaminants in water. One of the most used catalyst form is its suspension in water.

To maintain effective dispersion of the catalyst continuous mechanical stirring is required. Continuous aeration is also essential to scavenge the electrons and produce the reactive OH radicals in the water phase. The extent of dispersion can also be increased by sonication of the slurry using an ultrasonic bath for approximately 10–15 minutes (Mazzarino and Piccinini, 1999).

The advantage of using the suspension form is the close interaction of the pollutants molecules with the catalyst small particles. This property leads to the high degradation rate of pollutant at low catalyst load.

The use of suspended catalyst could lead to low catalyst performance due to low irradiation, which is caused by the opacity of the slurry (Ballari et al., 2010). After the detoxification process the catalyst particles must be separated from the water and transferred for further use. This process may need energy consuming filtration and complex regeneration processes.

For the above discussed reasons the use of TiO₂ suspension in industrial scale could be practically difficult and economically not feasible (Mukherjee and Ray, 1999).

2.4.2 Supported photocatalyst

An alternative to suspensions is the supported thin film photocatalyst. In this case the catalyst is permanently supported on the desired surface. The key advantages of this option are the possibilities to obtain an active crystalline structure of the catalyst and good stability of the catalyst layer in the reacting media.

Coated catalyst configurations, on the other hand, eliminate the need for catalyst filtration and centrifugation but generally result in a significant reduction in system efficiency.

A 60–70% reduction in performance is reported in aqueous systems for immobilized TiO₂ as compared to the unsupported catalyst (Kabra et al., 2004). Many kinds of support have been explored for TiO₂ photocatalyst particles which include aluminium (Chen et al., 2006), ceramic tiles (Kemmitt et al., 2004) and coated glass (Macedo et al., 2007). Since coatings are very thin, the actual active surface area of the photoreactor compared to the overall volume is low.

In TiO₂ heterogeneous photocatalysis, suspended catalysts, which can be agglomerated and sedimented after their use (Watts et al., 1995), usually show higher efficiencies than supported catalysts (Pozzo et al., 1997, 1999). Only in some cases TiO₂ coated on a support was found to be more efficient in organic compound removal than suspended TiO₂ (Kim et al., 2005; Kim et al., 2006).

The formation of the thin films by wash coating using a suspension of commercial products with a well-known photocatalytic activity can be easily obtained. However, the thin film obtained in this way is very sensitive to erosion by the liquid motion on the surface. Durable supported films can be obtained by different techniques like physical and chemical vapour deposition.

However, in this case the crystalline structure of the final product and consequently the catalytic activity of the TiO_2 might be difficult to control (Matthews, 1987). Thermal treatment at 500 °C can be used to increase the extent of crystalline nature of the catalyst obtained by physical or chemical vapour deposition.

TiO_2 coatings on sintered borosilicate glass (100–160 mm pore size) were prepared employing a synthetic route based on the hydrolysis of titanium oxysulfate (TiOSO_4) (Hidalgo et al., 2004). This method shows the coatings produced on sintered glass by the method appeared mechanically very robust and were not degraded even after repeated successive applications (4000 hours of continuous operation did not result in any appreciable decrease in the photocatalytic activity).

Scouring is another problem associated with films comprising immobilized powders of TiO_2 (Bideau et al., 1995) and reduced catalyst area to volume ratio of the immobilized photocatalyst is likely to cause mass transfer problems.

Butterfield has reported a modified fabrication technique and design of the reactor in order to eliminate scouring (Butterfield et al., 1997). In this technique oxide is actually grown on a titanium substrate as a defect film (a film that is electronically conducting even in dark), which also allows application of electric field with a view of enhancement in the extent of degradation. The batch reactor used in their work has been reported to remove 100% of *E. Coli* and 2 log units of *Cl. Perfringens* spores in 25 min. On the other hand, only approximately 20–30% disinfection was observed for UV light and UV light plus photocatalyst. However, this type of reactor needs to be tested on a large-scale and more importantly for the degradation of complex chemicals before firm conclusions can be made. In general, the immobilized or

supported catalytic reactor configuration offers many advantages like easy separation from the water and the elimination of high-pressure filtrations.

2.4.3 Pellet

Due to the potential separation problems in the large scale applications of suspended TiO₂ researchers have been seeking for alternative forms of TiO₂ catalyst, like pellets. Tan showed that the pellet type photocatalyst can be used for reduction of CO₂ to methane (Tan et al., 2006). They used cylindrically shaped TiO₂ pellets from Degussa Aerolyst 7708 (4 mm diameter and 4 mm height). The pellets were extruded from P25, Degussa's pyrogenic TiO₂, 80% anatase and 20% rutile, with particle size of 30 nm and surface area of 50 m² g⁻¹.

Horikoshi et al. reported the use of TiO₂ pellets and a microwave discharge electrodeless lamps (MDEL) for the photocatalytic degradation of acetaldehyde (Horikoshi et al., 2008). They found that the degradation of acetaldehyde using this system was very effective and they suggested the suitability of this system for effective removal of organic pollutants from air.

The TiO₂ pellets used by Horikoshi et al. were produced by Sachtleben Chemie GmbH and are named TiCat C. They are prepared from calcinated anatase TiO₂ at 800 °C (average length = 7 mm, average diameter = 5.5 mm). The BET surface area of the catalyst is approximately 30 m² g⁻¹.

2.5 The model compound (DCA)

DCA was chosen as the model compound because it is a relatively strong chloro-organic acid and a relevant industrial pollutant, the photodestruction of which has been extensively studied in different laboratories (Joyce et al., 2003; Marugán et al.,

2007; Lovato et al., 2011). The model compound DCA was selected for the following reasons:

- It is soluble in water
- It is easy to determine by TOC measurement.
- DCA represents the Toxic chlorinated organic compounds.
- Dichloroacetic acid (DCA) is a common pollutant found in lakes, rain, snow and water samples from diverse regions of the world (Scott et al., 2000; Rompp et al., 2001; Scott et al., 2002).

Sources of DCA contamination include water chlorination (Uden and Miller, 1983), use as a veterinary and human pharmaceutical (Park and Arieff, 1982; Weingand et al., 1986; Stacpoole, 1989; Stacpoole et al., 1992), and its use as a disinfectant and surfactant (Dalvi et al., 2000). DCA is also the microbial breakdown product of trichloroacetic acid (TCA) (Moghaddam et al., 1996).

Haloacetic acids (HAAs), such as DCA, are strong acids with low Henry's law constants in their ionized form so they are expected to partition into aquatic systems (Bowden et al., 1996, 1998b, a). Current environmental concentrations of DCA in European fog range from 0.12 to 5 mg L⁻¹ (Rompp et al., 2001). In Canada, DCA was the most abundant HAA in rain samples, having an average concentration of 0.02–1.58 mg L⁻¹ and in lake samples having concentrations as high as 1.5 mg L⁻¹ DCA (Scott et al., 2000).

Based on detailed mechanistic studies, the following reaction scheme for photocatalytic degradation of DCA is proposed (Lindner et al., 1997)





2.6 Photocatalytic reactors

Although scientific research on photocatalytic processes has been conducted for at least the three decades, industrial/commercial applications, engineering systems and engineering design methodologies have only been developed later (Parent et al., 1996; Blanco-Galvez et al., 2007; Blanco et al., 2009). Solar photochemical detoxification technologies can provide the environmental waste management industry with a powerful new tool to destroy pollutants with clean energy from the sun.

The specific hardware needed for solar photocatalytic applications is very similar to that used for conventional thermal applications with the following main differences (Blake et al., 1997; Malato, 1999) the fluid must be exposed to UV solar radiation so the absorber must be transparent to this radiation and no thermal insulation is required as the temperature does not play a significant role in the photocatalytic process.

Aluminium is the only metal surface that offers high reflectivity values in the UV spectrum. Photocatalytic reactors must be both transmissive and resistant to UV light. Common materials that meet these requirements are fluoropolymers, acrylic polymers and borosilicate glass and tubular photoreactor designs are the best option.

A wide variety of reactor configurations have been reported in the literature over the past 30 years including:

- annular photoreactor,

- packed bed photoreactor,
- photocatalytic Taylor vortex reactor,
- fluidised bed reactor,
- coated fibre optic cable reactor,
- falling film reactor,
- thin film fixed bed sloping plate reactor,
- swirl flow reactor,
- corrugated plate reactor.

These types of photoreactors have been discussed in detail in a recent review by McCullagh and co-authors (McCullagh et al., 2011).

2.7 Solar photocatalysis technology

The first outdoor engineering-scale reactor developed was a converted solar thermal parabolic through collector in which the absorber/glazing tube combination were replaced by a simple Pyrex glass tube through which contaminated water could flow (Tyner, 1990; Pacheco et al., 1991).

Since that time, research all over the world has advanced a number of reactor concepts and designs, including concentrating and non-concentrating reactors (Wendelin, 1992; Minero et al., 1993; Pacheco et al., 1993; Bockelmann et al., 1995; Curco et al., 1996b; Goswami, 1997; Goswami et al., 1997; Malato et al., 1997; vanWell et al., 1997; Dillert et al., 1999a).

The catalyst can be deployed in several ways, including as a fixed catalyst, slurry, or neutral-density large particles. As mentioned above, a simple modification of the parabolic through solar thermal collector was successfully developed and operated for

experiments in which the catalyst was deployed in suspension (Fernández-García et al., 2010).

Parabolic concentrating-type reactors have been used for applications such as groundwater remediation (Borthen and Leviten, 1992; Mehos et al., 1992), pesticide degradation (Malato et al., 1998; Muneer et al., 2004) and removal of metals from water (Prairie et al., 1991; Curco et al., 1996a; Marques et al., 1997).

A disadvantage of concentrating reactors is that they cannot concentrate diffuse solar radiation. This is not a major problem for solar thermal applications because diffuse radiation forms a small fraction of the total solar radiation. However, solar photocatalytic detoxification with TiO₂ as a catalyst uses only the UV portion of solar radiation, and as much as 50% or more of this may be present in diffuse form, especially at humid locations and during cloudy or partly cloudy periods.

Another disadvantage of concentrating reactors is that the quantum efficiency is low, due to a square root rather than linear dependence of rate on light flux (Ollis, 1991; Parent et al., 1996; Alfano et al., 2000). These disadvantages tend to favour the use of non-concentrating reactors (Pacheco et al., 1993; Romero et al., 1999).

Non-concentrating solar collectors are the choice for solar photocatalytic applications (Ajona and Vidal, 2000) they are more efficient than concentrator-based systems due to the use of both direct and diffuse UV light and their intrinsic simplicity.

A non-concentrating flat plate reactor is the double-skin sheet reactor (DSSR) which has been developed by Röhm GmbH Chemische Fabrik, Darmstadt, Germany and the Institut fuer Solarenergieforschung GmbH, Hannover, Germany (ISFH) (vanWell et al., 1997). The DSSR consists of a modified double-skin sheet (SDP 16/32) manufactured by the Röhm GmbH in Darmstadt, Germany. PLEXIGLAS® (polymethyl methacrylate) is used to produce the flat and structured box of the photoreactor.

The double skin sheet reactor made from Plexiglas[®] is able to use the diffuse as well as direct sunlight; the DSSR has many advantages when comparing with other types of reactor like thin film fixed bed reactor TFFBR (Dillert et al., 1999b).

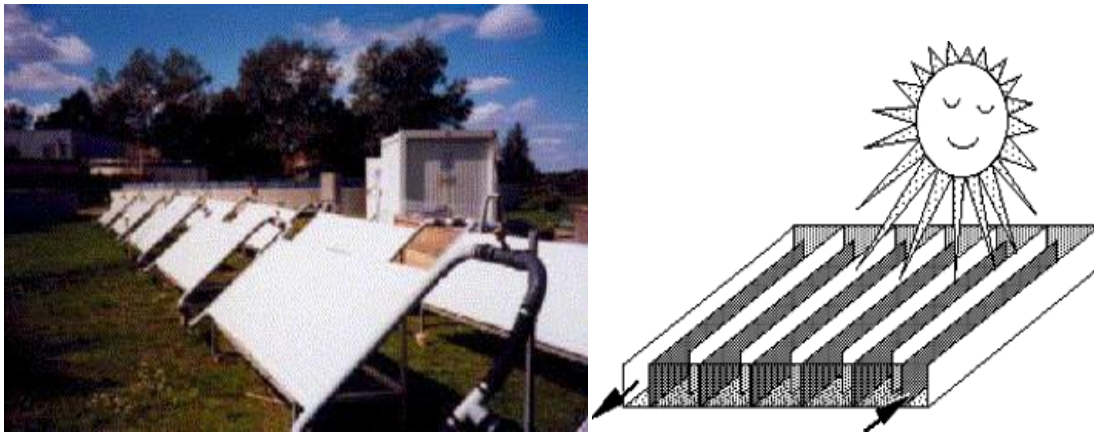


Figure 4: Left photo of pilot plant installed in the Wolfsburg factory of the Volkswagen AG (Photo: J. Lohmann, ISFH). Right, schematic view of DSSR showing the inner structure of the transparent box made of PLEXIGLAS[®] (Bahnemann, 2004).

Advantages of this type of reactor are that it uses total global UV – irradiation usable, due to the high turbulent flow conditions it has no mass transfer limitations, no vaporization of volatile contaminants because it is a nearly closed reactor and it has simple construction and low investment cost. While the disadvantages were as low optical efficiency, separation of photocatalyst from the treated water is needed; oxygen injection necessary and large reactor area is required for the purification of large wastewater volumes.

The CPC (Fig. 5) is a very interesting cross between trough concentrators and one-sun systems and have been found to provide the best optics for low concentration systems (Miranda-García et al., 2011). Almost all the UV radiation arriving at the CPC

aperture area (not only direct, but also diffuse) can be collected and is available for the process in the reactor.

The light reflected by the CPC is distributed around the back of the tubular photoreactor illuminating most of the reactor tube circumference. Due to the ratio of CPC aperture to tube diameter, the incident light on the reactor is very similar to that of a one-sun photoreactor, the performance being close to that of the simple tubular photoreactor.

As in a parabolic trough, the water is more easily piped and distributed than in many one-sun designs. All these factors contribute to excellent CPC collector performance in solar photochemical and photocatalytic applications.

One of the first solar reactors using a fixed photocatalyst and not applying a light-concentrating system for the photocatalytic process is the thin-film fixed-bed reactor (TFFBR) (Fig. 6). The most important part of the TFFBR is a sloping glass plate coated with the photocatalyst (e.g., titanium dioxide Aeroxide P25 or Sachtleben Sachtleben Hombikat UV100). The polluted water flows along the inclined glass pane forming a very thin film.



Figure 5: View of one CPC collector module (photo made at PSA, Spain) (Fernández et al., 2005).



Figure 6: Photograph of the TFFBR reactor installed at the Plataforma Solar de Almeria in Spain (Photo: D. Bockelmann) (Bahnemann, 2004).

Table 3 shows the main advantages and disadvantages between concentrating and non-concentrating photocatalytic reactors.

Table 3: Main advantages and drawback of concentrating and non-concentrating solar photocatalytic reactors

Concentrating reactors	Non-concentrating reactors
Advantages	
Smaller reactor volume. Smaller harvesting area.	Negligible optical losses. Direct and diffuse light utilization. Simple design and low investment cost. Linear dependence between efficiency and radiation intensity
Disadvantages	
High investment cost. Direct light utilized only. Square-root dependence between efficiency and radiation intensity.	High friction pressure losses. Larger reactor.

2.8 Solar photocatalysis applications

Solar photocatalytic water mineralization of organic and inorganic water pollutants using interaction between UV radiation and semiconductor catalysts has a strong potential in the industrial destruction of toxic materials in water as has been widely demonstrated in last decade (Goswami, 1997; Blanco et al., 1999; Herrmann, 1999; Rodríguez et al., 1999; Alfano et al., 2000) and the number of applications and target

compounds are numerous. Solar photocatalysis also has its potential for the detoxification of hydrogen sulphide containing waters from geothermal springs, or as they may be produced in oil and gas operations. This approach has been suggested even as an alternative to the established Claus process and has been also discussed for the production of hydrogen from H_2S (Zaman and Chakma, 1995).

Solar photocatalytic mineralization of organic water pollutants using interaction between UV radiation and semi-conductor catalysts has a strong potential in the industrial destruction of toxic organics in water as has been widely demonstrated in last decades (Goswami, 1997; Blanco et al., 1999; Herrmann, 1999; Rodríguez et al., 1999; Alfano et al., 2000) and the number of applications and target compounds are numerous. In zones with medium/high solar radiation solar detoxification is useful for treating water contaminants with the following characteristics:

- maximum organic concentration of several hundreds of $mg L^{-1}$;
- non-biodegradable contaminants and biocides;
- hazardous contaminants present within complex mixtures of organics and,
- Inorganic toxins, like H_2S (Gruzdkov et al., 1987; Sopyan, 2007) and HCN (Chiang et al., 2002).

At present and from the wide experience accumulated by many scientists and research groups during the last 30 years worldwide, solar detoxification seems to be a good solution with many interesting possible applications.

2.9 Slurry reactors and immobilized photocatalyst

The majority of reactor designs are using suspended slurries as photocatalysts. Generally, slurry reactors exhibit the following properties:

- Slurry systems have shown the largest photocatalytic activity when compared to reactors with immobilized photocatalyst (Chester et al., 1993),

- Slurry systems mostly use pure (in contrast to supported) photocatalyst on a relatively small scale,
- Optimized slurry type reactors offer a degradation rate faster than immobilized designs,
- Slurry reactor designs are mostly applied at the R&D stage of a technology development (Ballari et al., 2010).

Although, the suspension is more efficient in photocatalysis, it requires the separation of the photocatalyst which will add considerable costs to the process. This will turn into a particular worry when it comes to industrial and large scale applications. The decontamination process in slurry reactors requires removal of the catalyst by filtration.

While a simple separation, using flow type cyclones or settling by gravity might be a rather economic approach at a first glance, complete separation of photocatalyst from the solution may become quite cumbersome and expensive, in particular if filtration or centrifuge techniques have to be applied. Any process that could avoid the filtration step (for example, immobilizing the photocatalyst particles on a solid substrate) would be of great practical benefit (Matthews, 1987).

In addition to these concerns, slurry type designs may not be able to fully recover or reuse the photocatalyst and a continuous supply of add-up catalyst will be needed. This has to be considered in the budgeting and could considerably affect the business economics of a photocatalytic process, especially if the photocatalyst constitutes of expensive substances.

Therefore, and very similar to other industrial and chemical processes, the main advantage and driver of developing Photocatalytic reactors with immobilized (fixed bed) photocatalysts is pure business economics by eliminating the costly and maintenance intensive solid – from - liquid separation step (Bekbölet et al., 1996).

As known from other industrial catalytic processes, immobilized photoreactors theoretically can be subdivided into moving bed type and fixed bed type.

The concept of moving bed type of photoreactors, where the active photocatalyst continuously is supplied and spent or deactivated catalyst regenerated, may have some applications in photocatalytic processes other than photooxidation of water pollutants, like photocatalytic synthesis processes, and the use in large solar concentrators. Moving bed photocatalyst systems also will add costs and maintenance to a process and will not be studied in this work.

Thus, a perfectly operating photocatalytic reactor system for water detoxification should have no or very few moving or rotating equipments and an infinite lifetime of the photocatalyst. The polluted water, eventually after some kind of pre-screening or treatment, will flow through one or a series of long-life and virtually maintenance-free photocatalytic cells. The effluent after the photocatalytic process will be clean water, free of organic material, only containing inorganic ions in its oxidized form.

Not surprisingly, the up-scaling from suspension type reactors to large fixed bed type faces the same challenges as known from other industrial catalytic processes (Mukherjee and Ray, 1999):

- Finding the right support material for the photocatalyst.
- Minimize deactivation of photocatalyst.
- Minimize leaching and migration of photocatalyst.
- Cutting costs by designing an inexpensive photocatalyst.

These type of reactors used suspension of photocatalyst. They have these features:

- The majority of the photoreactors currently in use for water treatment are well-mixed slurry.
- Slurry systems have shown the largest photocatalytic activity when compared to reactors with immobilized photocatalyst.

- high degradation rate.

Although, the suspension is more efficient in photocatalysis, it requires the separation of the photocatalyst which is add more cost to the process. Photocatalytic reactors with immobilized TiO_2 have the advantages that requisite no separation of the photocatalyst. Table 4 summarize and compare some of the main advantages and setbacks between slurry type and immobilized reactors:

Table 4: Advantages and disadvantages of reactors with slurry and immobilized photocatalyst

Reactors with slurry photocatalyst	Reactors with immobilized photocatalyst
Advantages	
<ul style="list-style-type: none"> -Fairly uniform catalyst distribution. -High photocatalyst surface area to reactor volume ratio. -Min. Catalyst fouling. -Well mixed particle suspension. - Low pressure drop through the reactor. 	<ul style="list-style-type: none"> -Continuous operation. -Improved removal of organic material while using a support with adsorption properties. -No need for an additional catalyst separation operation.
Disadvantages	
<ul style="list-style-type: none"> Required post- process filtration Important light scattering and adsorption in particle suspended medium. 	<ul style="list-style-type: none"> Low light utilization efficiencies due to light scattering by immobilized photocatalyst. Restricted processing capacities due to possible mass transfer limitations. Possible catalyst deactivation and catalyst wash out

3 Material and methods

3.1 Materials

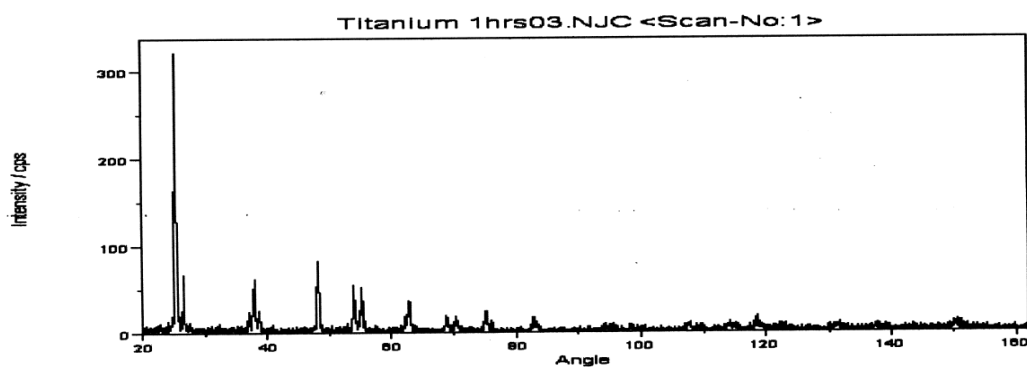
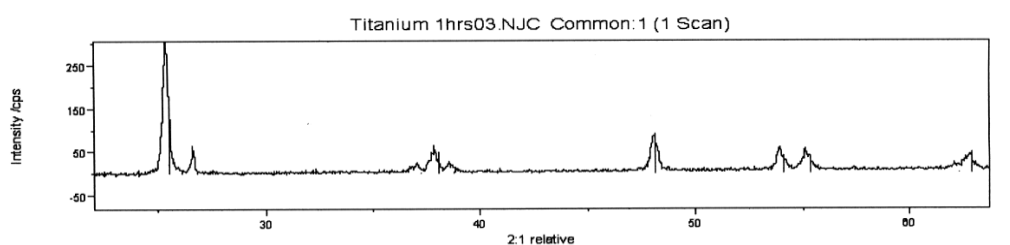
3.1.1 Photocatalysts

The photocatalysts used in this work was commercially available TiO₂ powder Aeroxide P25 (previously Degussa P25) and Sachtleben Hombikat UV100. Characteristics data for the commercial available TiO₂ powders are given in table (5) (Kirchnerova et al., 2005) and TiO₂ pellets from BASF.

Table 5: Main characteristics of two different commercial titania powders

Characteristic	Aeroxide P25	Sachtleben Hombikat UV100
Preparation method	Flame pyrolysis of TiCl ₄	Sulphate process, precipitation
Composition by XRD	70% anatase	100% anatase, not fully crystalline
Apparent powder density (g ml ⁻¹)	0.05	0.35
Primary crystallite size, XRD (nm)	30	<10
Morphology	Heterogeneous, wrinkled surface	Round agglomerated particles
Apparent particle size (µm)	<10	20–30
SSA _{BET} (m ² g ⁻¹)	50	289; 189; 300

It can be seen from Table (5) that the main differences between Aeroxide P25 and Sachtleben Hombikat UV 100 are the primary crystallite size, which is 30 nm for Aeroxide P25 and <10 nm for Sachtleben Hombikat UV 100, and the composition, which is pure anatase in case of Sachtleben Hombikat UV 100 while Aeroxide P25 is a mixture of 70% anatase and 30% rutile. BASF TiO₂ pellet photocatalyst, which is commercially not available, are cylindrical in shape with different sizes, the pellet size used were (3 mm . 3 and 5 mm . 5 mm). The X-ray run shows that the pellet consist of about 35 % of anatase TiO₂ and approximately 65% aluminium titanium silicate Al₄Ti₂SiO₁₂ (Fig. 7).



PDF-No	In Range	Matched	FOM	SOM	Name Min.	Formula
21-1272	39	26	1.108	1.186	Anatase, syn	Ti O ₂
22- 502	13	13	1.601	1.544	Aluminum Titanium Silicate	Al ₄ Ti ₂ Si O ₁₂

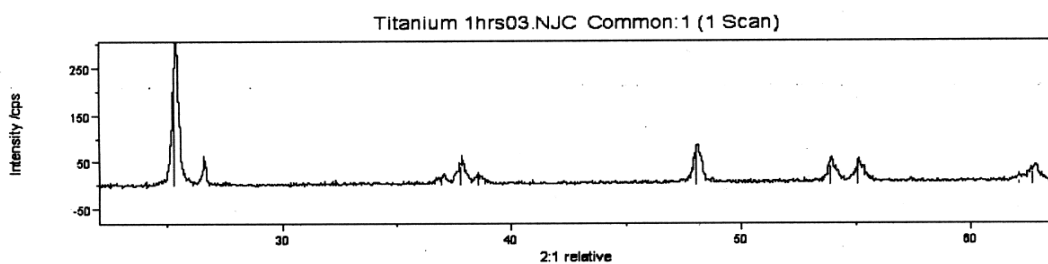


Figure 7: X-ray for TiO₂ Pellet from BASF, this analysis is performed in the laboratory of RASCO (Ras Lanuf Oil and Gas Processing Company) Ras Lanuf-Libya.

3.1.2 Chemicals

All chemicals used in this work such as dichloroacetic acid (DCA), potassium hydrogen phthalate (KHP), sodium bicarbonate, sodium carbonate, NaOH, KOH, and KNO₃ were of reagent grade and used as received without any further purification. All aqueous solutions and suspensions were prepared with deionized water purified by a Milli-Q/RO system (Millipore) resulting in a resistivity >18MΩcm.

3.1.3 Spiral glass reactor

The spiral glass reactor was built by a 4 meter long borosilicate glass tube (10 mm outer diameter and 8 mm internal diameter) wound in turns of diameter of 6 cm in order to be fit for UV lamp (UV-lamp 40 W from Osram Eversun type L 40 W/79K) which inserted in the spiral glass reactor (Fig. 8).



Figure 8: Glass spiral reactor

3.1.4 Preparation of coated spiral glass reactor

A spiral shape glass reactor the inside of which has been coated with TiO_2 employing a new sol-gel technique that has been developed in our laboratory (Hidalgo et al., 2004). The suspension which produced by the mentioned method was poured into the spiral reactor using a funnel from the top side and the pouring repeated for many times (Fig. 9). The wet reactor was dried at $110\text{ }^\circ\text{C}$ for 2 hours and calcined at $500\text{ }^\circ\text{C}$ for 1 hour, following heating rates of $5\text{ }^\circ\text{C}/\text{min}$.

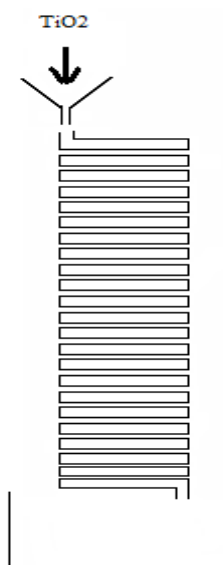


Figure 9: Coating procedure of the spiral reactor

3.2 Procedures

3.2.1 Preparation of DCA stock solution (500 mM)

DCA Stock solution was prepared by adding 41.66 ml of DCA liquid (purity of 99%) into 1000 ml of de-ionized water in order to make 500 mM of DCA.

Typically DCA solutions were prepared by adding of less than 2 L of de-ionized water into a 2 L volumetric flask. Then 4 ml of a dichloroacetic acid stock solution (500 mM) and 2.02 g of KNO_3 were added to the flask. After the salt was solved, the

volume was then adjusted by filling of de-ionised water to the 2 L mark, resulting in a solution containing 1mM and 10 mM of DCA and KNO_3 , respectively. This mixture named DCA solution and was used as a model compound solution in all photocatalytic experiments unless indicated.

3.2.2 Preparation of TiO_2 suspensions

Typically 3.0 g of the photocatalyst powder (Aeroxide P25 or Sachtleben Hombikat UV 100) was added into a conical flask containing 1000 ml of DCA solution (see 3.2.1) in order to prepare suspensions with a catalyst concentration of 3g L^{-1} .

This mixture was stirred for 30 minutes and then sonicated for another 30 minutes to insure total dispersion of the catalyst through the suspension (Ultrasonic bath type Branson 5200 from Branson). The suspension, according to the experiment (500 ml or 1000 ml) was poured into a double jacket flask (1000 ml) of the photocatalytical setup where it was stirred continuously. The pH (pH 91 from WTW) was adjusted to 3 by adding either 1N KOH or 1 N HNO_3 depending on the pH of the suspension. Air was pumped into the suspension to insure saturation with molecular oxygen, and the setup was thermostated to 20°C using circulation of cooled water through the jacket of the flask (thermostat HAAKE G, Haake, Germany). The suspension circulated in the dark for 30 minutes to reach adsorption equilibrium. Before the light was switched on, a sample was taken and then the light was switched on.

3.2.3 Spiral experimental setup

In order to prepare a packed column, the spiral glass was filled with TiO_2 pellet (dimension of 3 mm . 3 mm from BASF). The reactor was filled with 123 g of the TiO_2 pellet. The spiral glass reactor was fixed inside a box where the lamp was installed. One lamp (UV-lamp 40 W from Osram Eversun type L 40 W/79K) is inserted in the spiral reactor. Flexible tubes were connected at the inlet and the outlet

of the reactor, the inlet tube was connected to a centrifugal pump (type KrP 800, from Heidolph, Germany) in case of suspension and a membrane pump (type FM 1.3 KT 18, from KNF flodos, Germany) in case of pumping the solution into spiral packed reactor.

The solution or suspension was pumped from the flask to the upper part of the reactor. In the flask the solution or suspension was stirred by a magnetic stirrer. pH electrode and oxygen electrode conjugated with thermometer (microprocessor oximeter Oxi 2000, electrode TriOximatic EO200, from WTW Germany) were inserted into the solution or suspension. Air was supplied to the flask through small air pump (Fig. 10).

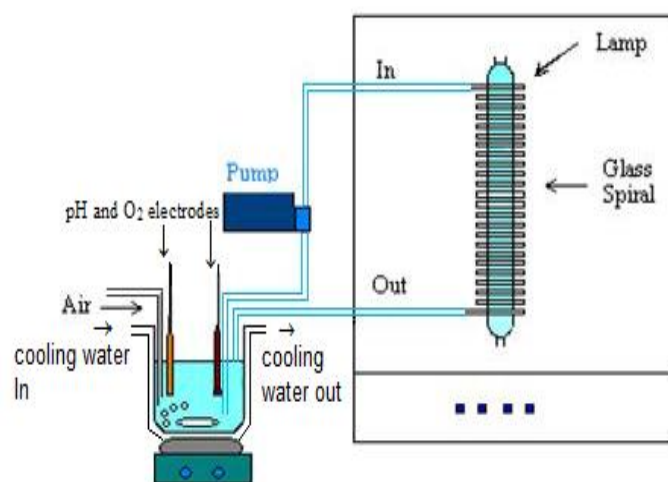


Figure 10: Spiral packed reactor experimental set up

3.2.4 Blank experiments

3.2.4.1 Effect of UV light on DCA degradation

To check the effect of direct UV light (photolysis) on the degradation of the model compound DCA, a clean spiral glass reactor was used without adding any

photocatalytic material. 1 L of DCA solution (1mM) was circulated in the spiral reactor with continues bubbling of air. The solution was illuminated during the experiment with UV-A light with an intensity of 30 W m^{-2} . The pH of the solution was adjusted to pH 3 in all experimental runs. Samples were taken each 30 minutes and subject of analysis.

3.2.4.2 Blank experiment (Spiral glass reactor)

The adsorption effect of photocatalyst on the model compound has been checked by a blank experiment where 500 ml of DCA solution was circulated through the reactor of 123 g packed column for 3 hours without employing the UV light. The pH of the solution was adjusted to 3. To guarantee a constant O_2 concentration the solution was continuously purged with air by means of an air pump. The flask which contains the solution was thermostated at $21 \pm 1 \text{ }^\circ\text{C}$. Samples were taken regularly.

3.2.5 Pan reactor

A pan made of polypropylene of the dimension of (25 cm . 19.5 cm) area of 0.04875 m^2 (Fig. 11), was filled with 400 g of TiO_2 pellets (5 mm . 5 mm) which spread in to it. 500 ml of a solution containing about 1.4 mM DCA were poured into the pan over the catalyst. The pan placed in the dark for 48 hours in order to measure the effect of adsorption; samples were taken on regular basis. After 48 hours the pan was irradiated with UV-A (light intensity 30 W m^{-2}) and samples for TOC measurements were taken.



Figure 11: Polypropylene pan filled with 400 g of 5 mm . 5 mm of pellet type photocatalyst

3.2.6 Flat packed reactor

A flat tray was made of PVC with dimension of 33 cm long, 28 cm wide and 1.0 cm height. Amount of TiO_2 pellets (size of 5 mm . 5 mm) was spread in the tray to the height of 0.5 cm of the tray; the irradiated area was 0.0924 m^2 . Two flexible hoses were connected to the inlet and outlet connections of a centrifugal pump (type KrP 800, from Heidolph, Germany) the inlet tube to the pump was immersed into the flask where the model compound which to be degraded (Fig. 12 and 13). The light employed was from solar simulator full technical description can found in (Sagawe et al., 2001). The reactor received 30 W m^{-2} from the solar simulator.

The other hose the outlet of the pump was connected to the tube. This tube is laid horizontally on the tray. The tube was perforated which enable the circulated solution to be sprayed uniformly over the pellet from the reservoir to the reactor (Fig. 13) to enable the solution to be circulated. The circulated solution passed over the pellet to the flask (reservoir); pH and oxygen electrodes were immersed into the solution in order to monitor pH and oxygen content. Air was pumped into the suspension to insure saturation with molecular oxygen.

When the flat reactor was employed outdoor and directly subjected to sunlight, a substantial amount of solution was lost. This disadvantage has triggered the idea of designing a closed system which was the tubular packed reactor.



Figure 12: Flat packed reactor, BASF Pellet catalyst size of 5 mm . 5 mm

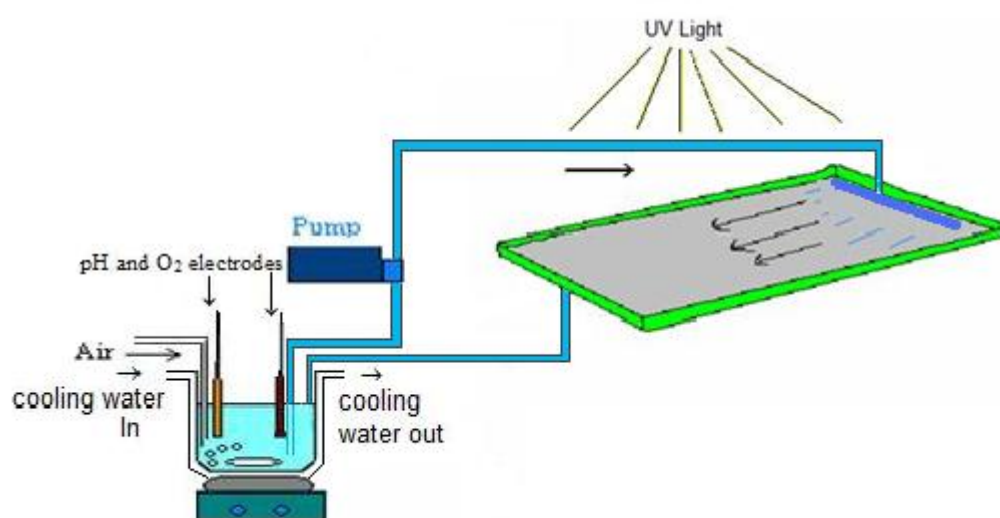


Figure 13: Flat packed reactor setup experiment with circulation, irradiated area is 0.0924m².

3.2.7 Tubular packed reactor

To overcome of the problem of the flat packed reactor, a tubular glass reactor was investigated. The tubular reactor consists of 12 tubes (23 cm long and 1cm inner diameter); each tube was filled with 10 g of 3 mm . 3 mm TiO₂ pellet. The tubes were

connected together using flexible hoses. One end was connected to a centrifugal pump (Type KrP 800 from Heidolph with flow rate of 8 L min^{-1}) and the other end was connected to the flask as an outlet of the system.

pH electrode was immersed into the flask; oxygen analyzer and thermometer were also installed in the system. Air was pumped into the suspension to insure saturation with molecular oxygen. Solution was pumped through the reactor tubes for 30 minutes in order to allow the system to be in equilibrium state. A sample was taken before the system was exposed to the UV light. UV light was from the solar simulator. In regular intervals, reading of pH, temperature and oxygen content were recorded. Samples were taken to be analyzed using TOC. The total irradiated area was 0.04335 m^2 (Fig. 14).

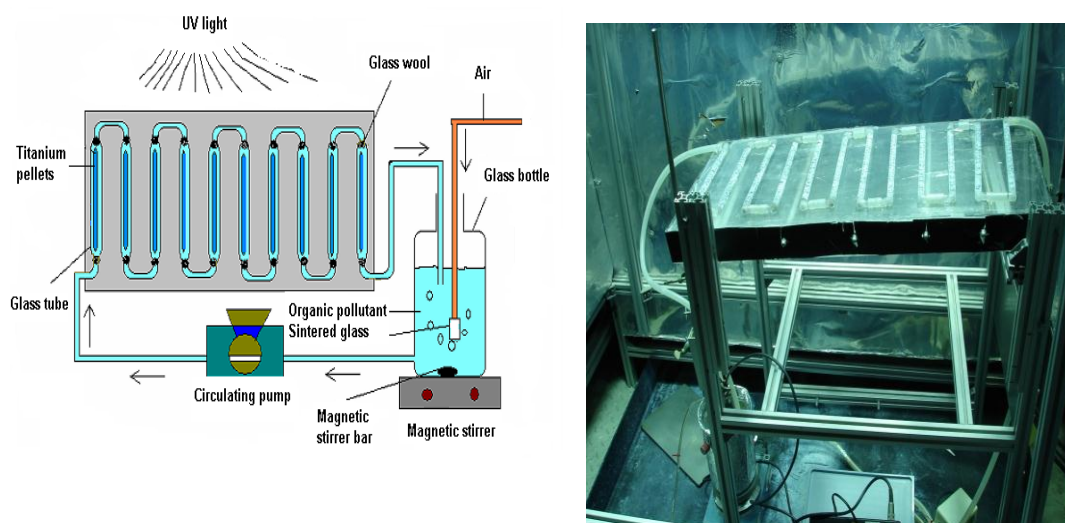


Figure 14: Tubular packed reactor setup

3.2.8 Analytical procedure

At specific time intervals, the samples (5 ml) were withdrawn from the reservoir of the photocatalytic set-up and in the case of suspension centrifuged at a speed of 4000 rpm for 40 minutes (Centrifuge, type Megafuge 1.0 from Heraeus). The supernatant liquid was transferred to the TOC analyzer (TOC 5000 from Shimadzu)

in order to measure the total organic carbon in the sample. The COD of the supernatant liquid was measured by a Dr. Lange cuvette test (LCK314 with measuring range 15-150 mg L⁻¹, or LCK114 with measuring range 150-1000 mg L⁻¹). The oxygen concentration of the aqueous solutions and suspensions were determined employing a dissolved oxygen meter (WTW Oxi 2000). The irradiance in the UV-A region was measured with a radiometer (Dr. Hönle UV-Technik).

3.3 Real wastewater (Solvay sample)

Solvay is a chemical producing company specialized in the production of essential chemicals including soda ash, caustic soda, hydrogen peroxide and special chemicals. A real wastewater was received from Solvay in order to check the ability of the photocatalytic technique to treat it. Sample was orange in colour with pH of 12.84 and the organic content of this wastewater was 1476 mg L⁻¹ as TOC and 5400 mg L⁻¹ as COD. Samples with a volume of 250 mL were treated in the spiral reactor after mixing with 1 g L⁻¹ Evonik-Degussa Aeroxide P25, stirring for 30 minutes and sonication for 15 minutes in the dark, without any additional treatment or dilution. The samples were then irradiated for 7 hours. Samples were taken in appropriate time intervals and diluted 100 times in order to measure the TOC and COD.

4 Results

4.1 The spiral glass reactor

4.1.1 Blank experiments

To create a base line for the investigation of the photocatalytic DCA degradation blank experiments were carried out. To determine the possible photolysis of the DCA in the absence of titanium dioxide, a DCA solution with a concentration of ~ 1 mM was prepared and introduced into the reservoir of the spiral reactor. The solution was circulated through the photoreactor with a flow rate of approximately 105 L h^{-1} resulting in a residence time $t_r = 0.18$ min. The spiral reactor was irradiated with one UV-A lamp ($\lambda_{\text{max}} = 360$ nm) centered in the axis of the glass spiral. The TOC values measured at different points in time during the experimental runs are plotted in Figure 15 versus the irradiation time. As it becomes obvious from this Figure the TOC of the solution showed only minor decrease during 720 minutes of UV-A irradiation which can be neglected within experimental error

The second blank experiment was the combination of DCA in an aqueous titanium dioxide suspension and the absence of UV-A light. The objective of this experiment was to measure the amount of DCA, which could possibly be adsorbed on the catalyst surface. The experimental results of this experimental run are presented in Figure 16. No change of the TOC value (within experimental error) during the recirculation of the suspension through the reactor for a period of 120 minutes was observed.

These results are in agreement with results published in a recent work (Singh et al., 2003; Zalazar et al., 2005b).

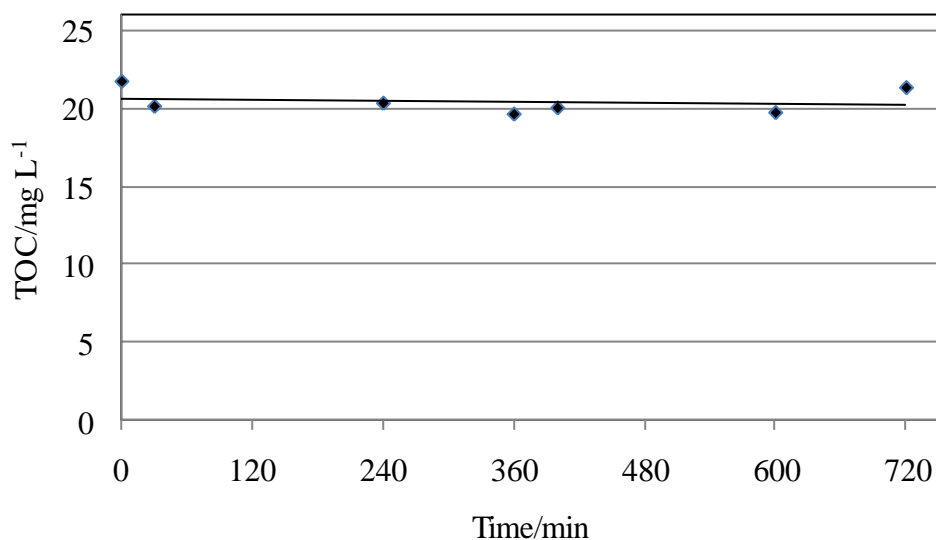


Figure 15: Plot of TOC versus irradiation time during UV-A irradiation of a homogeneous DCA solution circulating through the spiral glass reactor. *Experimental conditions:* $c_{\text{DCA},0} = 1 \text{ mM}$, $\text{pH } 3.0$, $V = 500 \text{ mL}$, $F = 105 \pm 2 \text{ L h}^{-1}$, $I_{\text{hv}} = 28 \text{ W m}^{-2}$, $T = 21 \pm 1^\circ\text{C}$.

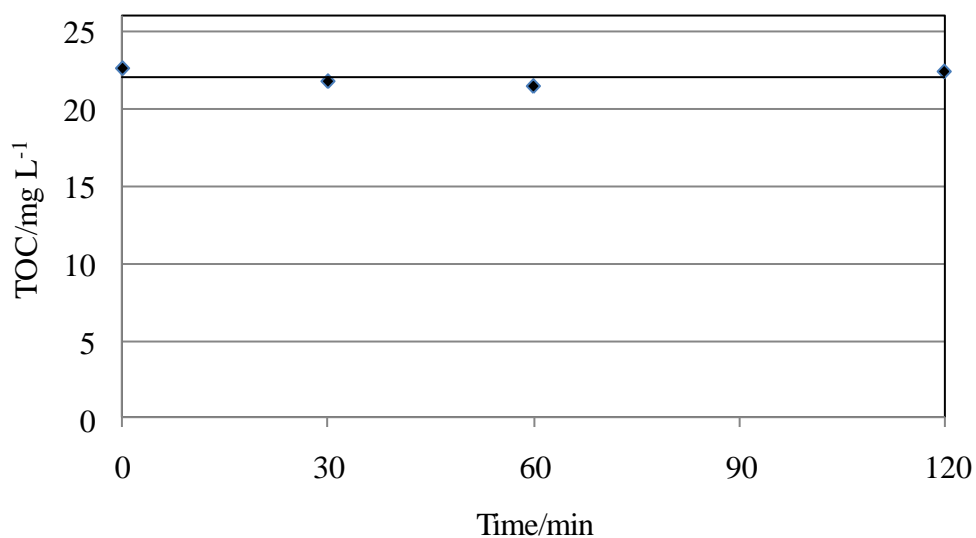


Figure 16: Plot of TOC versus time during recirculation of a DCA containing TiO_2 suspension through the spiral glass reactor in the dark. *Experimental conditions:* $c_{\text{DCA},0} = 1 \text{ mM}$, Sachtleben Hombikat UV 100, $c_{\text{cat}} = 3.0 \text{ g L}^{-1}$, $\text{pH } 3.0$, $V = 500 \text{ mL}$, $F = 105 \pm 2 \text{ L h}^{-1}$, $I_{\text{hv}} = 0 \text{ W m}^{-2}$, $T = 21 \pm 1^\circ\text{C}$.

4.1.2 The spiral glass reactor with suspended photocatalyst

The photocatalytic degradation of DCA ($c_0 = 1 \text{ mM}$) in the spiral glass reactor was investigated in aqueous suspensions of two different types of suspended photocatalysts (Sachtleben Hombikat UV 100, and Evonik Aeroxide P25; $c_{\text{cat}} = 3 \text{ g L}^{-1}$). The volume of the air-purged suspension circulating through the photoreactor was varied ($V = 500$ and 1000 mL) while the flow rate ($F = 105 \pm 2 \text{ L h}^{-1}$) of the suspension was maintained constant.

The change of the TOC of the DCA-containing suspension with irradiation time ($I_{\text{hv}} = 28 \text{ W m}^{-2}$) for two typical experimental runs employing Hombikat UV 100 as the photocatalyst and suspension volumes of 500 mL and 1000 mL , respectively, are presented in the Figures 17 and 18. As can be seen from these Figures the TOC of the suspensions decreased within 30 minutes of UV-A irradiation from 24.03 to 2.19 mg L^{-1} and 25.23 to 4.47 mg L^{-1} when 500 and 1000 mL were treated, clearly indicating the photocatalytic mineralization of the probe molecule. These decrease of the TOC values correspond to a conversion of 91% and 82% of the initially present DCA.

The photocatalytic reduction of the TOC was associated with an initial decrease of the oxygen concentration of the suspension, which was monitored online during the entire experimental run, during the first 5 minutes of UV-A irradiation (cf. Fig. 19). Then the oxygen concentration returns to the level of about 8 mg L^{-1} which is typical for an air-saturated aqueous suspension at ambient temperature.

Typical results of the respective experimental runs employing Evonik Aeroxide P 25 as the photocatalyst are presented in the Figure 20 to 23. When 500 mL of suspension was used the TOC decreased from initially 24.04 mg L^{-1} to a final value of 2.45 mg L^{-1} within 30 minutes of UV-A irradiation corresponding with a conversion of 90% of the initially present DCA (Fig 20). An initial decrease of the oxygen concentration from a starting concentration of 8.36 mg L^{-1} to a minimum value of 5.74 mg L^{-1} after 20 minutes of UV-A irradiation was observed (Fig. 21). Subsequently, the oxygen concentration increased again within the later 10 minutes of the experimental run reaching a value of 8.0 mg L^{-1} .

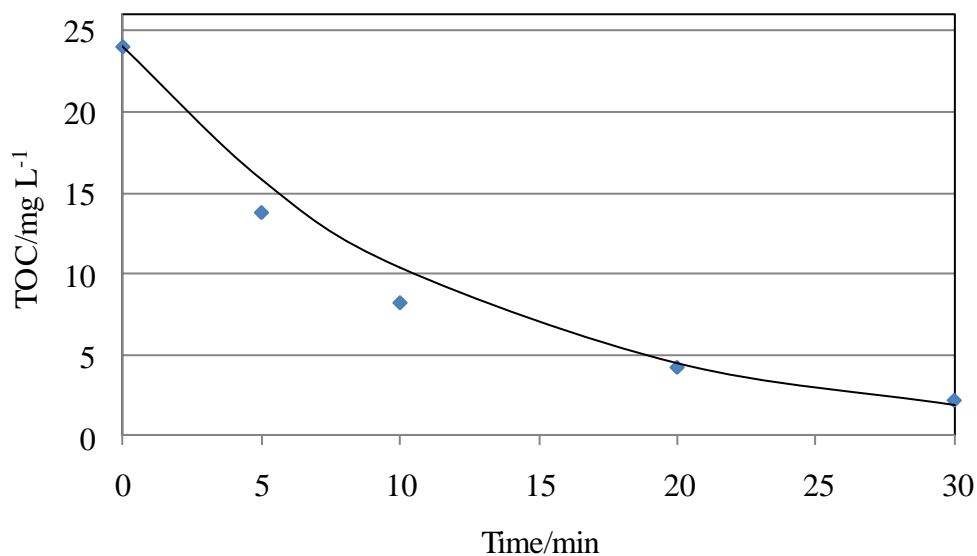


Figure 17: Plot of TOC versus irradiation time during recirculation of a DCA containing TiO_2 suspension through the spiral glass reactor. *Experimental conditions:* $c_{\text{DCA},0} = 1 \text{ mM}$, Sachtleben Hombikat UV 100, $c_{\text{cat}} = 3.0 \text{ g L}^{-1}$, pH 3.0, $V = 500 \text{ mL}$, $F = 105 \pm 2 \text{ L h}^{-1}$, $I_{\text{hv}} = 28 \text{ W m}^{-2}$, $T = 21 \pm 1^\circ\text{C}$.

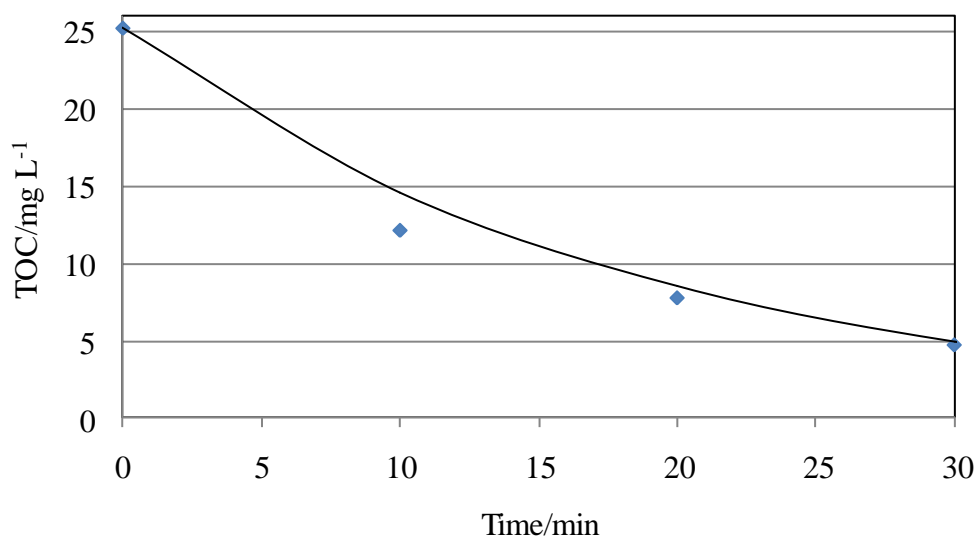


Figure 18: Plot of TOC versus irradiation time during recirculation of a DCA containing TiO_2 suspension through the spiral glass reactor. *Experimental conditions:* $c_{\text{DCA},0} = 1 \text{ mM}$, Sachtleben Hombikat UV 100, $c_{\text{cat}} = 3.0 \text{ g L}^{-1}$, pH 3.0, $V = 1000 \text{ mL}$, $F = 105 \pm 2 \text{ L h}^{-1}$, $I_{\text{hv}} = 28 \text{ W m}^{-2}$, $T = 21 \pm 1^\circ\text{C}$.

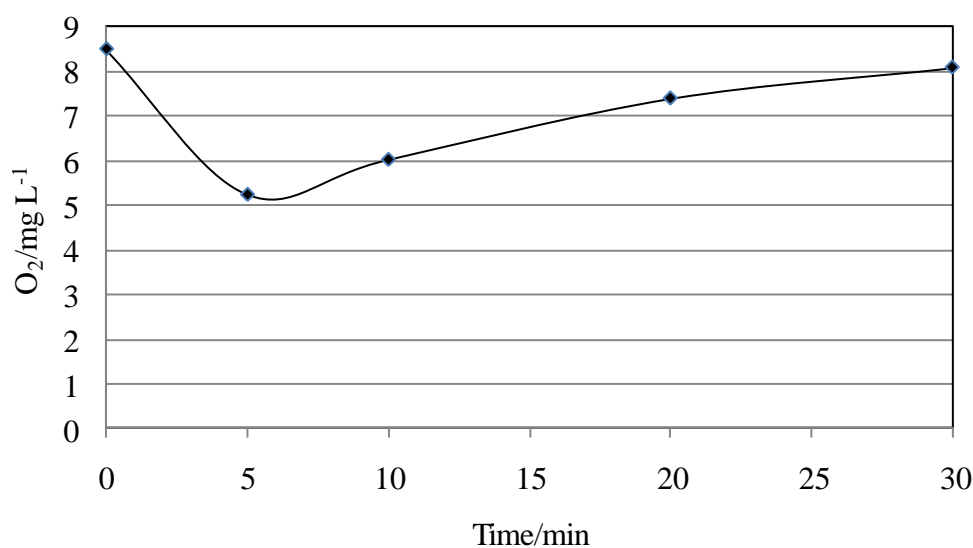


Figure 19: Plot of the oxygen concentration versus irradiation time during recirculation of a DCA containing TiO₂ suspension through the spiral glass reactor. *Experimental conditions:* as given in the legend of Fig. 17.

When 1000 mL of a DCA-containing Evonik Aeroxid P25 suspension was used in the photocatalytic runs under otherwise unchanged experimental conditions the TOC decreased from initially 22.05 mg L⁻¹ to a value of 6.41 mg L⁻¹ within 30 minutes of UV-A irradiation corresponding with a conversion of 71% of the initially present DCA (Fig 22). Again, a decrease of the oxygen concentration from a starting concentration of 9.55 mg L⁻¹ to a minimum value of 6.91 mg L⁻¹ during the first 10 minutes under UV-A irradiation was observed (Fig. 23). Subsequently, the oxygen concentration increased again reaching a value of 9.0 mg L⁻¹ after 30 minutes from the start of the experimental run.

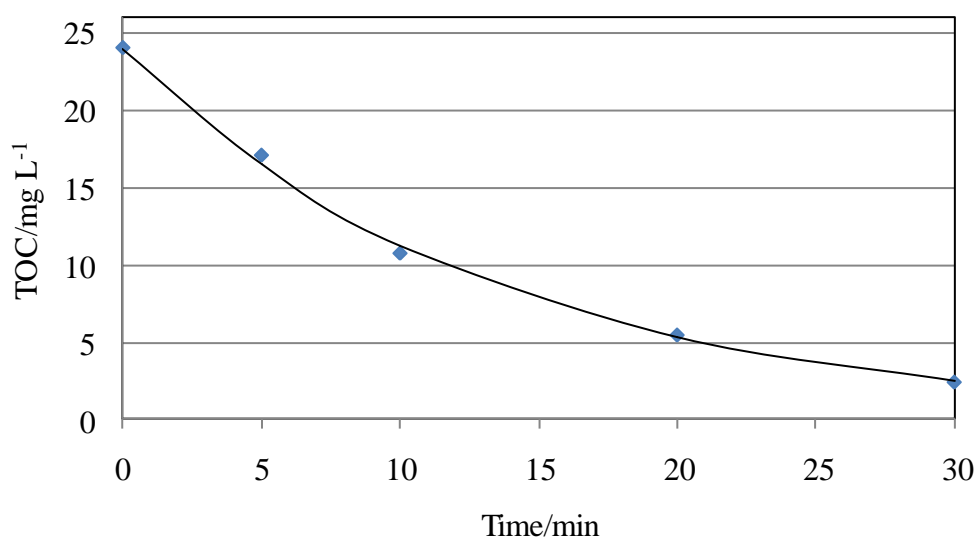


Figure 20: Plot of TOC versus irradiation time during recirculation of a DCA containing TiO_2 suspension through the spiral glass reactor. *Experimental conditions:* $c_{\text{DCA},0} = 1 \text{ mM}$, Evonik Aeroxide P25, $c_{\text{cat}} = 3.0 \text{ g L}^{-1}$, pH 3.0, $V = 500 \text{ mL}$, $F = 105 \pm 2 \text{ L h}^{-1}$, $I_{\text{hv}} = 28 \text{ W m}^{-2}$, $T = 21 \pm 1^\circ\text{C}$.

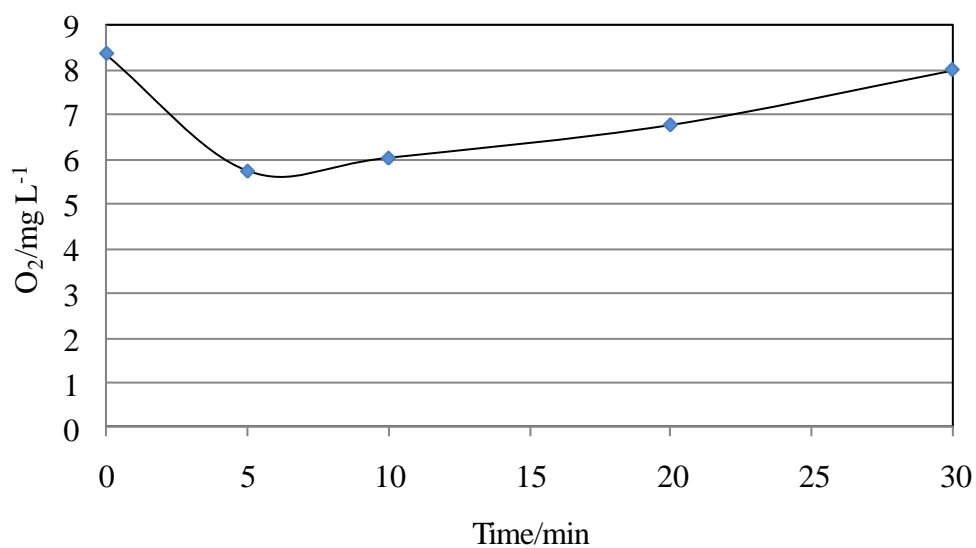


Figure 21: Plot of the oxygen concentration versus irradiation time during recirculation of a DCA containing TiO_2 suspension through the spiral glass reactor. *Experimental conditions:* as given in the legend of Fig. 20.

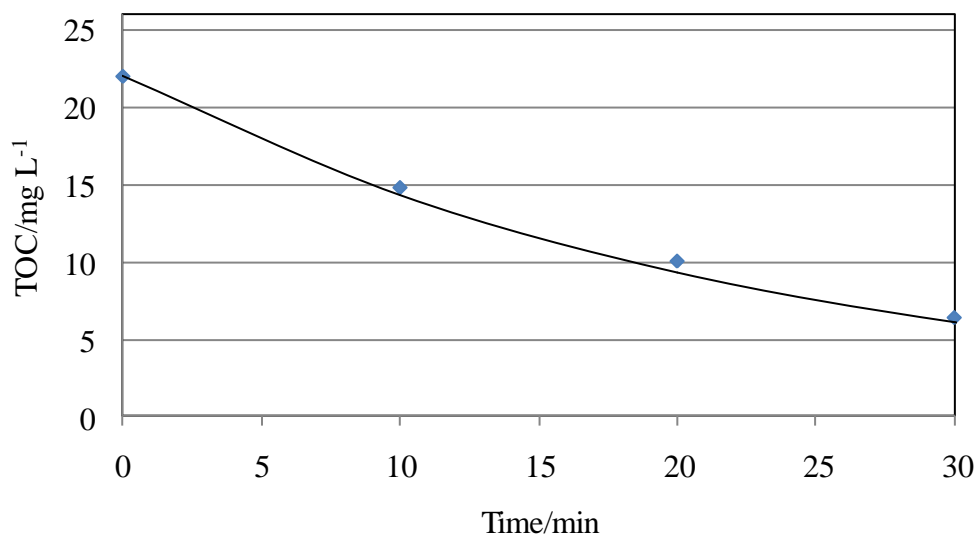


Figure 22: Plot of TOC versus irradiation time during recirculation of a DCA containing TiO_2 suspension through the spiral glass reactor. *Experimental conditions:* $c_{\text{DCA},0} = 1 \text{ mM}$, Evonik Aeroxide P25, $c_{\text{cat}} = 3.0 \text{ g L}^{-1}$, pH 3.0, $V = 1000 \text{ mL}$, $F = 105 \pm 2 \text{ L h}^{-1}$, $I_{\text{hv}} = 28 \text{ W m}^{-2}$, $T = 21 \pm 1^\circ\text{C}$.

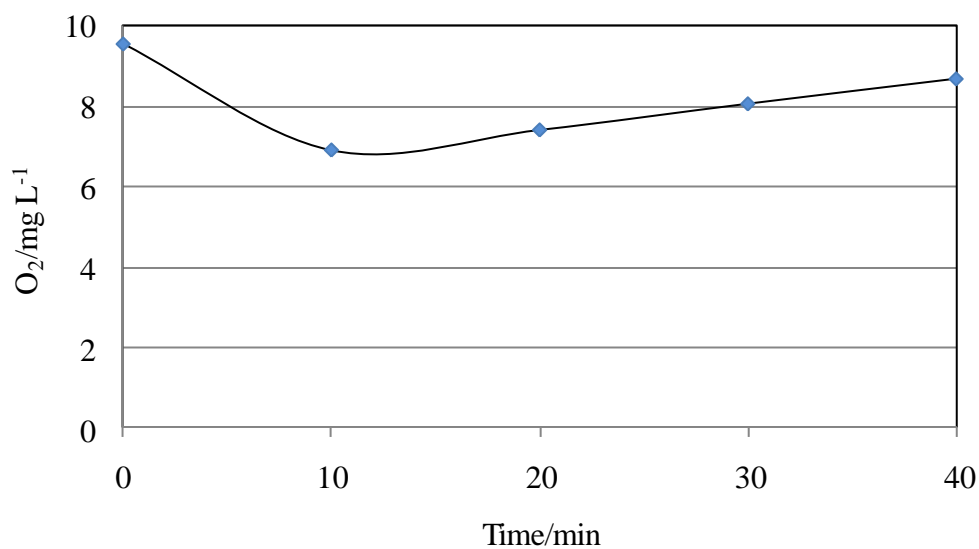


Figure 23: Plot of the oxygen concentration versus irradiation time during recirculation of a DCA containing TiO_2 suspension through the spiral glass reactor. *Experimental conditions:* as given in the legend of Fig. 22.

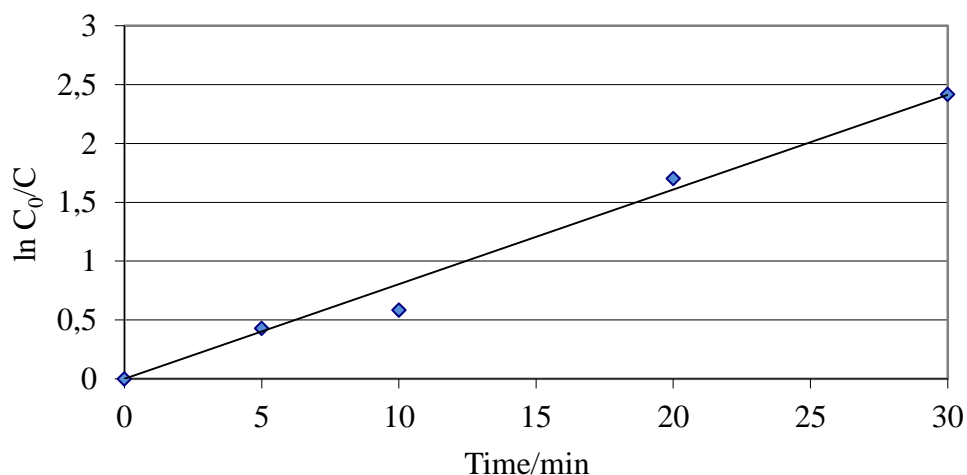


Figure 24: Logarithmic plot of the normalized DCA concentration versus irradiation time during recirculation of 500 mL DCA-containing Hombikat UV100 suspension through the spiral glass reactor. Correlation coefficient of the regression line: $R^2 = 0.9856$. *Experimental conditions:* as given in the legend of Fig. 17.

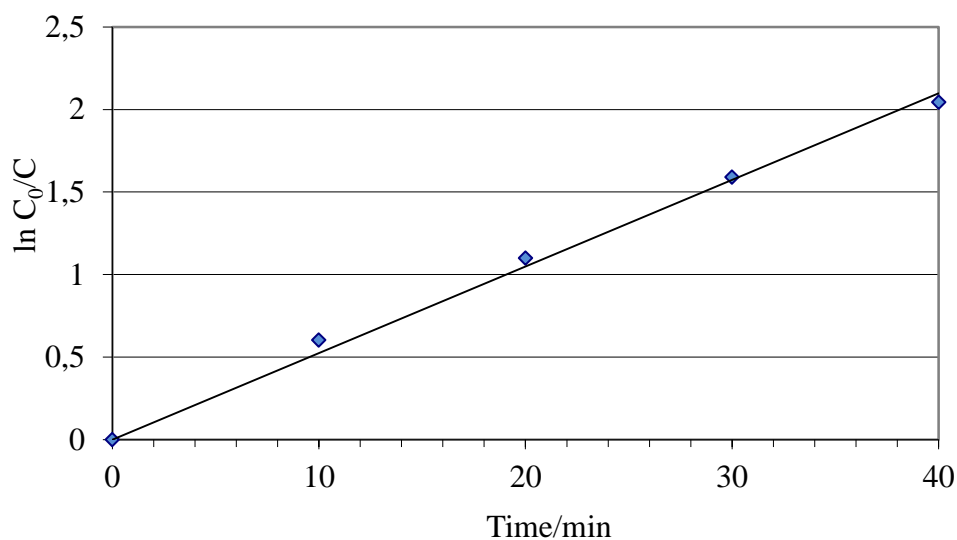


Figure 25: Logarithmic plot of the normalized DCA concentration versus irradiation time during circulation of 1000 mL DCA-containing Hombikat UV100 suspension through the spiral glass reactor. Correlation coefficient of the regression line: $R^2 = 0.9955$. *Experimental conditions:* as given in the legend of Fig. 18.

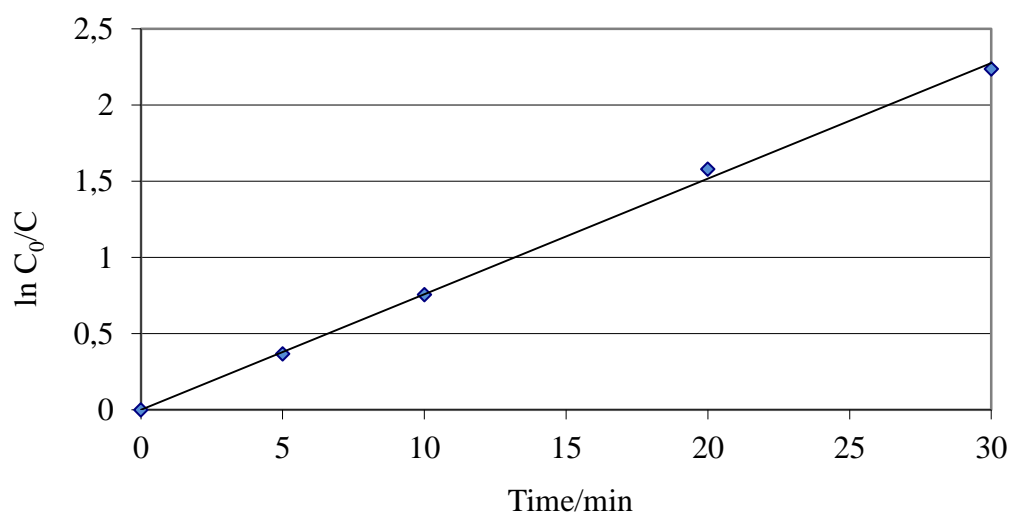


Figure 26: Logarithmic plot of the normalized DCA concentration versus irradiation time during recirculation of 500 mL DCA-containing Evonik Aeroxide P25 suspension in the spiral glass reactor. Correlation coefficient of the regression line: $R^2=0.9983$. *Experimental conditions:* as given in the legend of Fig. 20.

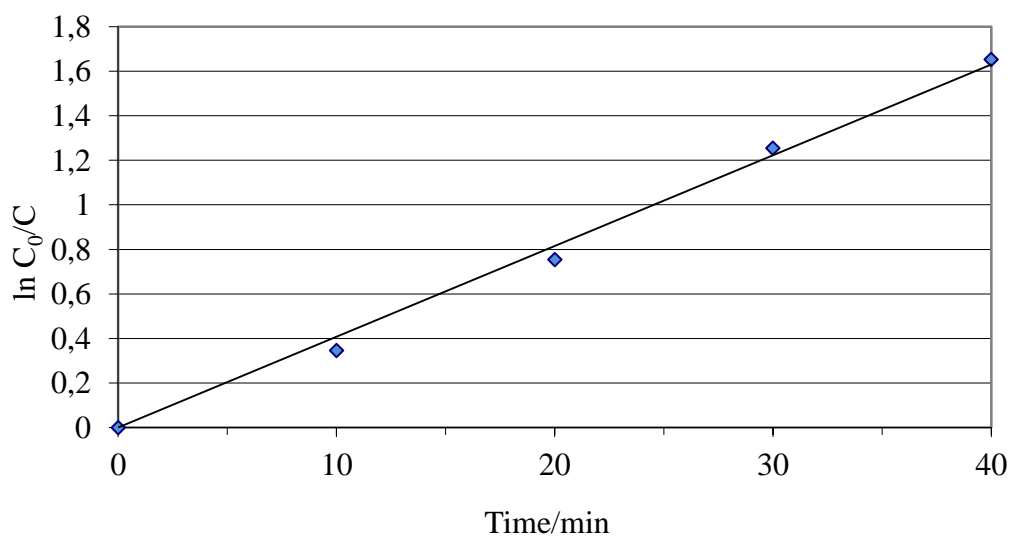


Figure 27: Logarithmic plot of the normalized DCA concentration versus irradiation time during recirculation of 1000 mL DCA-containing Evonik Aeroxide P25 suspension in the spiral glass reactor. Correlation coefficient of the regression line: $R^2=0.9950$. *Experimental conditions:* as given in the legend of Fig. 22.

A kinetic analysis of the experimental data was performed by plotting the logarithm of the normalized DCA concentration c_0/c (which is equivalent to the normalized TOC, TOC_0/TOC) versus the irradiation time (Figures 24 to 27). As can be seen from these figures a linear correlation between $\ln(c_0/c)$ and the irradiation time t is observed in all cases having correlation coefficients $R^2 > 0.98$. Therefore, the photocatalytic degradation of DCA in aqueous suspension circulating through a spiral glass reactor can be described by a first-order kinetic with a first-order rate constant k given by the slope of the regression line of the $(\ln(c_0/c), t)$ data. By multiplication of the obtained rate constant k with the initial DCA concentration c_0 of the experimental run under consideration the initial reaction rate $r_0 = k \cdot c_0$ can be calculated.

To compare different photocatalytic experiments the photonic efficiency ζ has been defined as the ratio of the number of substrate molecules reacted to the total number of photons during the reaction period (Serpone et al., 1993) and can be calculated as the ratio of the reaction rate to the incoming photon flux (Eq. 32):

$$\zeta = \frac{dc/dt}{d[\text{Photons}]/dt} \quad (32)$$

Using this approach the initial photonic efficiency ζ_0 is given by

$$\zeta_0 = \frac{r_0}{d[\text{Photons}]/dt} = \frac{kc_0}{d[\text{Photons}]/dt} \quad (33)$$

The calculated rate constants, initial reaction rates, and initial photonic efficiencies for the experimental runs performed with DCA-containing TiO_2 suspensions in the spiral glass reactor are presented in Table 6. All experimental runs have been repeated three times to insure the repeatability of the experimental set-up. As can be seen from this Table the deviation of the rate constants from their respective mean values is always smaller than 7% indicating a fairly good reproducibility of the experiments in the chosen experimental set-up.

Table 6: Calculated reaction rate constants k , initial degradation rates r_0 , and initial photonic efficiencies ζ_0 of the photocatalytic DCA degradation in TiO_2 suspensions employing the spiral glass reactor.

photocatalyst	V / mL	c_0 / mM	k / min^{-1}	r_0 / $\mu\text{M min}^{-1}$	ζ_0 /%
Hombikat UV 100	500	1.00	0.084	84.4	13.3
		1.00	0.081	80.8	12.7
		1.00	0.092	91.6	14.4
	1000	1.05	0.054	57.0	18.0
		1.03	0.058	59.5	18.8
		1.03	0.060	61.3	19.4
Aeroxide P25	500	1.00	0.076	75.7	11.9
		1.00	0.080	80.4	12.7
		1.00	0.080	80.4	12.7
	1000	0.94	0.044	41.0	12.9
		0.92	0.043	39.5	12.4
		0.92	0.040	36.4	12.4

To check whether the reactor design presented here is suitable for the treatment of real wastewater test have been performed with polluted water supplied by different companies (Delta, Solvay and other). As one example experimental results obtained with a highly polluted wastewater from Solvay is presented here. 250 ml of this wastewater was mixed with the photocatalyst Evonik Aeroxide P25 resulting in a catalyst concentration of 4.0 g L^{-1} . Then the suspension was poured into the glass reactor and irradiated for 7 hours with UV-A light (28 W m^{-2}). The change of the TOC and the COD during this time is plotted in the Figures 28 and 29. A reduction of the TOC from initially 1476 mg L^{-1} to 1140 mg L^{-1} within 420 minutes and a reduction of the COD from initially $5400 \text{ mg O}_2 \text{ L}^{-1}$ to $3500 \text{ mg O}_2 \text{ L}^{-1}$ within 420 minutes was observed under UV(A)-irradiation of the suspension circulating through the reactor with a flow rate of 105 L h^{-1} .

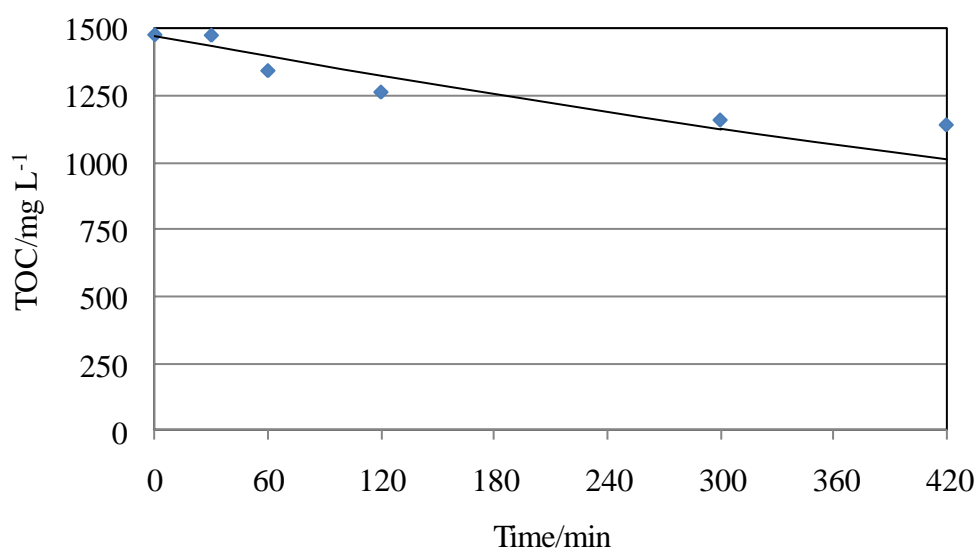


Figure 28: Plot of TOC versus irradiation time during circulation of a wastewater (Solway) containing Evonik Aeroxide P25 through the spiral glass reactor.
Experimental conditions: $c_{\text{cat}} = 4.0 \text{ g L}^{-1}$, natural pH, $V = 250 \text{ mL}$, $F = 105 \pm 2 \text{ L h}^{-1}$, $I_{\text{hv}} = 28 \text{ W m}^{-2}$, $T = 21 \pm 1 \text{ }^\circ\text{C}$.

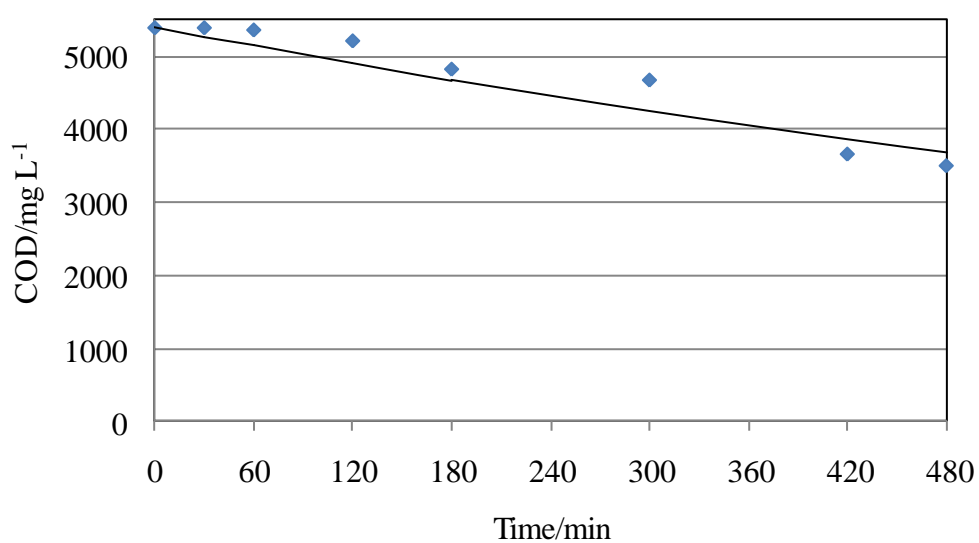


Figure 29: Plot of COD versus irradiation time during circulation of a wastewater (Solway) containing Evonik Aeroxide P25 through the spiral glass reactor.
Experimental conditions: as given in the legend of Fig. 28.

4.1.3 The spiral glass reactor with a photocatalytic coating

To overcome the restrictions in wastewater treatment associated with the use of photocatalyst suspensions (cf. Chapter 2.4.1) the inside wall of the spiral shape glass reactor was coated with TiO₂ employing a sol-gel technique that has been developed by Bahnemann and co-authors. (Hidalgo et al., 2004). Dichloroacetic acid was used as a model compound to assess the activity of this support concept. The decrease of the TOC was monitored under irradiation with UV(A)-light in order to determine the activity of the reactor. The change of TOC with irradiation time of a typical experimental run is presented in Figure 30. As can be seen from this Figure the TOC of the aqueous DCA solution decreased from 24.24 to 9.31 mg L⁻¹ within 420 minutes of UV-A irradiation which is equal to a 62% reduction of the DCA initially present in the solution. The plot of the logarithm of the normalized pollutant concentration versus the irradiation time (Fig. 31) shows a linear dependence indicating that also in this case the photocatalytic mineralization of DCA can be described by a first order kinetics.

The calculated reaction rate constants k , initial degradation rates r_0 , and initial photonic efficiencies ζ_0 of three repetitive experimental runs of the photocatalytic DCA degradation in the coated spiral glass reactor are presented in Table 7.

Table 7: Calculated reaction rate constants k , initial degradation rates r_0 , and initial photonic efficiencies ζ_0 of the photocatalytic DCA degradation employing the spiral glass reactor with a photocatalytic coating.

c_0 / mM	k / min^{-1}	$r_0 / \mu\text{M min}^{-1}$	$\zeta_0 / \%$
1.01	0.002	2.0	0.6
0.89	0.002	1.8	0.6
1.04	0.002	2.2	0.7

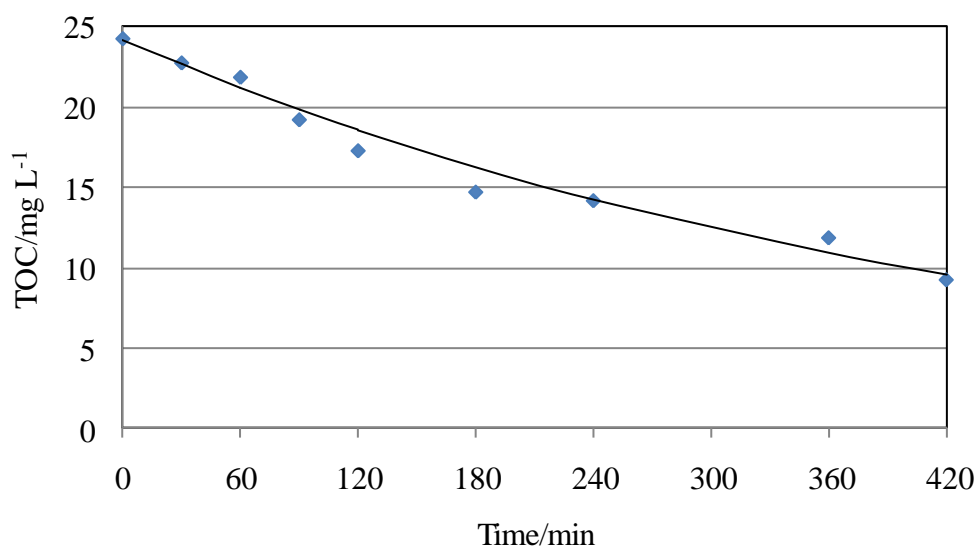


Figure 30: Plot of TOC versus irradiation time during recirculation of a DCA solution through the TiO₂ coated spiral glass reactor. *Experimental conditions:* $c_{\text{DCA},0} = 1 \text{ mM}$, pH 3.0, $V = 1000 \text{ mL}$, $F = 105 \text{ L h}^{-1}$, $I_{\text{hv}} = 30 \text{ W m}^{-2}$, $T = 21 \pm 1^\circ\text{C}$.

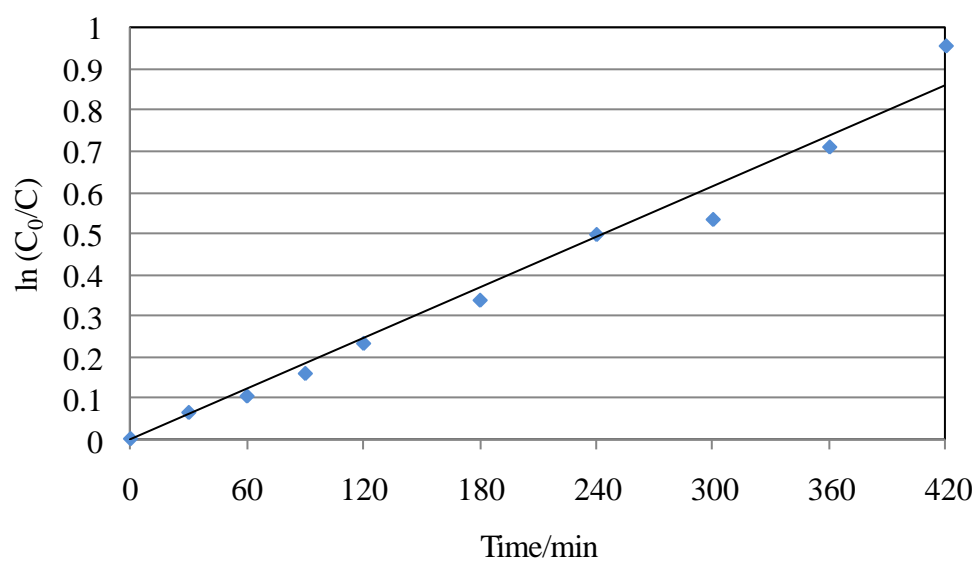


Figure 31: Logarithmic plot of the normalized DCA concentration versus irradiation time during recirculation of a DCA solution through the TiO₂ coated spiral glass reactor. Correlation coefficient of the regression line: $R^2=0.9784$. *Experimental conditions:* as given in the legend of Fig. 30.

The comparison of the values presented in this Table with the data tabulated in Table 7 shows that the coated spiral glass reactor has a much lower photonic efficiency than the spiral glass reactor charged with a polluted TiO₂ suspension. Attempts to increase the photocatalytic activity by using other formulations for the coating sol were not successful (data not shown).

4.1.4 The spiral glass reactor packed with photocatalyst pellets

Since the coated spiral glass reactor was found to be substantially less effective than the spiral glass reactor charged with a polluted TiO₂ suspension another approach was investigated to overcome the restrictions due to the use of photocatalyst suspensions. The spiral glass reactor was filled with a bed of BASF TiO₂ pellets having the dimensions of 3 mm · 3 mm (cf. Fig. 8).

In typical experimental runs 1000 ml of a DCA solution ($c_{\text{DCA},0} = 1\text{mM}$) was circulated through the packed photoreactor with a flow rate of $8 \pm 2 \text{ L h}^{-1}$ by means of a membrane pump. This flow rate corresponds to a residence time of 1.9 minutes.

The TOC values measured in regular time intervals during UV-A irradiation of the photocatalytic reactor are plotted versus the irradiation time in Figure 32. In a typical experimental run a 96% decrease of the TOC to a final concentration of 1.02 mg L^{-1} was observed within 90 minutes of UV-A irradiation of 1000 mL of a solution containing 1 mM DCA.

The kinetic analysis of the experimental data revealed that the mineralization of DCA in this packed spiral glass photoreactor followed a first order kinetics. The calculated reaction rate constants k , initial degradation rates r_0 , and initial photonic efficiencies ζ_0 of three repetitive experimental runs are presented in Table 8. The comparison of the values presented in this Table with the respective data tabulated in Table 6 for the spiral glass reactor charged with a polluted TiO₂ suspension shows that the packed

spiral glass reactor has a photonic efficiency being approximately one third lower than the identical suspension reactor.

Table 8: Calculated reaction rate constants k , initial degradation rates r_0 , and initial photonic efficiencies ζ_0 of the photocatalytic DCA degradation employing the spiral glass reactor packed with photocatalyst pellets.

c_0 / mM	k / min^{-1}	$r_0 / \mu\text{M min}^{-1}$	$\zeta_0 / \%$
1.00	0.055	55.4	8.7
1.02	0.052	53.2	8.4
1.05	0.045	46.8	7.4

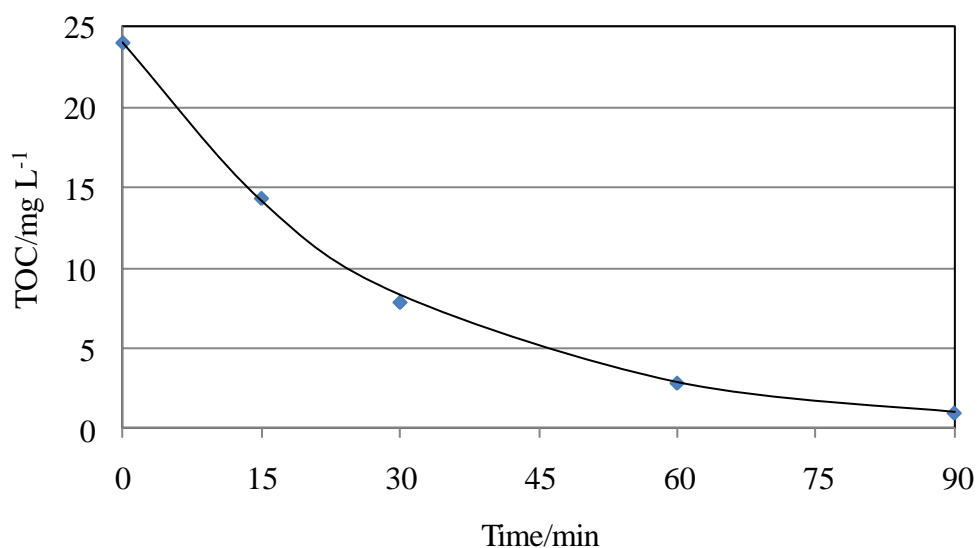


Figure 32: Plot of TOC versus irradiation time during recirculation of a DCA solution through the spiral glass reactor containing catalyst pellets. *Experimental conditions:* $c_{\text{DCA},0} = 1 \text{ mM}$, BASF catalyst pellets $3 \text{ mm} \cdot 3 \text{ mm}$, pH 3.0, $V = 500 \text{ mL}$, $F = 8 \pm 2 \text{ L h}^{-1}$, $I_{\text{hv}} = 28 \text{ W m}^{-2}$, $T = 21 \pm 1^\circ\text{C}$.

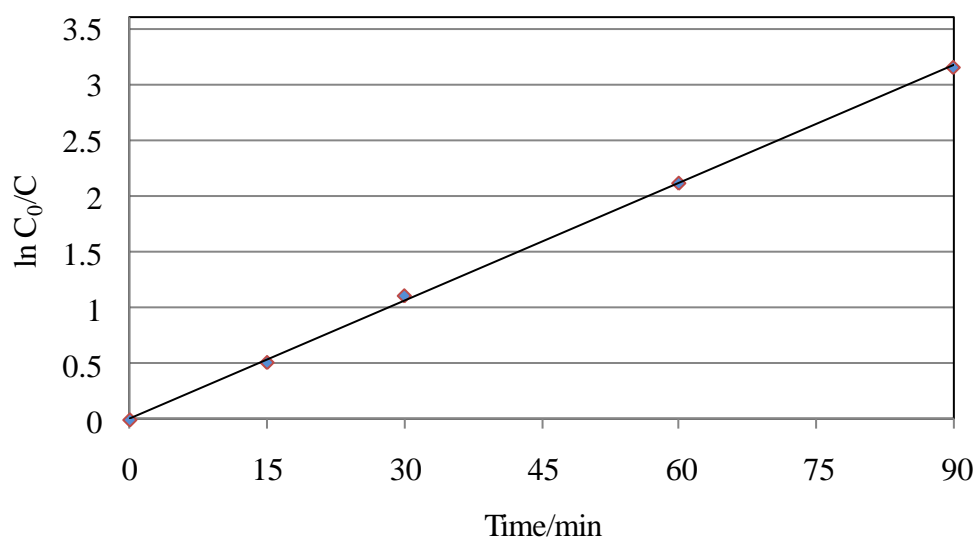


Figure 33: Logarithmic plot of the normalized DCA concentration versus irradiation time during recirculation of a DCA solution through the spiral glass reactor containing catalyst pellets. Correlation coefficient of the regression line: $R^2=0.999$. *Experimental conditions:* as given in the legend of Fig. 32.

Applying the same reactor for real wastewater treatment, 400 ml of wastewater from Solvay were circulated in the spiral glass packed reactor without adjusting of pH of the sample which was 11.2, the sample circulated for 30 minutes in the dark. A reduction of TOC from 1486 to 1075 mg L⁻¹ was observed and that was due to the dark adsorption, which represents about 27% of reduction due to adsorption. Then the illumination started. In Figure 34 the TOC versus irradiation time is plotted. The first sample taken after 200 minutes of UV-A irradiation had a TOC content of 707 mg L⁻¹ associated with reduction of pH to 7.92. Another sample taken after 270 minutes of irradiation had a TOC of 692 mg L⁻¹ and the pH was 7.78.

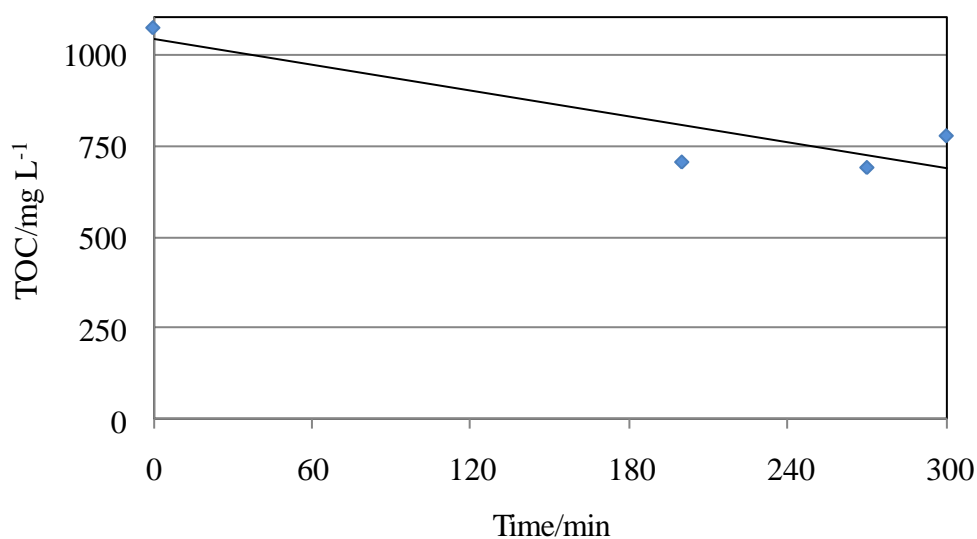


Figure 34: Plot of TOC versus irradiation time during recirculation of a wastewater (Solway) through the spiral glass packed reactor containing catalyst pellets. *Experimental conditions:* BASF catalyst pellets 3 mm · 3 mm, pH 3.0, V = 400 mL, F = 6 L h⁻¹, I_{hv} = 28 W m⁻², T = 21±1°C

4.2 The pan reactor with photocatalyst pellets

The sufficient high activity of the photocatalytically active TiO₂ pellets encouraged the determination of the activity of this photocatalyst in other types of photoreactors which are expected to be more suitable for applications in solar wastewater treatment than the spiral glass reactor. The simplest design of a solar-driven photocatalytic reactor is a basin containing the polluted water in contact with the photocatalyst. Therefore, a pan reactor was filled with 5 mm · 5 mm BASF TiO₂ pellet photocatalyst as described in Chapter 3.2.5 and the amount of a 1 mM DCA solution necessary to cover the photocatalyst bed (500 – 1000 mL). The pan was left without movement during the experimental run.

Before exposing the pan reactor to the UV-light the DCA solution in contact with the pellets was left for 48 hours in the dark to determine the quantity of DCA

disappearing by adsorption. It was found that only 3% DCA has disappeared by dark adsorption at the photocatalyst surface. Considering the experimental error this amount is negligible.

The top of the pan was exposed to the UV light and the reduction of the DCA concentration was measured as TOC. Typical experimental data are presented in Figure 34 for two different amounts of DCA (34 and 64 mg L⁻¹ organic carbon). Employing a small solution volume and a low initial DCA concentration a rapid decrease of the TOC decreases from 34.0 to 4.69 mg L⁻¹ within 240 minutes was observed (86% conversion). If a higher DCA concentration (TOC₀ = 64.4 mg L⁻¹) and a larger volume of the solution (V = 1000 mL) is subjected to this treatment only 64% of the initially present DCA is mineralized under otherwise identical experimental conditions.

The kinetic analysis of the experimental data revealed that the light-induced mineralization of DCA in this reactor configuration can be described by a first order kinetics (Figure 35). Calculated reaction rate constants k, initial degradation rates r₀, and initial photonic efficiencies ζ₀ for the experimental runs presented in Fig. 35 are tabulated in Table 9.

Table 9: Calculated reaction rate constants k, initial degradation rates r₀, and initial photonic efficiencies ζ₀ of the photocatalytic DCA degradation employing the pan reactor filled with photocatalyst pellets.

V / mL	c ₀ / mM	k / min ⁻¹	r ₀ / μM min ⁻¹	ζ ₀ /%
500	1.42	0.008	11.6	2.4
1000	2.68	0.002	6.4	2.6

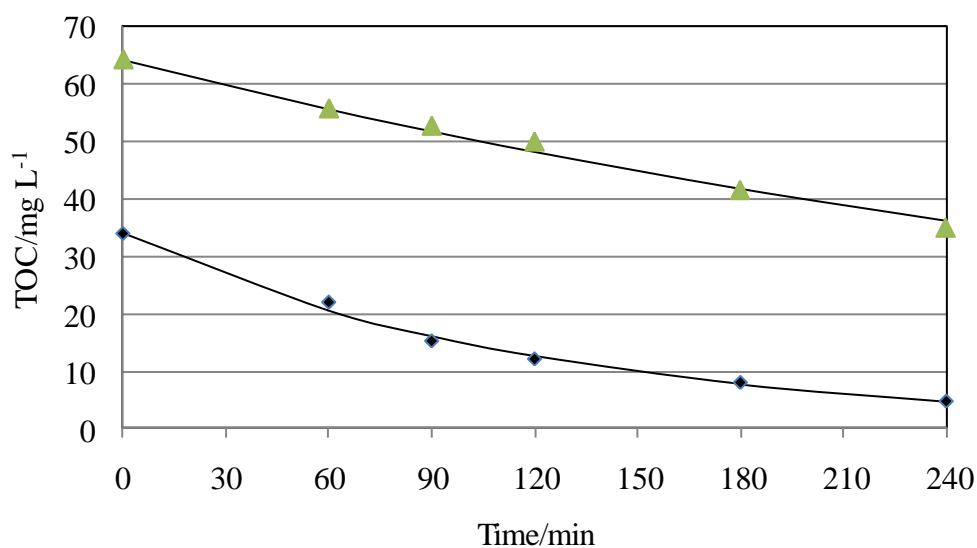


Figure 35: Plot of TOC versus irradiation time during treatment of a DCA solution in the pan reactor containing catalyst pellets. *Experimental conditions:* a) $\text{TOC}_0 = 34 \text{ mg L}^{-1}$, $V = 500 \text{ mL}$ (\blacklozenge), and b) $\text{TOC}_0 = 64 \text{ mg L}^{-1}$, $V = 1000 \text{ mL}$ (\blacktriangle); BASF catalyst pellets $5 \text{ mm} \cdot 5 \text{ mm}$, pH 3.0, $I_{\text{hv}} = 23 \text{ W m}^{-2}$, ambient T.

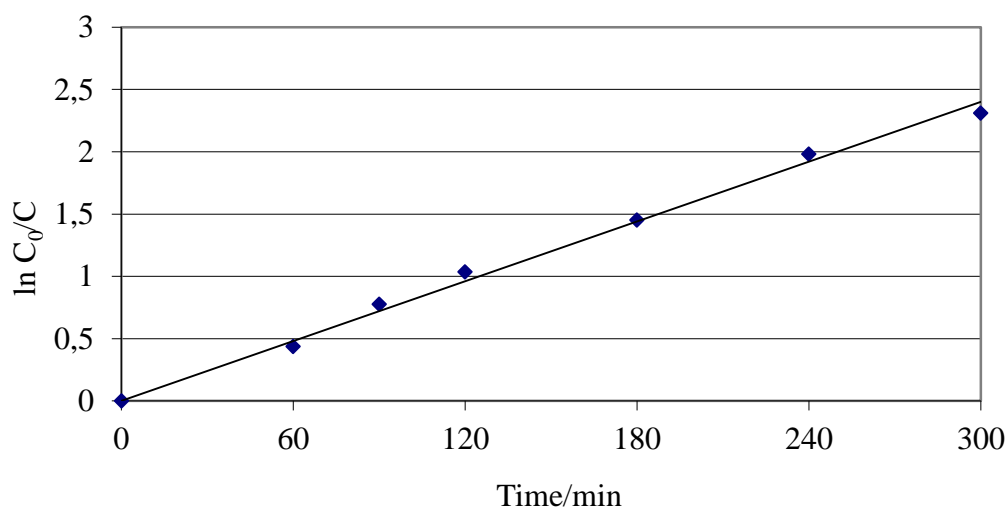


Figure 36: Logarithmic plot of the normalized DCA concentration versus irradiation time during treatment of a DCA in the pan reactor containing catalyst pellets. Correlation coefficient of the regression line: $R^2 = 0.9944$. *Experimental conditions:* $\text{TOC}_0 = 34 \text{ mg L}^{-1}$, BASF catalyst pellets $5 \text{ mm} \cdot 5 \text{ mm}$, pH 3.0, $V = 500 \text{ mL}$, $I_{\text{hv}} = 23 \text{ W m}^{-2}$, ambient T.

4.3 The flat packed reactor with photocatalyst pellets

While the pan reactor showed only low initial photonic efficiencies ($\zeta_0 \approx 2.5\%$; cf. Table 10) which is possibly due to mass transport limitations in this batch reactor the reactor concept was enhanced to the continuously charged flat packed reactor with 5 mm · 5 mm BASF TiO₂ pellets and equipped with a perforated tube to distribute the incoming aqueous DCA solution ($c_{\text{DCA},0} = 0.9 - 1.0$ mM) uniformly over the width of the reactor (see Figure 12 and 13). To measure the relationship between the DCA degradation rate and the flow rate F of the solution the flow rate was varied between 30 L h⁻¹ and 120 L h⁻¹. The TOC at the different flow rates were measured and recorded. Figure 36 illustrates the decrease of the TOC at the different flow rates.

During the experimental runs the temperature of the aqueous solution increased reaching values higher than 30°C within 1 hour of UV-A irradiation using a solar simulator.

The kinetic analysis of the experimental data revealed a first order kinetic for the photocatalytic DCA degradation under the experimental conditions of this study. The calculated reaction rate constants k , initial degradation rates r_0 , and initial photonic efficiencies ζ_0 obtained with the flat packed reactor containing BASF TiO₂ pellets are given in Table 10. Photonic efficiencies nearly as high as those found with BASF TiO₂ pellets inside the spiral glass reactor (cf. Table 8) were obtained.

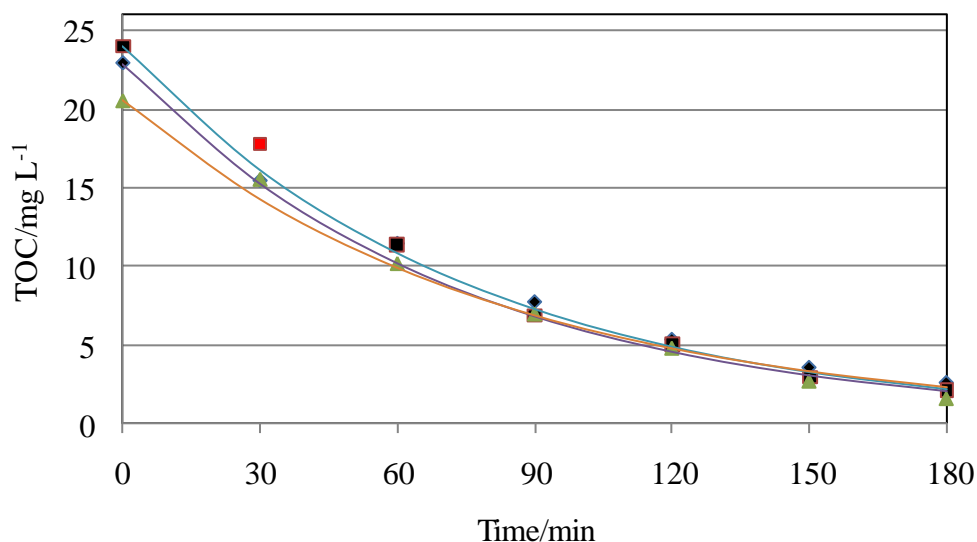


Figure 37: Plot of TOC versus irradiation time during recirculation of a DCA solution through the flat packed reactor containing catalyst pellets. *Experimental conditions:* $c_{\text{DCA},0} = 1 \text{ mM}$, BASF catalyst pellets $5 \text{ mm} \cdot 5 \text{ mm}$, pH 3.0, $V = 2000 \text{ mL}$, $F = 30$ (\blacklozenge), 60 (\blacksquare), and 120 L h^{-1} (\blacktriangle), $I_{\text{hv}} = 33.6 \text{ W m}^{-2}$, no control of T.

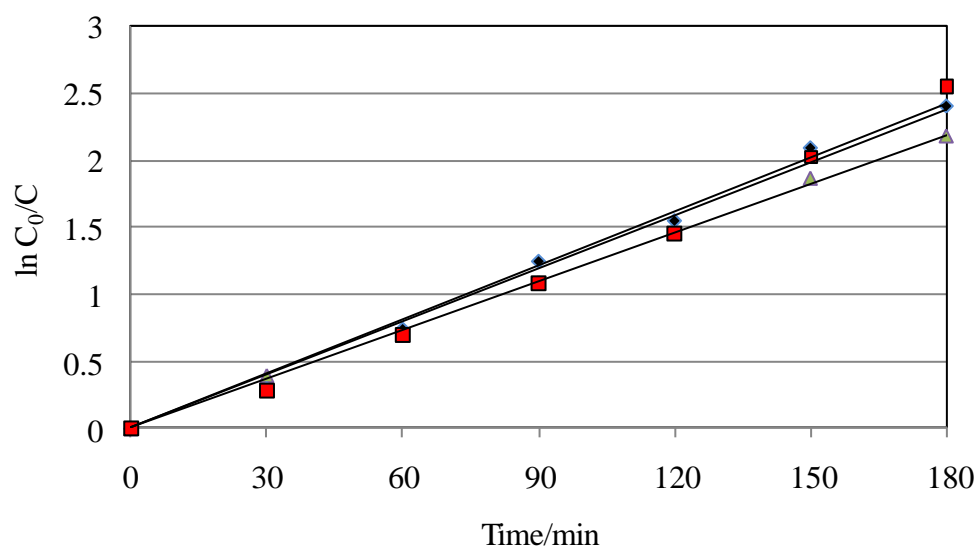


Figure 38: Logarithmic plot of the normalized DCA concentration versus irradiation time during recirculation of a DCA solution through the flat packed reactor containing catalyst pellets. Correlation coefficient of the regression line: $R^2=0.999$. *Experimental conditions:* as given in the legend of Fig. 36.

Table 10: Calculated reaction rate constants k , initial degradation rates r_0 , and initial photonic efficiencies ζ_0 of the photocatalytic DCA degradation employing the flat packed reactor containing photocatalyst pellets.

$F / \text{L h}^{-1}$	c_0 / mM	k / min^{-1}	$r_0 / \mu\text{M min}^{-1}$	$\zeta_0 / \%$
30	0.95	0.013	12.6	6.6
60	1.00	0.014	13.5	7.0
120	0.86	0.012	10.5	5.5

4.4 The tubular reactor packed with photocatalyst pellets

When the flat packed reactor was employed outdoor (data not shown), it was directly subjected to sunlight. As an unintended consequence, a substantial amount of the solution was lost by evaporation. Therefore, an open solar-driven photocatalytic reactor as the pan reactor and the flat packed reactor seems not to be suitable for photocatalytic water treatment in warmer countries like Libya. A closed photocatalytic reactor system like the tubular reactor described in Chapter 3.2.7 was considered.

The photocatalytic degradation of DCA in was investigated employing a tubular reactor with an irradiated surface area of 0.043 m^2 filled with BASF photocatalyst pellets ($3 \text{ mm} \cdot 3 \text{ mm}$). A volume of 1000 mL of an air-purged DCA solution ($c_0 = 1 \text{ mM}$) was circulating through the photoreactor with a flow rate $F = 18 \text{ L h}^{-1}$) by means of a membrane pump resulting in a residence time inside the photoreactor of 0.72 min.

For a typical experimental run the TOC values measured during irradiation of the photoreactor with simulated solar light ($I_{\text{hv}} = 33.6 \text{ W m}^{-2}$) are plotted versus the irradiation time in Figure 38. As can be seen from this Figures the TOC of the suspensions decreased within 120 minutes of UV-A irradiation from 22.9 to 3.43 mg L^{-1} , clearly indicating the photocatalytic mineralization of the probe molecule. This decrease of the TOC value corresponds to a conversion of 85% of the initially present DCA.

During the experimental runs the temperature of the aqueous solution increased reaching values higher than 30°C in less than 1 hour of UV-A irradiation using a solar simulator.

The logarithmic plots of the normalized DCA concentration versus irradiation time during recirculation of a DCA solution through the tubular reactor containing catalyst pellets always showed a linear dependence of $\ln(c_0/c)$ on the irradiation time t with correlation coefficient (R^2) of the regression line being > 0.99 .

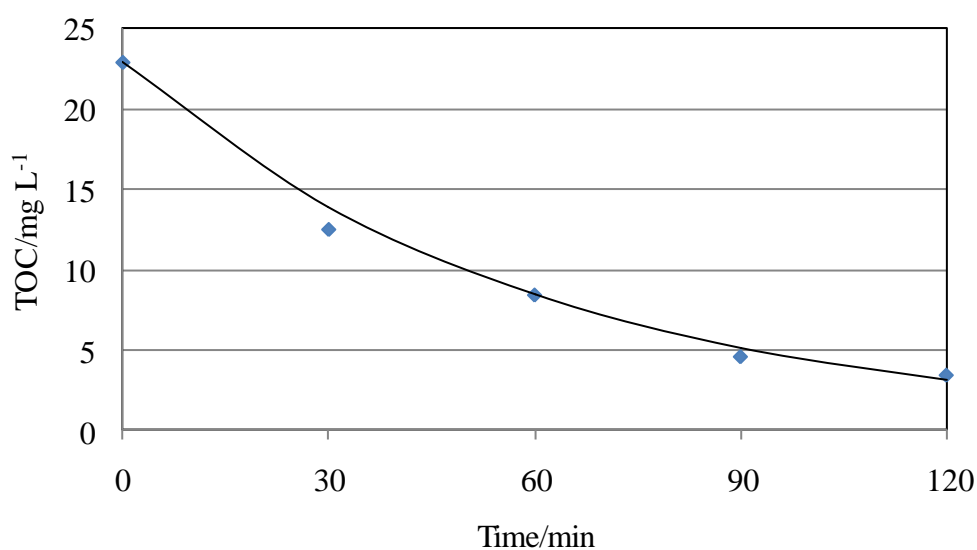


Figure 39: Plot of TOC versus irradiation time during recirculation of a DCA solution through the tubular reactor containing catalyst pellets. *Experimental conditions:* $c_{\text{DCA},0} = 1 \text{ mM}$, BASF catalyst pellets $3 \text{ mm} \cdot 3 \text{ mm}$, pH 3.0, $V = 1000 \text{ mL}$, $F = 18 \text{ L h}^{-1}$, $I_{\text{hv}} = 33.6 \text{ W m}^{-2}$, no control of T (start: $T = 21 \pm 1^\circ\text{C}$).

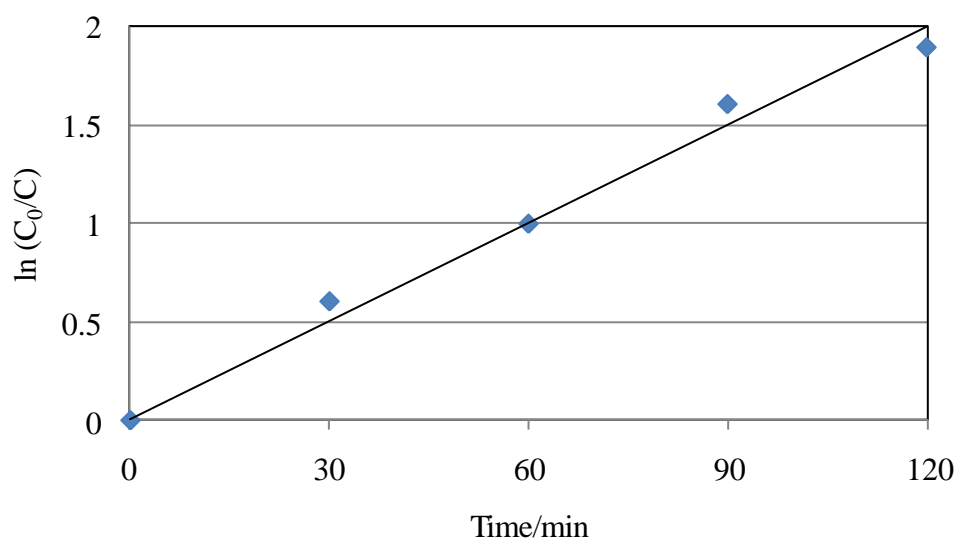


Figure 40: Logarithmic plot of the normalized DCA concentration versus irradiation time during recirculation of a DCA solution through the tubular reactor containing catalyst pellets. Correlation coefficient of the regression line: $R^2=0.986$.
Experimental conditions: as given in the legend of Fig. 39.

The calculated reaction rate constants k , initial degradation rates r_0 , and initial photonic efficiencies ζ_0 of three repetitive experimental runs are presented in Table 11. The comparison of the values presented in this Table with the respective data tabulated in Table 8 for the spiral glass reactor packed with BASF photocatalyst pellets shows that the tubular reactor containing the same photocatalyst has a photonic efficiency being approximately 25% lower than the former.

Figure 40 shows the change of the TOC during irradiation of a DCA solution circulating through the packed tubular reactor with natural sunlight light. The TOC decreased from initially 22.45 mg L^{-1} to 0.5 mg L^{-1} within 300 minutes. In 120 minutes of irradiation a 59% conversion of the DCA initially present in the solution was observed.

Table 11: Calculated reaction rate constants k , initial degradation rates r_0 , and initial photonic efficiencies ζ_0 of the photocatalytic DCA degradation employing the tubular reactor containing photocatalyst pellets.

c_0 / mM	k / min^{-1}	$r_0 / \mu\text{M min}^{-1}$	$\zeta_0 / \%$
1.04	0.017	17.5	6.6
0.95	0.017	15.9	6.0
0.93	0.017	16.0	6.1

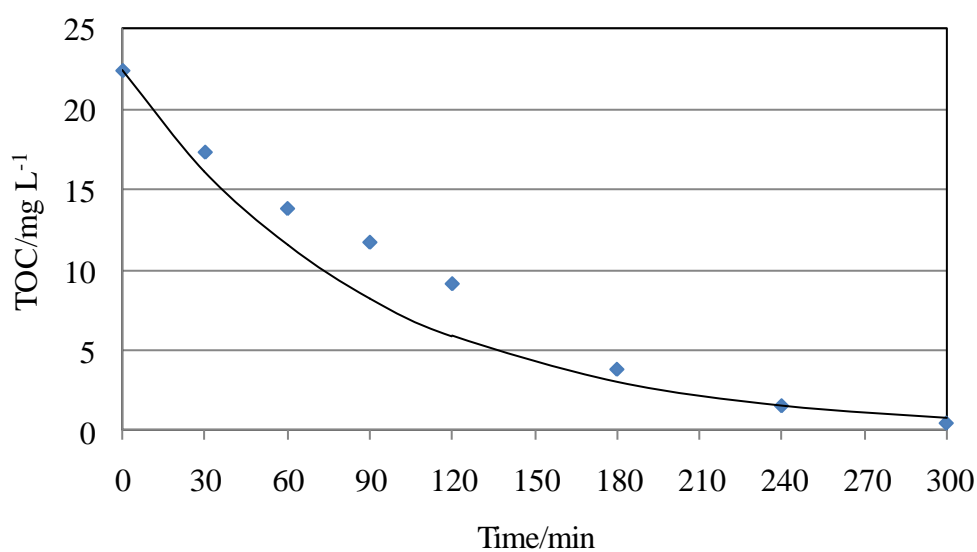


Figure 41: Plot of TOC versus irradiation time during recirculation of a DCA solution through the tubular reactor containing catalyst pellets. *Experimental conditions:* $c_{\text{DCA},0} = 1 \text{ mM}$, BASF catalyst pellets $3 \text{ mm} \cdot 3 \text{ mm}$, pH 3.0, $V = 1000 \text{ mL}$, $F = 18 \text{ L h}^{-1}$, direct solar light, ambient T.

5 Discussion

5.1 Introductory remarks

The objective of this work is the development of a simple photocatalytic reactor suitable for the treatment of small quantities of polluted water in rural areas of North Africa.

Therefore, different types of TiO₂ photocatalysts (suspensions, thin film, and pellets) in different types of photocatalytic reactors, *i. e.*, spiral reactor, pan reactor, flat packed reactor and tubular packed reactor, have been studied. An overview over the different combinations of photocatalyst type and phototocatalytic reactor studied is presented in Table 12.

Table 12: Overview over the combinations of photocatalyst type and phototocatalytic reactor studied in this thesis.

Type	Photocatalyst	Photoreactor			
		Spiral	Pan	Flat packed	Tubular
Suspension	Hombikat UV 100	X			
	Aeroxide P25	X			
Coated	Sol – Gel	X			
Pellet	BASF	X	X	X	X

To determine the effectiveness of the respective combination of photocatalyst and photocatalytic reactor for the photocatalytic treatment of polluted water dichloroacetic acid (DCA) was chosen as the model pollutant due to its water-solubility and easy monitoring by TOC measurements. In all combinations of photocatalyst type and photocatalytic reactor studied here the mineralization of DCA according to



was observed during irradiation with UV-A light, while no reaction occurred in the dark or in the absence of a photocatalyst. The kinetic analysis of the experimental data was performed by plotting the logarithm of the normalized DCA concentration c_0/c (which is equivalent to the normalized TOC: TOC_0/TOC) versus the irradiation time. In all experimental runs performed in this work a linear correlation between $\ln(c_0/c)$ and the irradiation time t having correlation coefficients $R^2 > 0.98$ was observed indicating that the decay of the concentration of the probe molecule during UV-A irradiation in the presence of a photocatalyst can be described by a first order rate law

$$r = k \cdot c \quad (35)$$

As has been mentioned in Chapter 2.3 this is a special case of a more general rate law usually observed when low concentrations of organic compounds dissolved in an aqueous phase are photocatalytically degraded. For the photocatalytic DCA degradation many authors have reported that the decay of the DCA concentration follows a first order kinetics at concentrations lower than 1 mM (Kandiel et al., 2010b; Ismail and Bahnemann, 2011).

The photocatalytic reactors employed in this work differ in their reactor volume V_R and in the irradiated surface area A_R . By technical reasons the intensities of the UV-A light used to irradiate the photocatalyst was different for the different combinations of photocatalyst type and photoreactor. Details concerning the illuminated reactor areas A_R and the reactor volumes V_R , the total volume V_S of the suspensions or solutions treated in each experiment, the average value of the initial concentrations $c_{0,m}$ of the pollutant, and the average values of the UV-A light intensities $I_{\text{hv},m}$ are presented in Table 13.

To compare different photocatalytic experiments the photonic efficiency ζ , defined as the ratio of the number of substrate molecules reacted to the total number of photons impinging the photocatalyst during the reaction period, is usually used (Serpone et al., 1993; Serpone and Salinaro, 1999)

$$\zeta = \frac{dc/dt}{d[\text{Photons}]/dt} \quad (24)$$

Table 13: Experimental data of the laboratory experiments of the photocatalytic degradation of DCA.

Type of photoreactor	Catalyst	V_R / 10^{-4} m^3	V_S / L	$c_{0,m}$ / mM	A_R / m^2	$I_{hv,m}$ / W m^{-2}	$\zeta_{0,m}$ / %
Spiral glass reactor	Suspension (Hobikat UV100)	3.14	0.5	1.00	0.0624	28.0	13.5
		3.14	1.0	1.04	0.0624	28.0	18.7
	Suspension (Aeroxide P25)	3.14	0.5	1.00	0.0624	28.0	12.4
		3.14	1.0	0.92	0.0624	28.0	12.6
Pan reactor	TiO ₂ -coated	3.14	1.0	0.98	0.0624	28.0	0.6
	BASF pellets 3 mm · 3 mm	3.14	0.5	1.02	0.0624	28.0	8.2
	BASF pellets 5 mm · 5 mm	5.00	0.5	1.42	0.0488	26.0	2.4
		10.00	1.0	2.68	0.0488	26.0	2.6
Flat packed reactor	BASF pellets 5 mm · 5 mm	4.62	2.0	0.94	0.0924	30.0	6.3
Tubular packed reactor	BASF pellets 3 mm · 3 mm	2.17	1.0	0.97	0.0434	33.6	6.2

In this work the initial photonic efficiency

$$\zeta_0 = \frac{V_S k c_0}{A_R I_{h\nu}} \times \frac{N_A h c_{h\nu}}{\lambda} \quad (36)$$

was calculated for all experimental runs for the purpose of comparison.

5.2 The spiral glass reactor

5.2.1 The spiral glass reactor with suspended photocatalyst

To get a benchmark for future experimental designs first experimental runs have been performed employing a spiral glass reactor continuously charged with aqueous DCA-containing TiO₂ suspensions. This photoreactor consisted of a borosilicate glass tube (4 m long, 10 mm outer diameter, and 8 mm internal diameter) wounded in turns of 6 cm diameter. The light source was centered in the axis of the reactor. The UV-A irradiated surface area was 0.0624 m². It has to be mentioned that this reactor design is scarcely suitable for solar applications.

The photocatalytic degradation of DCA ($c_0 = 1$ mM) in the spiral glass reactor was investigated in aqueous suspensions of two different types of suspended photocatalysts (Sachtleben Hombikat UV 100, and Evonik Aeroxide P25; $c_{\text{cat}} = 3$ g L⁻¹) at pH 3. The volume of the air-purged suspension circulating through the photoreactor was varied. The flow rate of the suspension through the photoreactor was kept constant resulting in a residence time of 0.18 minutes.

The reaction rate constants k , the initial degradation rates r_0 , and the initial photonic efficiencies ζ_0 for the experimental runs employing TiO₂ suspensions are tabulated in Table 6. For both suspended photocatalysts the reaction rate constant was found to decrease with increasing volume V_S of the suspension treated in the flow-through photocatalytic reactor clearly indicating that the rate constant is only an apparent rate constant being a function of the volume V_S . The apparent rate constants of the

photocatalytic DCA degradation were found to be significantly lower for Aeroxide P25 than for Hombikat UV 100. (Lindner et al., 1997).

The photonic efficiencies for Hombikat UV 100 in 500 ml and 1000 ml suspension volumes were calculated to be 13,5% and 18,7% (average of three experimental runs), respectively, while the respective photonic efficiencies for Aeroxide P25 were calculated to be 12.4 and 12.6 (average of three experimental runs). These results suggest that Sachtleben Hombikat UV100 is photocatalytically more effective than Aeroxide P25. The photonic efficiencies determined in this work are significantly higher than the values reported by Dillert and co-authors for the treatment of DCA-containing suspensions of the above mentioned photocatalysts in a laboratory-scale double-skin sheet reactor. But they found higher photonic efficiencies for Hombikat UV 100 in comparison with Aeroxide P25 as well. (Lindner et al., 1997).

5.2.2 The spiral glass reactor with a photocatalytic coating

As has been pointed out (*cf.* 4.1.3) the use of suspensions in industrial scale water treatment could become economically less attractive and impractical due to the necessity to separate the solid photocatalyst from the treated water. One approach to avoid this separation step in water treatment is the use of a thin TiO₂ coating at the side of the light transparent tubes of the photoreactor being in contact with the polluted water (Feitz et al., 2000; Lizama et al., 2005; Camurlu et al., 2012). Therefore the inner side of the above described spiral glass reactor was coated by a titanium dioxide layer employing a sol gel technique with titanium oxysulfate being the titanium source (*cf.* Chapter 3.1.4).

When an aqueous DCA solution was circulated through this coated spiral glass reactor a slow decrease of the concentration of the probe molecule was observed under UV-A irradiation. The initial degradation rate of 1 mM DCA solution was determined to be 2.0 $\mu\text{mol L}^{-1} \text{s}^{-1}$ corresponding to a photonic efficiency of 0.6% (average of three measurements). This initial reaction rate is much lower than that

observed for any other reactor configuration employed in this study. The low initial rate could be attributed to irregular formation of a film with sufficient high surface area on the glass. In addition, the preparation of the thin film was carried out in the laboratory under relatively poor controlled conditions, which could negatively affect the efficiency of the catalyst. As has been mentioned in Chapter 3.1.4 attempts to increase the photocatalytic activity by using other formulations for the coating sol were not successful.

5.2.3 The spiral glass reactor packed with photocatalyst pellets

Since the coated spiral glass reactor was found to be substantially less effective than the spiral glass reactor charged with a DCA-containing TiO₂ suspension another approach was investigated to overcome the restrictions due to the use of photocatalyst suspensions. The application of the catalyst suspension form at industrial scale is costly and needs substantial efforts in engineering, such as high-pressure filtration or cyclones. To overcome this problem, pellet forms of titanium dioxide have been chosen and its photocatalytic degradation activity was investigated as major part of this work. The first objective of this investigation is to determine the feasibility of using the pellet form and the effect of this form on the degradation efficiency of the catalyst.

TiO₂ photocatalyst pellets became available from different companies; here pellets supplied by BASF with the dimensions 3 mm · 3 mm and 5 mm · 5 mm were used. BASF TiO₂ pellets were used to fill the spiral glass reactor which is continuously charged with an aqueous solution containing the organic pollutant(s). The filling of the glass tube by TiO₂ pellets caused a significant pressure drop. Therefore, the solution was circulated with a flow rate of only 10 L h⁻¹ through the reactor.

The effectivity of this combination of photocatalyst type and photocatalytic reactor was determined by measuring the change of the TOC during UV irradiation of a DCA solution and a highly polluted real wastewater passing the photoreactor.

In a typical experimental run employing a DCA solution an average photonic efficiency of 8.2% was determined (cf. Table 13). The comparison of this value with the respective data found for the spiral glass reactor charged with a polluted TiO₂ suspension (cf. Table 13) shows that the packed spiral glass reactor has a photonic efficiency being approximately one third lower than the identical suspension reactor. This decrease of the initial photonic efficiency can be explained by the lower active surface area of the photocatalyst pellets in comparison with the suspended photocatalyst particles (cf. Table 13) and by possible mass transport limitations of the probe molecule from the bulk solution to the photocatalyst surface.

To increase the available photocatalytically active surface area smaller TiO₂ pellets have to be used. Actually, smaller cylindrical shaped pellets were available from Sachtleben. These materials with the trade name HombiCat C have been successfully used for the photocatalytic oxidation of acetaldehyde in the gas phase. (Horikoshi et al., 2008). Unfortunately, they were found to be unstable under the experimental conditions used here yielding a TiO₂ suspension (data not presented in this work).

To proof whether the BASF TiO₂ pellets are also suitable for the treatment of real wastewater experiments have been performed with highly polluted water supplied by the chemical company Solvay (TOC₀ ≈ 1500 mg L⁻¹) in the spiral glass reactor packed with these pellets (cf. Chapter 4.1.3). The results have been compared with the results obtained with this wastewater and suspended TiO₂ (Chapter 4.1.2). It was found in both cases that the degradation rate followed zero order kinetics. This behaviour can be attributed to the high initial concentration of the pollutant which results in a blocking of all adsorption sites at the photocatalyst surface. The catalyst type didn't have any significant impact on the degradation rate of the pollutants in the wastewater tested.

The above results clearly show that it is possible to degrade real wastewater using the spiral reactor and photocatalyst pellets. It is obvious from the experimental results presented above that the total detoxification of the wastewater will depend on the initial TOC and the time of water circulation.

From the above results it is concluded that the pellet form could have huge potential for industrial applications in photocatalytic water treatment. On the other hand, since the spiral glass photoreactor has not a suitable shape for a solar-powered photocatalytic reactor the TiO₂ pellets have to be applied in combination with photoreactors of another design.

5.3 The pan reactor with photocatalyst pellets

The high activity of the photocatalytically active TiO₂ pellets observed during DCA degradation in the spiral glass reactor was encouraging the determination of the activity of this photocatalyst type in other types of photoreactors which are expected to be more suitable for applications in solar wastewater treatment than the spiral glass reactor. The simplest design of a solar-driven photocatalytic reactor is a basin containing the polluted water in contact with the photocatalyst. The geometry of photoreactor type is very similar to geometry of the wastewater ponds which are typical in industrial complexes and effluent treatment plants.

The pan reactor was filled with 5 mm · 5 mm BASF TiO₂ pellet photocatalyst (cf. Chapter 3.2.5) and 0.5 to 1 L DCA solution which was necessary to cover the photocatalyst bed. The pan which was operated as batch reactor was exposed to the UV light and the reduction of the DCA concentration was measured as TOC.

Employing this pan reactor it was observed that the DCA concentration of a 500 ml solution with an initial pollutant concentration of 1 mM decreased by 86% within 240 minutes. An initial photonic efficiency of approximately 2.5% was determined which is not affected by the volume of the aqueous solution.

These results show that in principal it is possible to eliminate organic pollutants from water by just adding titanium dioxide pellets into simple ponds exposed to UV-light. Based on the above results it is imaginable that a pellet catalyst could be added into an open shallow pond under natural conditions. The organic pollutant then will be

decomposed without using any further steps or additional energy for circulation or filtration.

5.4 The flat packed reactor with photocatalyst pellets

While the pan reactor showed only low initial photonic efficiencies ($\zeta_0 \approx 2.5\%$; cf. Table 13) which is possibly due to mass transport limitations in this batch reactor the reactor concept was enhanced to the continuously charged flat packed reactor with 5 mm · 5 mm BASF TiO₂ pellets and equipped with a perforated tube to distribute the incoming aqueous DCA solution ($c_{\text{DCA},0} = 0.9 - 1.0 \text{ mM}$) uniformly over the width of the reactor (Chapter 3.2.6). The irradiated surface area of this reactor type was 0.0924 m²; the flow rate of the DCA solution was between 30 L h⁻¹ and 120 L h⁻¹ corresponding to a residence time of 0.9 to 0.2 minutes.

With 30 L h⁻¹ flow rate the TOC decreased by 88% within 180 minutes of UV-A irradiation. Increasing the flow rate to 60 L h⁻¹ led to an increase of the degradation rate by 16%. A further increase of the flow rate to 120 L h⁻¹ increased the degradation rate by only 1%. It was observed that the initial degradation rate at this flow rate decreased back to its original value at 30 L h⁻¹ flow rate. Photonic efficiencies of approximately 6.3% were achieved under these experimental conditions. It becomes clear from the experimental results that the change in the reaction rate is small and within the experimental error. These results clearly show that the flow rate of the water does not have any significant effect on the degradation rate.

5.5 The tubular reactor packed with photocatalyst pellets

When the pan reactor and the flat packed reactor were employed outdoor with the sun being the source of the UV-A light a substantial amount of the water was lost by evaporation due to the unintended warming of the aqueous solution (data not shown).

Therefore, an open solar-driven photocatalytic reactor as the pan reactor and the flat packed reactor seems not to be suitable for photocatalytic water treatment in warmer countries like Libya. A closed photocatalytic reactor system like the tubular reactor described in Chapter 3.2.7 was therefore considered. This tubular reactor with an irradiated surface area of 0.043 m^2 was filled with BASF photocatalyst pellets (3 mm · 3 mm) and continuously charged with a DCA solution.

Typically a decrease of the DCA concentration $> 90\%$ was achieved during 120 minutes of UV-A irradiation with a light intensity of 33.6 W m^{-2} . An initial photonic efficiency of 6.2% was determined. The comparison of this value with the photonic efficiency obtained with the spiral glass reactor packed with BASF photocatalyst pellets shows that the tubular reactor containing the same photocatalyst has a photonic efficiency being approximately 25% lower than the former (cf. Table 13).

To study the effect of the sunlight on the photocatalytic degradation of DCA and comparing it to the artificial UV-light the tubular reactor filled with TiO_2 pellets was used. The reactor was exposed to natural sunlight for 5h. The TOC of the recirculating DCA solution decreased by 97% within the first 5 hours of solar irradiation. The initial degradation rate was determined to be $10.4 \text{ } \mu\text{mol L}^{-1} \text{ min}^{-1}$ which is lower than the initial rates observed in the experimental runs employing an artificial light source. This difference might be due to the lower light intensity (averaged value: 25 W m^{-2}) in the solar experiment.

From the experimental results presented above it is concluded that DCA degradation rate under the natural sunlight conditions is very similar to the degradation rate under the laboratory conditions. This result is very promising for transferring results from laboratory to field conditions.

5.6 Comparison of the photocatalytic systems

For the purpose of an easy comparison of the experimental results average values of the photonic efficiencies obtained with the different combinations of photocatalyst type and photoreactor studied here are summarized in Table 13. As it becomes obvious from these data the highest initial photonic efficiencies are obtained when TiO₂ suspensions are employed to degrade organic water pollutants. The initial photonic efficiencies obtained with BASF TiO₂ pellets are approximately 33% to 50% lower than the values found with suspensions. But it has to be emphasized that the pellets have an initial photonic efficiency making them suitable for photocatalytic water treatment.

It has to be mentioned that (initial) photonic efficiencies are useful for laboratory experiments, because, under these circumstances, the photon flux should be constant and well known, and very often the degradation rate can be determined by the slope of the concentration versus time profile. However, for comparing solar outdoor experiments under fluctuating radiation conditions, the photonic efficiency cannot be used in a straightforward manner. Therefore, the concept of initial photonic efficiencies was not used in this work to analyse the results of the solar-driven photocatalytic degradation experiments.

Photonic efficiency, reaction rate or a kinetic constant determined directly from the slope of the concentration-time profile do not provide enough information for scaling-up a solar catalytic water treatment plant from laboratory-scale experiments. For this purpose, a useful kinetic approach has to include (Dillert et al., 1999a).

- (i) the pollutant concentration or related variable (e.g., TOC, COD),
- (ii) the photon density flux reaching the reactor area,
- (iii) the total volume of the suspension to be treated,
- (iv) the light harvesting area,
- (v) the photoreactor volume, and

(vi) the irradiation time

as the minimum design variables.

Recently a kinetic approach has been derived by Dillert and co-authors (Dillert et al., 1999a). The basic ideas are as follow:

Consider a typical degradation unit made of a solar-irradiated reactor (volume V_R) and a storage tank (volume V_T) forming the main parts of a batch recirculating system containing a total suspension volume V_S . When the reactor operates under low conversions per pass inside the loop of a well-mixed batch system, it can be shown that

$$r_V = -\frac{V_S}{V_R} \frac{dc}{dt} = -\frac{V_S}{V_R} r \quad (37)$$

where dc/dt is the change in concentration measured in the tank. In photocatalytic water degradation systems, this equation will be more valid when the recirculating flow rate is high. The real challenge when working with real wastewaters, and usually variable solar irradiation rates, is the formulation of the left-hand side of Eq. (37).

In formulating r_V , two approximations will be made:

- (i) it is directly proportional to the volume and time averaged photon absorption rate $\langle\langle e \rangle_{V_R} \rangle_t$, and
- (ii) it is directly proportional to the concentration of the organic pollutant c (determined as total organic carbon, TOC, in this work).

$$r_V = k^1 \langle\langle e \rangle_{V_R} \rangle_t c \quad (38)$$

The two approximations used in Eq. (38) are not always valid. First-order dependence with respect to the photonic absorption rate has been reported when the irradiation rate is low (below 1 sun is the order of magnitude usually referred to). First-order dependence with respect to the organic compound has been found usually at low

pollutant concentrations (a limiting case of the more general apparent Langmuir–Hinshelwood (L–H) kinetics; see Chapter 2.3).

The volume averaged photon absorption rate is given by an additional simplification in terms of the photon density flux arriving at the reactor surface:

$$\langle e \rangle_{V_R} = k^2 \alpha \frac{A_R}{V_R} I_{hv} \quad (39)$$

The dimensionless parameter α ($\alpha \leq 1$) is related to the ability of a reactor system to use the available light, and takes into account the losses of the photon energy due to scattering, reactor wall reflection and absorption, etc. Again, this assumption is only approximate because it does not consider variations of the photon absorption rate with the reactor depth. Additionally, scattering, as well as reactor wall reflection and absorption, can hardly be well modeled with a single constant.

We can further assume that the irradiation is monochromatic, and I_{hv} is an average value over the wavelength range of the useful radiation density flux. Once again, this is an approximation. For the case of solar irradiation in the 300–400 nm range, the radiation density flux arriving at the surface of the reactor decreases when one moves towards the shorter wavelengths (Bird et al., 1983). On the other hand, titanium dioxide absorption has just the opposite trend (Cabrera et al., 1996). Thus, some form of compensation effect may be possible. Unfortunately, I_{hv} is not constant along the day of a typical solar reactor operation. Instead, an average value over the exposure time will be used.

Substituting Eq. (39) into Eq. (38) yields the reaction rate per unit suspension volume:

$$r_V = k^1 k^2 \alpha \frac{A_R}{V_R} I_{hv} c \quad (40)$$

Inserting this result into Eq. (37), and using the abbreviations $k^3 = k^1 k^2 \alpha$ finally yields the time rate of change of the pollutant concentration in the tank:

$$r = -k^3 \frac{A_R}{V_S} I_{hv} c \quad (41)$$

For constant radiation fluxes, Eq. (41) is equivalent to a first-order rate law in concentrations as it was observed in the DCA degradation experiments performed in this work. After integration within the limits $c = c_0$ at time $t = 0$ and $c = c$ at time t , the usual exponential expression is obtained:

$$c = c_0 \exp\left(-k^3 \frac{A_R}{V_S} I_{hv} t\right) \quad (42)$$

Rearrangement of Eq. (42) yields an expression to calculate the kinetic parameter k^3 :

$$k^3 = \frac{V_S}{A_R} \frac{1}{I_{hv} t} \ln\left(\frac{c_0}{c}\right) \quad (43)$$

Note that the kinetic parameter k^3 is not a true kinetic constant. On one hand, it was obtained under the following assumptions:

- (i) the reaction is first order with respect to the photon absorption rate;
- (ii) the reaction is first order with respect to the ‘pollutant’ concentration;
- (iii) for complex reaction mixtures, the pollutant concentration can be well represented by a single ‘composition’, indicated by the TOC;
- (iv) the radiation is pseudo-monochromatic;
- (v) a simplified expression is used for the time average of the reactor volume average photon absorption rate;
- (vi) the photon absorption rate is represented by the flux of arriving photons affected by a constant to account for all non-absorbed photons; and
- (vii) this constant is the same for all reactors, independent of wavelength.

On the other, this very simple kinetic model does not take into account

- (i) the type of catalyst;
- (ii) the catalyst concentration;
- (iii) the molecular oxygen concentration in the reactor;

(iv) pH effects; and

(v) those effects on the reaction derived from the existence of impurities in the incoming stream of fluid.

This kinetic approach resulting in a mathematical expression to calculate the kinetic parameter k^3 was used to analyse the experimental results of this work. Average values of k^3 are given in Table 14. These values are in very good agreement with values which have recently published by Dillert and co-authors for photocatalytic DCA degradation experiments comparing the DSSR with a CPCIR irradiated by artificial and solar light (Dillert et al., 1999a)

Using a rearranged form of Eq. 43

$$A_R = V_S \frac{1}{k^3 I_{hv} m t} \ln \left(\frac{c_0}{c} \right) \quad (44)$$

the data presented in Table 14 can be used to calculate the irradiated reactor area A_R being necessary for the treatment of a given volume V_S of a contaminated water. To perform these calculation appropriate assumptions concerning the light intensity I_{hv} , the treatment time t , and the desired removal (c_0/c) have to be made.

Wavelengths shorter than 400 nm are essential for the excitation of TiO_2 , at present the most suitable semiconducting material for photocatalysis. In the solar spectrum, the wavelength range that can be used for the excitation of TiO_2 , i.e., the UV-A region between 300 and 400 nm, approximately 50 W m^{-2} radiation from the sun is reaching the surface of the earth under AM 1.5 conditions (Bird et al., 1983). Assuming that

- (i) a continuously operating tubular packed reactor with BASF TiO_2 pellets is used ($k^3 = 19.3 \cdot 10^{-8} \text{ m}^3 \text{ W}^{-1} \text{ s}^{-1}$; cf. Table 14)
- (ii) an average of 25 W m^{-2} is available during a period of 8 hours (= 28800 s) and that
- (iii) a 98% reduction of the pollutant concentration ($\ln(c_0/c) = 3.91$) is aspired

approximately 28 m² irradiated reactor area are necessary for the treatment of 1 m³ polluted water.

Much higher values for the kinetic parameter k^3 are obtained for the pan reactor filled with BASF TiO₂ pellets. With the assumptions made above only 15 to 16 m² irradiated reactor area becomes necessary for the treatment of 1 m³ polluted water without energy consumption for the recirculation of the liquid phase.

But it has to be mentioned again that the temperature of the aqueous solution in the pan (and in the flat packed reactor as well) increased reaching values higher than 30°C within 1 hour of UV-A irradiation using a solar simulator or direct sun light and that a significant amount of the water evaporated. Therefore, a reactor design allowing an unhindered exchange of water from the aqueous phase to the open atmosphere seems not to be suitable in arid countries like Libya.

Table 14: Experimental data and the kinetic parameter k_m^3 (average value) of the laboratory experiments of the photocatalytic degradation of DCA .

Type of photoreactor	Catalyst	V_R $/ 10^{-4} \text{ m}^3$	V_S $/ \text{ L}$	$c_{0,m}$ $/ \text{ mM}$	A_R $/ \text{ m}^2$	$I_{hv,m}$ $/ \text{ W m}^{-2}$	k_m^3 $/ 10^{-8} \text{ m}^3 \text{ W}^{-1} \text{ s}^{-1}$
Spiral glass reactor	Suspension (Hobikat UV100)	3.14	0.5	1.00	0.0624	28.0	40.5
		3.14	1.0	0.92	0.0624	28.0	54.2
	Suspension (Aeroxide P25)	3.14	0.5	1.00	0.0624	28.0	37.3
		3.14	1.0	0.92	0.0624	28.0	40.0
	TiO ₂ -coated	3.14	1.0	0.98	0.0624	28.0	1.9
	BASF pellets 3 mm · 3 mm	3.14	0.5	1.02	0.0624	28.0	24.0
Pan reactor	BASF pellets 5 mm · 5 mm	5.00	0.5	1.42	0.0488	26.0	33.3
		10.00	1.0	2.68	0.0488	26.0	35.5
Flat packed reactor	BASF pellets 5 mm · 5 mm	4.62	2.0	0.94	0.0924	30.0	15.6
Tubular packed reactor	BASF pellets 3 mm · 3 mm	2.17	1.0	0.97	0.0434	33.6	19.3

6 Conclusion and outlook

The main objective of this work was to investigate the photocatalytic effectiveness of a novel pellet form TiO_2 catalyst and compare its effectiveness to the mostly used suspension types. The goal and objective of this work is to solve the separation problems of TiO_2 suspensions in the large scale after the treatment process. In addition, the photocatalytic degradation of DCA using four different reactor configurations was investigated and compared. The degradation of DCA obtained in the laboratory using UV light was compared to the degradation using direct sunlight using the tubular reactor as an example.

The results of the investigations obtained in this work are summarized as follow:

- The degradation rate of DCA in the spiral reactor using Sachtleben Hombikat UV 100 suspensions was found to be superior to the degradation rate in the case of Aeroxide P25. These results can be explained by the higher reactive sites of the Sachtleben Hombikat UV 100 compared to the Aeroxide P25. In general the TOC of the DCA decreased sharply within the first 30 minutes (over 91% in both cases). These results clearly showed the effectiveness of the spiral configuration of the reactor in the DCA degradation, using suspension approach.
- The same spiral reactor was packed with BASF TiO_2 pellets and the DCA solution was circulated in the same manner as in the suspension experiment. The degradation rate of DCA was found to be 50% lower than the suspension form under the same conditions and the same irradiation time. This difference is explained by the higher surface area in the suspension compared to the pellet form. The photonic efficiency was found to be 33% less than the photonic efficiency in case of using the suspension. Despite the observed decrease in the degradation when using the pellet form, the results are encouraging and show that the TiO_2 pellets exhibit substantial advantages due to their suitability for use in large industrial large-scale operations, compared to suspension.

- To investigate the effect of different reactor configuration, a tubular reactor was packed with BASF pellets and the DCA solution was circulated. The DCA degradation rate was found to be 1.37 % with much lower values compared to the spiral reactor. This low value can be attributed to the smaller catalyst area exposed to the UV-light. Due to the reactor design and experimental setup, the reactor was exposed to the UV light only from one side, leading to lower degradation. These results clearly show the importance of a large surface area in the case of using tubular configuration for real applications.
- The tubular reactor configuration was used to degrade DCA, using direct sunlight. This experiment was carried out to determine the effectiveness of the TiO₂ pellet form under field conditions. The results clearly show that the pellet form is also very efficient under natural sunlight. The TOC decreased by 97% within 5 hours. The degradation rate was found to be $0.93 \cdot 10^{-2} \text{ mmol}\cdot\text{min}^{-1}$, 32% less than the degradation rate using UV-lamp. Despite the low degradation rate one can conclude that the TiO₂ pellet form offers a huge potential to be used in large-scale and field applications.
- The effectiveness of the BASF TiO₂ pellets in DCA degradation was tested in the flat packed reactor. The degradation rate of DCA was found to be the same as for the tubular reactor after 120 minutes of the solution circulation. The circulation rate of the solution and its effect on the degradation rate was measured. It was found that the circulation rate does not have a significant effect on the degradation rate.
- The use of a low rate of circulation design could simplify the application of TiO₂ photo purification technology in the real world and substantially will bring the costs down for possible applications and devices. It will have potential applications for the preparation of potable water in remote areas or developing countries.

- The BASF TiO₂ pellet form was further investigated using a pan reactor configuration. The pan reactor is simple and it resembles a water pond in a conventional wastewater plant or even a natural shallow lake. The pellets were added to the DCA solution in the pan and irradiated with UV-light. Within 240 minutes the TOC decreased by 86%. Increasing the DCA solution volume to double slowed the TOC disappearance by 50%.
- The above results confirmed the effectiveness of the pan configuration in DCA degradation without any agitation or oxygen purging. At this point it appears to be the most cost effective configuration for large-scale applications or cleanup of contaminated lakes with shallow beaches.
- Another possibility to avoid using TiO₂ suspension is the concept of a coated reactor. For this purpose the spiral reactor was coated with TiO₂ using sol gel technique. The DCA degradation rate was found to be very low compared to all other reactors. This was attributed to the smaller catalyst surface area or defects in the surface area preparation. This technique needs more future investigation in order to be able to make a final judgment about its effectiveness and potential areas of application.
- To determine the photocatalytic activity of the TiO₂ pellet in a real wastewater, a sample received from Solvay was circulated in the spiral reactor filled with the TiO₂ pellets. It was found that the degradation rate followed zero order kinetics. This behaviour can be attributed to the high initial concentration of the pollutant (> 1400 mg L⁻¹ TOC value). A decrease in TOC was observed and was not continued to the total degradation.
- This work clearly shows that BASF TiO₂ pellets can replace conventional TiO₂ suspensions. The application of pellets has the potential to solve the major catalyst separation problems, facing large-scale applications.

- Therefore, we conclude that the TiO_2 pellets offer the potential of bringing the TiO_2 technology in wastewater treatment one step further towards large-scale industrial application.

7 References

- Ahmed, S., Ollis, D.F., 1984. Solar photoassisted catalytic decomposition of the chlorinated hydrocarbons trichloroethylene and trichloromethane. *Solar Energy* 32, 597-601.
- Ajona, J.I., Vidal, A., 2000. The use of cpc collectors for detoxification of contaminated water: Design, construction and preliminary results. *Solar Energy* 68, 109-120.
- Alfano, O.M., Bahnemann, D., Cassano, A.E., Dillert, R., Goslich, R., 2000. Photocatalysis in water environments using artificial and solar light. *Catal. Today* 58, 199-230.
- Alhakimi, G., Studnicki, L.H., Al-Ghazali, M., 2003. Photocatalytic destruction of potassium hydrogen phthalate using TiO_2 and sunlight: Application for the treatment of industrial wastewater. *J. Photochem. Photobiol. A-Chem.* 154, 219-228.
- Alsayyed, G., Doliveira, J.C., Pichat, P., 1991. Semiconductor-sensitized photodegradation of 4-chlorophenol in water. *J. Photochem. Photobiol. A-Chem.* 58, 99-114.
- Atkins, P., 1985. *Physical chemistry*. Oxford university press.
- Augugliaro, V., Palmisano, L., Sclafani, A., Minero, C., Pelizzetti, E., 1988. Photocatalytic degradation of phenol in aqueous titanium-dioxide dispersions. *Toxicol. Environ. Chem.* 16, 89-109.
- Bahnemann, D., 1999. Photocatalytic detoxification of polluted waters. In: Boule, P. (Ed.). *Handbook of environmental photochemistry*. Springer, Heidelberg, pp. 285-351.
- Bahnemann, D., 2004. Photocatalytic water treatment: Solar energy applications. *Solar Energy* 77, 445-459.
- Bahnemann, D., Bockelmann, D., Goslich, R., 1991. Mechanistic studies of water detoxification in illuminated TiO_2 suspensions. *Solar Energy Materials* 24, 564-583.
- Bahnemann, D., Cunningham, J., Fox, M., Pelizzetti, E., Pichat, P., Serpone, N., 1994. Photocatalytic treatment of waters. In: Helz, G., Zepp, R., Crosby, D. (Eds.). *Aquatic and surface photochemistry*. Lewis, Boca Raton, Florida, pp. 261-316.
- Ballari, M.d.l.M., Alfano, O.M., Cassano, A.E., 2010. Mass transfer limitations in slurry photocatalytic reactors: Experimental validation. *Chem. Eng. Sci.* 65, 4931-4942.

-
- Bekbolet, M., 2009. Occurrence and consequences of disinfection by-products in drinking waters as related to water shortage problems in Istanbul metropolitan city. In: Hlavinek, P.P.C.M.J.M.I.K.T. (Ed.). Risk management of water supply and sanitation systems, pp. 125-134.
- Bekbölet, M., Lindner, M., Weichgrebe, D., Bahnemann, D.W., 1996. Photocatalytic detoxification with the thin-film fixed-bed reactor (tffbr): Clean-up of highly polluted landfill effluents using a novel TiO₂-photocatalyst. *Solar Energy* 56, 455-469.
- Bideau, M., Claudel, B., Dubien, C., Faure, L., Kazouan, H., 1995. On the immobilization of titanium-dioxide in the photocatalytic oxidation of spent waters. *J. Photochem. Photobiol. A-Chem.* 91, 137-144.
- Bielansky, P., Reichhold, A., Schoenberger, C., 2010. Catalytic cracking of rapeseed oil to high octane gasoline and olefins. *Chemical Engineering and Processing: Process Intensification* 49, 873-880.
- Bird, R.E., Hulstrom, R.L., Lewis, L.J., 1983. Terrestrial solar spectral data sets. *Solar Energy* 30, 563-573.
- Blake, D., Magrini-Bair, K., Wolfrum, E., 1997. Material issues in solar detoxification of air and water. In: Lampert, C., Granquist, C., Gratzel, M., Deb, S. (Eds.). *Materials technology for energy efficiency and solar energy conversion XVSPiE*, The International Society for Optical Engineering, pp. 154-162.
- Blanco-Galvez, J., Fernandez-Ibanez, P., Malato-Rodriguez, S., 2007. Solar photocatalytic detoxification and disinfection of water: Recent overview. *Journal of Solar Energy Engineering-Transactions of the ASME* 129, 4-15.
- Blanco, J., Malato, S., Fernandez-Ibanez, P., Alarcon, D., Gernjak, W., Maldonado, M.L., 2009. Review of feasible solar energy applications to water processes. *Renewable & Sustainable Energy Reviews* 13, 1437-1445.
- Blanco, J., Malato, S., Fernandez, P., Vidal, A., Morales, A., Trincado, P., Oliveira, J.C., Minero, C., Musci, M., Casalle, C., Brunotte, M., Tratzky, S., Dischinger, N., Funken, K.H., Sattler, C., Vincent, M., Collares-Pereira, M., Mendes, J.F., Rangel, C.M., 1999. Compound parabolic concentrator technology development to commercial solar detoxification applications. *Solar Energy* 67, 317-330.
- Bockelmann, D., Weichgrebe, D., Goslich, R., Bahnemann, D., 1995. Concentrating versus non-concentrating reactors for solar water detoxification. *Sol. Energy Mater. Sol. Cells* 38, 441-451.

-
- Bond, T., Henriot, O., Goslan, E.H., Parsons, S.A., Jefferson, B., 2009. Disinfection byproduct formation and fractionation behavior of natural organic matter surrogates. *Environmental Science & Technology* 43, 5982-5989.
- Borthen, J., Leviten, D., 1992. Making solar detoxification of contaminated groundwater a reality. *Solar Energy* 1, 57-63.
- Bowden, D.J., Clegg, S.L., Brimblecombe, P., 1996. The henry's law constant of trifluoroacetic acid and its partitioning into liquid water in the atmosphere. *Chemosphere* 32, 405-420.
- Bowden, D.J., Clegg, S.L., Brimblecombe, P., 1998a. The henry's law constant of trichloroacetic acid. *Water Air and Soil Pollution* 101, 197-215.
- Bowden, D.J., Clegg, S.L., Brimblecombe, P., 1998b. The Henry's law constants of the haloacetic acids. *Journal of Atmospheric Chemistry* 29, 85-107.
- Brunet, R., Bourbigot, M.M., Dore, M., 1984. Oxidation of organic-compounds through the combination ozone-hydrogen peroxide. *Ozone-Science & Engineering* 6, 163-183.
- Butterfield, I.M., Christensen, P.A., Curtis, T.P., Gunlazuardi, J., 1997. Water disinfection using an immobilised titanium dioxide film in a photochemical reactor with electric field enhancement. *Water Res.* 31, 675-677.
- Cabrera, M.a.I., Alfano, O.M., Cassano, A.E., 1996. Absorption and scattering coefficients of titanium dioxide particulate suspensions in water. *The Journal of Physical Chemistry* 100, 20043-20050.
- Camurlu, H.E., Kesmez, O., Burunkaya, E., Kiraz, N., Yesil, Z., Asilturk, M., Arpac, E., 2012. Sol-gel thin films with anti-reflective and self-cleaning properties. *Chemical Papers* 66, 461-471.
- Carey, J.H., Lawrence, J., Tosine, H.M., 1976. Photo-dechlorination of pcbs in presence of titanium-dioxide in aqueous suspensions. *Bulletin of Environmental Contamination and Toxicology* 16, 697-701.
- Chen, S.-Z., Zhang, P.-Y., Zhu, W.-P., Chen, L., Xu, S.-M., 2006. Deactivation of TiO₂ photocatalytic films loaded on aluminium: Xps and afm analyses. *Appl. Surf. Sci.* 252, 7532-7538.
- Chester, G., Anderson, M., Read, H., Esplugas, S., 1993. A jacketed annular membrane photocatalytic reactor for waste-water treatment - degradation of formic-acid and atrazine. *J. Photochem. Photobiol. A-Chem.* 71, 291-297.

Chiang, K., Amal, R., Tran, T., 2002. Photocatalytic degradation of cyanide using titanium dioxide modified with copper oxide. *Advances in Environmental Research* 6, 471-485.

Chong, M.N., Jin, B., Chow, C.W.K., Saint, C., 2010. Recent developments in photocatalytic water treatment technology: A review. *Water Res.* 44, 2997-3027.

Cossee, P., 1964. Ziegler-natta catalysis i. Mechanism of polymerization of α -olefins with ziegler-natta catalysts. *J. Catal.* 3, 80-88.

Cunningham, J., Sedlak, P., 1993. Initial rates of TiO₂-photocatalyzed degradations of water pollutants - influences of adsorption, ph and photon-flux.

Curco, D., Malato, S., Blanco, J., Gimenez, J., 1996a. Photocatalysis and radiation absorption in a solar plant. *Sol. Energy Mater. Sol. Cells* 44, 199-217.

Curco, D., Malato, S., Blanco, J., Gimenez, J., Marco, P., 1996b. Photocatalytic degradation of phenol: Comparison between pilot-plant-scale and laboratory results. *Solar Energy* 56, 387-400.

da Costa, E., Zamora, P.P., Zarbin, A.J.G., 2012. Novel TiO₂/c nanocomposites: Synthesis, characterization, and application as a photocatalyst for the degradation of organic pollutants. *J. Colloid Interface Sci.* 368, 121-127.

Dalvi, A.G.I., Al-Rasheed, R., Javeed, M.A., 2000. Haloacetic acids (haas) formation in desalination processes from disinfectants. *Desalination* 129, 261-271.

Di Paola, A., Addamo, M., Bellardita, M., Cazzanelli, E., Palmisano, L., 2007. Preparation of photocatalytic brookite thin films. *Thin Solid Films* 515, 3527-3529.

Dillert, R., Cassano, A.E., Goslich, R., Bahnemann, D., 1999a. Large scale studies in solar catalytic wastewater treatment. *Catal. Today* 54, 267-282.

Dillert, R., Vollmer, S., Schober, M., Theurich, J., Bahnemann, D., Arntz, H.J., Pahlmann, K., Wienefeld, J., Schmedding, T., Sager, G., 1999b. Photocatalytic treatment of an industrial wastewater in the double-skin sheet reactor. *Chemical Engineering & Technology* 22, 931-934.

Dorazio, L., Ruettinger, W., Castaldi, M.J., Farrauto, R., 2008. Deactivation, regeneration, and stable performance of a ptmore water gas shift catalyst for on-site hydrogen generation: Part 2. *Top. Catal.* 51, 68-75.

Duquet, J.P., Bruchet, A., Mallevalle, J., 1989. New advances in oxidation processes - the use of the ozone hydrogen-peroxide combination for micropollutant removal in drinking-water. *Iwsa Specialised Conference on Organic Micropollutants* 7, 115-123.

-
- Feitz, A.J., Boyden, B.H., Waite, T.D., 2000. Evaluation of two solar pilot scale fixed-bed photocatalytic reactors. *Water Res.* 34, 3927-3932.
- Fernández-García, A., Zarza, E., Valenzuela, L., Pérez, M., 2010. Parabolic-trough solar collectors and their applications. *Renewable and Sustainable Energy Reviews* 14, 1695-1721.
- Fernández, P., Blanco, J., Sichel, C., Malato, S., 2005. Water disinfection by solar photocatalysis using compound parabolic collectors. *Catal. Today* 101, 345-352.
- Fetwell, J., 1989. Semiconductors help the sun to clean water. *New Scientist* June 10, 36.
- Frenken, K., 2005. Irrigation in africa in figures - aquastat survey. FAO, Rome.
- Fujishima, A., Rao, T., D., T., 2000. Titanium dioxide photocatalysis. *Journal of Photochemistry and Photobiology C-Photochemistry Reviews* 1, 1-21.
- Gallard, H., von Gunten, U., 2002. Chlorination of natural organic matter: Kinetics of chlorination and of thm formation. *Water Res.* 36, 65-74.
- Gerischer, H., Heller, A., 1991. The role of oxygen in photooxidation of organic-molecules on semiconductor particles. *J. Phys. Chem.* 95, 5261-5267.
- Goswami, D.Y., 1997. A review of engineering developments of aqueous phase solar photocatalytic detoxification and disinfection processes. *Journal of Solar Energy Engineering-Transactions of the Asme* 119, 101-107.
- Goswami, D.Y., Sharma, S.K., Mathur, G.D., Jotshi, C.K., 1997. Techno-economic analysis of solar detoxification systems. *Journal of Solar Energy Engineering-Transactions of the Asme* 119, 108-113.
- Grätzel, M., 2001. Photoelectrochemical cells. *Nature* 414, 338-344.
- Grätzel, M., Rotzinger, F.P., 1985. The influence of the crystal-lattice structure on the conduction-band energy of oxides of titanium(iv). *Chem. Phys. Lett.* 118, 474-477.
- Gruzdkov, Y.A., Savinov, E.N., Parmon, V.N., 1987. Photocatalytic decomposition of hydrogen sulfide in the presence of polymer immobilized cadmium sulfide. Promotion by i and viii group metals. *Int. J. Hydrogen Energy* 12, 393-401.
- Herrmann, J.M., 1999. Heterogeneous photocatalysis: Fundamentals and applications to the removal of various types of aqueous pollutants. *Catal. Today* 53, 115-129.
- Hidaka, H., 1998. Photodegradation of surfactants with TiO₂ semiconductor for the environmental wastewater treatment. *Journal of Chemical Sciences* 110, 215-228.

-
- Hidalgo, M.C., Sakthivel, S., Bahnemann, D., 2004. Highly photoactive and stable TiO₂ coatings on sintered glass. *Applied Catalysis A: General* 277, 183-189.
- Hoffmann, M.R., Martin, S.T., Choi, W.Y., Bahnemann, D.W., 1995. Environmental applications of semiconductor photocatalysis. *Chem. Rev.* 95, 69-96.
- Horikoshi, S., Kajitani, M., Horikoshi, N., Dillert, R., Bahnemann, D.W., 2008. Use of microwave discharge electrodeless lamps (MDEL) - ii. Photodegradation of acetaldehyde over TiO₂ pellets. *J. Photochem. Photobiol. A-Chem.* 193, 284-287.
- Ismail, A.A., Bahnemann, D.W., 2011. Mesostructured pt/TiO₂ nanocomposites as highly active photocatalysts for the photooxidation of dichloroacetic acid. *Journal of Physical Chemistry C* 115, 5784-5791.
- IWRM, 2007. Current status and the way forward demonstrated by national, regional and international experiences. workshop 11-12 April, Tripoli - Libya.
- Joyce, M.D., Hend, G.-G., William, B., John, J.L., Kara, B.A., 2003. Toxicological review of dichloroacetic acid. EPA.
- Kabra, K., Chaudhary, R., Sawhney, R.L., 2004. Treatment of hazardous organic and inorganic compounds through aqueous-phase photocatalysis: A review. *Industrial & Engineering Chemistry Research* 43, 7683-7696.
- Kalbasi, R.J., Mosaddegh, N., 2012. Palladium nanoparticles supported on poly(2-hydroxyethyl methacrylate)/kit-6 composite as an efficient and reusable catalyst for suzuki-miyaura reaction in water. *J. Inorg. Organomet. Polym. Mater.* 22, 404-414.
- Kandiel, T.A., Dillert, R., Feldhoff, A., Bahnemann, D.W., 2010a. Direct synthesis of photocatalytically active rutile TiO₂ nanorods partly decorated with anatase nanoparticles. *Journal of Physical Chemistry C* 114, 4909-4915.
- Kandiel, T.A., Feldhoff, A., Robben, L., Dillert, R., Bahnemann, D.W., 2010b. Tailored titanium dioxide nanomaterials: Anatase nanoparticles and brookite nanorods as highly active photocatalysts. *Chem. Mater.* 22, 2050-2060.
- Katsoyiannis, I.A., Canonica, S., von Gunten, U., 2011. Efficiency and energy requirements for the transformation of organic micropollutants by ozone, o₃/h₂o₂ and uv/h₂o₂. *Water Res.* 45, 3811-3822.
- Kemmitt, T., Al-Salim, N.I., Waterland, M., Kennedy, V.J., Markwitz, A., 2004. Photocatalytic titania coatings. *Current Applied Physics* 4, 189-192.
- Kim, H., Lee, S., Han, Y., Park, J., 2005. Preparation of dip-coated TiO₂ photocatalyst on ceramic foam pellets. *Journal of Materials Science* 40, 5295-5298.

-
- Kim, H., Lee, S., Han, Y., Park, J., 2006. Preparation of dip-coated TiO₂ photocatalyst on ceramic foam pellets. *Journal of Materials Science* 41, 6150-6153.
- Kirchnerova, J., Cohen, M.L.H., Guy, C., Klvana, D., 2005. Photocatalytic oxidation of n-butanol under fluorescent visible light lamp over commercial TiO₂ (hombicat uv100 and degussa p25). *Applied Catalysis a-General* 282, 321-332.
- Kormann, C., Bahnemann, D.W., Hoffmann, M.R., 1991. Photolysis of chloroform and other organic-molecules in aqueous TiO₂ suspensions. *Environmental Science & Technology* 25, 494-500.
- Lee, J.H., Yang, Y.S., 2005. Effect of HCl concentration and reaction time on the change in the crystalline state of TiO₂ prepared from aqueous TiCl₄ solution by precipitation. *J. Eur. Ceram. Soc.* 25, 3573-3578.
- Legrini, O., Oliveros, E., Braun, A.M., 1993. Photochemical processes for water-treatment. *Chem. Rev.* 93, 671-698.
- Liang, H.-c., Li, X.-z., Yang, Y.-h., Sze, K.-h., 2008. Effects of dissolved oxygen, pH, and anions on the 2,3-dichlorophenol degradation by photocatalytic reaction with anodic TiO₂ nanotube films. *Chemosphere* 73, 805-812.
- Lindner, M., Bahnemann, D.W., Hirthe, B., Griebler, W.D., 1997. Solar water detoxification: Novel TiO₂ powders as highly active photocatalysts. *Journal of Solar Energy Engineering-Transactions of the Asme* 119, 120-125.
- Liu, X., Garoma, T., Chen, Z., Wang, L., Wu, Y., 2012. Smx degradation by ozonation and uv radiation: A kinetic study. *Chemosphere* 87, 1134-1140.
- Lizama, C., Bravo, C., Caneo, C., Ollino, M., 2005. Photocatalytic degradation of surfactants with immobilized TiO₂: Comparing two reaction systems. *Environ. Technol.* 26, 909-914.
- Lovato, M.E., Martín, C.A., Cassano, A.E., 2011. A reaction-reactor model for O₃ and UVC radiation degradation of dichloroacetic acid: The kinetics of three parallel reactions. *Chem. Eng. J.* 171, 474-489.
- Macedo, L.C., Zaia, D.A.M., Moore, G.J., de Santana, H., 2007. Degradation of leather dye on TiO₂: A study of applied experimental parameters on photoelectrocatalysis. *J. Photochem. Photobiol. A-Chem.* 185, 86-93.
- Malato, S., 1999. Solar photocatalytic decomposition of pentachlorophenol dissolved in water. CIEMAT, Madrid, Spain.

-
- Malato, S., Blanco, J., Richter, C., Braun, B., Maldonado, M.I., 1998. Enhancement of the rate of solar photocatalytic mineralization of organic pollutants by inorganic oxidizing species. *Applied Catalysis B-Environmental* 17, 347-356.
- Malato, S., Blanco, J., Richter, C., Curco, D., Gimenez, J., 1997. Low-concentrating cpc collectors for photocatalytic water detoxification: Comparison with a medium concentrating solar collector. *Water Sci. Technol.* 35, 157-164.
- Marques, P., Rosa, M.F., Mendes, F., Pereira, M.C., Blanco, J., Malato, S., 1997. Wastewater detoxification of organic and inorganic toxic compounds with solar collectors. *Desalination* 108, 213-220.
- Martin, S.T., Herrmann, H., Choi, W.Y., Hoffmann, M.R., 1994a. Time-resolved microwave conductivity .1. TiO_2 photoreactivity and size quantization. *Journal of the Chemical Society-Faraday Transactions* 90, 3315-3322.
- Martin, S.T., Herrmann, H., Hoffmann, M.R., 1994b. Time-resolved microwave conductivity .2. Quantum-sized TiO_2 and the effect of adsorbates and light-intensity on charge-carrier dynamics. *Journal of the Chemical Society-Faraday Transactions* 90, 3323-3330.
- Marugán, J., Aguado, J., Gernjak, W., Malato, S., 2007. Solar photocatalytic degradation of dichloroacetic acid with silica-supported titania at pilot-plant scale. *Catal. Today* 129, 59-68.
- Matthews, R.W., 1986. Photooxidation of organic material in aqueous suspensions of titanium-dioxide. *Water Res.* 20, 569-578.
- Matthews, R.W., 1987. Photooxidation of organic impurities in water using thin-films of titanium-dioxide. *J. Phys. Chem.* 91, 3328-3333.
- Matthews, R.W., 1991. Photooxidative degradation of colored organics in water using supported catalysts - TiO_2 on sand. *Water Res.* 25, 1169-1176.
- Matthews, R.W., McEvoy, S.R., 1992. Destruction of phenol in water with sun, sand, and photocatalysis. *Solar Energy* 49, 507-513.
- Mazzarino, I., Piccinini, P., 1999. Photocatalytic oxidation of organic acids in aqueous media by a supported catalyst. *Chem. Eng. Sci.* 54, 3107-3111.
- McCullagh, C., Skillen, N., Adams, M., Robertson, P.K.J., 2011. Photocatalytic reactors for environmental remediation: A review. *J. Chem. Technol. Biotechnol.* 86, 1002-1017.
- Mehos, M., Turchi, C., Pacheco, J., Boegel, A.J., Merrill, T., Stanley, R., 1992. Pilot-scale study of the solar detoxification of voc-contaminated groundwater.

-
- Memming, R., 1984. Electron-transfer process with excited molecules at semiconductor electrodes. *Prog. Surf. Sci.* 17, 7-73.
- Mills, A., Davies, R.H., Worsley, D., 1993. Water-purification by semiconductor photocatalysis. *Chem. Soc. Rev.* 22, 417-425.
- Minero, C., Pelizzetti, E., Malato, S., Blanco, J., 1993. Large solar plant photocatalytic water decontamination - degradation of pentachlorophenol. *Chemosphere* 26, 2103-2119.
- Miranda-García, N., Suárez, S., Sánchez, B., Coronado, J.M., Malato, S., Maldonado, M.I., 2011. Photocatalytic degradation of emerging contaminants in municipal wastewater treatment plant effluents using immobilized TiO₂ in a solar pilot plant. *Applied Catalysis B: Environmental* 103, 294-301.
- Moghaddam, A.P., Abbas, R., Fisher, J.W., Stavrou, S., Lipscomb, J.C., 1996. Formation of dichloroacetic acid by rat and mouse gut microflora, an in vitro study. *Biochem. Biophys. Res. Commun.* 228, 639-645.
- Mukherjee, P.S., Ray, A.K., 1999. Major challenges in the design of a large-scale photocatalytic reactor for water treatment. *Chemical Engineering & Technology* 22, 253-260.
- Muneer, M., Saquib, M., Qamar, M., Bahnemann, D., 2004. Titanium-dioxide-mediated photocatalysis reaction of three selected pesticide derivatives. *Res. Chem. Intermed.* 30, 663-672.
- Nakamura, R., Nakato, Y., 2004. Primary intermediates of oxygen photoevolution reaction on TiO₂ (rutile) particles, revealed by in situ ftir absorption and photoluminescence measurements. *J. Am. Chem. Soc.* 126, 1290-1298.
- Nishida, K., Ohgaki, S., 1994. Photolysis of aromatic chemical-compounds in aqueous TiO₂ suspensions. *Water Sci. Technol.* 30, 39-46.
- Ollis, D., 1988. Photocatalysis and environment, trends and applications. In: Schiavello, M. (Ed.). Kluwer, Dordrecht.
- Ollis, D., 1991. Solar-assisted photocatalysis for water purification: Issues, data, questions. Photochemical conversion and storage of solar energy. Kluwer academic publishers.
- Ollis, D., Al-Ekabi, H. (Eds.), 1993. Photocatalytic purification and treatment of water and air. Elsevier, Amsterdam.

-
- Ollis, D.F., Turchi, C., 1990. Heterogeneous photocatalysis for water-purification - contaminant mineralization kinetics and elementary reactor analysis. *Environ. Prog.* 9, 229-234.
- Pacheco, J., Prairie, M., Yellowhorse, L., 1990. Photocatalytic destruction of chlorinated solvents with solar energy.
- Pacheco, J.E., Prairie, M.R., Yellowhorse, L., 1993. Photocatalytic destruction of chlorinated solvents in water with solar-energy. *Journal of Solar Energy Engineering-Transactions of the Asme* 115, 123-129.
- Pacheco, K., Prairie, M., L., Y.H., 1991. Photocatalytic destruction of chlorinated solvents with solar energy. *ASME/JSME/JSES international solar energy conference*, p. 275.
- Parent, Y., Blake, D., MagriniBair, K., Lyons, C., Turchi, C., Watt, A., Wolfrum, E., Prairie, M., 1996. Solar photocatalytic processes for the purification of water: State of development and barriers to commercialization. *Solar Energy* 56, 429-437.
- Park, R., Arieff, A.I., 1982. Treatment of lactic-acidosis with dichloroacetate in dogs. *Journal of Clinical Investigation* 70, 853-862.
- Peyton, G.R., Glaze, W.H., 1988. Destruction of pollutants in water with ozone in combination with ultraviolet-radiation .3. Photolysis of aqueous ozone. *Environmental Science & Technology* 22, 761-767.
- Pozzo, R.L., Baltanas, M.A., Cassano, A.E., 1997. Supported titanium oxide as photocatalyst in water decontamination: State of the art. *Catal. Today* 39, 219-231.
- Pozzo, R.L., Baltanas, M.A., Cassano, A.E., 1999. Towards a precise assessment of the performance of supported photocatalysts for water detoxification processes. *Catal. Today* 54, 143-157.
- Prairie, M.R., Pacheco, J., Evans, L.R., 1991. Solar detoxification of water containing chlorinated solvents and heavy metals via TiO₂ photocatalysis.
- Prat, C., Vicente, M., Esplugas, S., 1990. Ozone and ozone uv decolorization of bleaching waters of the paper-industry. *Industrial & Engineering Chemistry Research* 29, 349-355.
- Robert, D., Malato, S., 2002. Solar photocatalysis: A clean process for water detoxification. *Sci. Total Environ.* 291, 85-97.
- Rodríguez, S.M., Gálvez, J.B., Herrmann, J.M., 1999. Solar catalysis for water decontamination - introduction by the guest editors. *Catal. Today* 54, 191-192.

-
- Romero, M., Blanco, J., Sanchez, B., Vidal, A., Malato, S., Cardona, A.I., Garcia, E., 1999. Solar photocatalytic degradation of water and air pollutants: Challenges and perspectives. *Solar Energy* 66, 169-182.
- Rompp, A., Klemm, O., Fricke, W., Frank, H., 2001. Haloacetates in fog and rain. *Environmental Science & Technology* 35, 1294-1298.
- Rook, J., 1974. Formation of haloforms during chlorination of natural water. *Water Treat. Exam.* 23, 234-243.
- Rosario-Ortiz, F.L., Wert, E.C., Snyder, S.A., 2010. Evaluation of UV/H₂O₂ treatment for the oxidation of pharmaceuticals in wastewater. *Water Res.* 44, 1440-1448.
- Rothenberger, G., Moser, J., Gratzel, M., Serpone, N., Sharma, D.K., 1985. Charge carrier trapping and recombination dynamics in small semiconductor particles. *J. Am. Chem. Soc.* 107, 8054-8059.
- Sagawe, G., Brandi, R.J., Bahnemann, D., Cassano, A.E., 2003a. Photocatalytic reactors for treating water pollution with solar illumination. I: A simplified analysis for batch reactors. *Chem. Eng. Sci.* 58, 2587-2599.
- Sagawe, G., Brandi, R.J., Bahnemann, D., Cassano, A.E., 2003b. Photocatalytic reactors for treating water pollution with solar illumination. II: A simplified analysis for flow reactors. *Chem. Eng. Sci.* 58, 2601-2615.
- Sagawe, G., Brandi, R.J., Bahnemann, D., Cassano, A.E., 2004. Photocatalytic reactors for treating water pollution with solar illumination. III: A simplified analysis for recirculating reactors. *Solar Energy* 77, 471-489.
- Sagawe, G., Brandi, R.J., Bahnemann, D., Cassano, A.E., 2005. Photocatalytic reactors for treating water pollution with solar illumination: A simplified analysis for n-steps flow reactors with recirculation. *Solar Energy* 79, 262-269.
- Sagawe, G., Lehnard, A., Lubber, M., Bahnemann, D., 2001. The insulated solar fenton hybrid process: Fundamental investigations. *Helv. Chim. Acta* 84, 3742-3759.
- Sagawe, G., Satuf, M.L., Brandi, R.J., Muschner, J.P., Federer, C., Alfano, O.M., Bahnemann, D., Cassano, A.E., 2010. Analysis of photocatalytic reactors employing the photonic efficiency and the removal efficiency parameters: Degradation of radiation absorbing and nonabsorbing pollutants. *Industrial & Engineering Chemistry Research* 49, 6898-6908.
- Schaffer, S., Gruber, J., Ng, L.F., Fong, S., Wong, Y.T., Tang, S.Y., Halliwell, B., 2011. The effect of dichloroacetate on health- and lifespan in *c. Elegans*. *Biogerontology* 12, 195-209.

-
- Scheminski, A., Krull, R., Hempel, D.C., 2000. Oxidative treatment of digested sewage sludge with ozone. *Water Sci. Technol.* 42, 151-158.
- Scott, B.F., Mactavish, D., Spencer, C., Strachan, W.M.J., Muir, D.C.G., 2000. Haloacetic acids in canadian lake waters and precipitation. *Environmental Science & Technology* 34, 4266-4272.
- Scott, B.F., Spencer, C., Marvin, C.H., MacTavish, D.C., Muir, D.C.G., 2002. Distribution of haloacetic acids in the water columns of the laurentian great lakes and lake malawi. *Environmental Science & Technology* 36, 1893-1898.
- Serpone, N., Salinaro, A., 1999. Terminology, relative photonic efficiencies and quantum yields in heterogeneous photocatalysis. Part I: Suggested protocol (technical report). *Pure Appl. Chem.* 71, 303-320.
- Serpone, N., Terzian, R., Lawless, D., Kennepohl, P., Sauve, G., 1993. On the usage of turnover numbers and quantum yields in heterogeneous photocatalysis. *J. Photochem. Photobiol. A-Chem.* 73, 11-16.
- Singh, H.K., Muneer, M., Bahnemann, D., 2003. Photocatalysed degradation of a herbicide derivative, bromacil, in aqueous suspensions of titanium dioxide. *Photochemical & Photobiological Sciences* 2, 151-156.
- Song, H., Dai, M., Guo, Y.-T., Zhang, Y.-J., 2012. Preparation of composite TiO₂-Al₂O₃ supported nickel phosphide hydrotreating catalysts and catalytic activity for hydrodesulfurization of dibenzothiophene. *Fuel Process. Technol.* 96, 228-236.
- Sopyan, I., 2007. Kinetic analysis on photocatalytic degradation of gaseous acetaldehyde, ammonia and hydrogen sulfide on nanosized porous TiO₂ films. *Science and Technology of Advanced Materials* 8, 33-39.
- Stacpoole, P.W., 1989. The pharmacology of dichloroacetate. *Metabolism-Clinical and Experimental* 38, 1124-1144.
- Stacpoole, P.W., Wright, E.C., Baumgartner, T.G., Bersin, R.M., Buchalter, S., Curry, S.H., Duncan, C.A., Harman, E.M., Henderson, G.N., Jenkinson, S., Lachin, J.M., Lorenz, A., Schneider, S.H., Siegel, J.H., Summer, W.R., Thompson, D., Wolfe, C.L., Zorovich, B., 1992. A controlled clinical-trial of dichloroacetate for treatment of lactic-acidosis in adults. *New England Journal of Medicine* 327, 1564-1569.
- Tan, S.S., Zou, L., Hu, E., 2006. Photocatalytic reduction of carbon dioxide into gaseous hydrocarbon using TiO₂ pellets. *Catal. Today* 115, 269-273.
- Tanaka, S., Saha, U.K., 1994. Effects of pH on photocatalysis of 2,4,6-trichlorophenol in aqueous TiO₂ suspensions. *Water Sci. Technol.* 30, 47-57.

-
- Theurich, J., Lindner, M., Bahnemann, D.W., 1996. Photocatalytic degradation of 4-chlorophenol in aerated aqueous titanium dioxide suspensions: a kinetic and mechanistic study. *Langmuir* 12, 6368-6376.
- Tölgyessy, P., 1988. The degradation of bentazone and chlorotoluron in aqueous-solutions by gamma-radiation - biodegradability and toxicity to tubifex tubifex of radiolysis products. *Journal of Radioanalytical and Nuclear Chemistry-Letters* 128, 321-329.
- Torres, A.R., Azevedo, E.B., Resende, N.S., Dezotti, M., 2007. A comparison between bulk and supported TiO₂ photocatalysts in the degradation of formic acid. *Brazilian Journal of Chemical Engineering* 24, 185-192.
- Turchi, C.S., Ollis, D.F., 1989. Mixed reactant photocatalysis - intermediates and mutual rate inhibition. *J. Catal.* 119, 483-496.
- Twigg, M.V., 2011. Catalytic control of emissions from cars. *Catal. Today* 163, 33-41.
- Tyner, C.E., 1990. Application of solar thermal technology to the destruction of hazardous wastes. *Solar Energy Materials* 21, 113-129.
- Uden, P.C., Miller, J.W., 1983. Chlorinate acids and chloral in drinking-water. *Journal American Water Works Association* 75, 524-527.
- Valentin, M., Valentin, N., Alexander, V., Denis, K., Panagiotis, S., 2012. *Photocatalysis: Catalysts, kinetics and reactors*. John Wiley & Sons.
- Van Geluwe, S., Braeken, L., Van der Bruggen, B., 2011. Ozone oxidation for the alleviation of membrane fouling by natural organic matter: A review. *Water Res.* 45, 3551-3570.
- vanWell, M., Dillert, R.H.G., Bahnemann, D.W., Benz, V.W., Mueller, M.A., 1997. A novel nonconcentrating reactor for solar water detoxification. *Journal of Solar Energy Engineering-Transactions of the Asme* 119, 114-119.
- Vogna, D., Marotta, R., Napolitano, A., Andreozzi, R., d'Ischia, M., 2004. Advanced oxidation of the pharmaceutical drug diclofenac with UV/H₂O₂ and ozone. *Water Res.* 38, 414-422.
- Wang, J.L., Xu, L.J., 2012. Advanced oxidation processes for wastewater treatment: Formation of hydroxyl radical and application. *Critical Reviews in Environmental Science and Technology* 42, 251-325.

Watts, R.J., Kong, S.H., Lee, W., 1995. Sedimentation and reuse of titanium-dioxide - application to suspended-photocatalyst reactors. *Journal of Environmental Engineering-Asce* 121, 730-735.

Weingand, K.W., Fettman, M.J., Phillips, R.W., Hand, M.S., 1986. Effects of sodium dichloroacetate in awake, healthy, yucatan miniature swine. *American Journal of Veterinary Research* 47, 441-446.

Wendelin, T., 1992. A survey of potential low-cost concentrator concepts for use in low-temperature water detoxification. In: Stine, W., Kreider, J., Koichi, W. (Eds.). *ASME International Solar Energy Conference*, New York, pp. 15-21.

WHO, 2007. Water supply, sanitation and hygiene development in water (water scarcity), sanitation and health.

Zalazar, C.S., Martin, C.A., Cassano, A.E., 2005a. Photocatalytic intrinsic reaction kinetics. II: Effects of oxygen concentration on the kinetics of the photocatalytic degradation of dichloroacetic acid. *Chem. Eng. Sci.* 60, 4311-4322.

Zalazar, C.S., Romero, R.L., Martin, C.A., Cassano, A.E., 2005b. Photocatalytic intrinsic reaction kinetics I: Mineralization of dichloroacetic acid. *Chem. Eng. Sci.* 60, 5240-5254.

Zaman, J., Chakma, A., 1995. Production of hydrogen and sulfur from hydrogen-sulfide. *Fuel Process. Technol.* 41, 159-198.

Zhang, D., Qiu, R., Song, L., Eric, B., Mo, Y., Huang, X., 2009. Role of oxygen active species in the photocatalytic degradation of phenol using polymer sensitized TiO₂ under visible light irradiation. *J. Hazard. Mater.* 163, 843-847.

Zhang, X.W., Zhou, M.H., Lei, L.C., 2005. Preparation of anatase TiO₂ supported on alumina by different metal organic chemical vapor deposition methods. *Applied Catalysis a-General* 282, 285-293.

Zhang, Y., Crittenden, J.C., Hand, D.W., Perram, D.L., 1994. Fixed-bed photocatalysts for solar decontamination of water. *Environmental Science & Technology* 28, 435-442.

Zheng, Y.Q., Erwei, S., Cui, S.X., Li, W.J., Hu, X.F., 2000a. Hydrothermal preparation and characterization of brookite-type TiO₂ nanocrystallites. *J. Mater. Sci. Lett.* 19, 1445-1448.

Zheng, Y.Q., Shi, E.W., Cui, S.X., Li, W.J., Hu, X.F., 2000b. Hydrothermal preparation of nanosized brookite powders. *J. Am. Ceram. Soc.* 83, 2634-2636.

8 Appendix

8.1 Table of Figures

Figure 1: Reaction progress with and without catalysis (source www.wikimedia.org)	12
Figure 2: Simple diagram showing the photocatalysis process	19
Figure 3: Semiconductor photocatalysis process	21
Figure 4: Left photo of pilot plant installed in the Wolfsburg factory of the Volkswagen AG (Photo: J. Lohmann, ISFH). Right, schematic view of DSSR showing the inner structure of the transparent box made of PLEXIGLAS® (Bahnemann, 2004).	42
Figure 5: View of one CPC collector module (photo made at PSA, Spain) (Fernández et al., 2005).	44
Figure 6: Photograph of the TFFBR reactor installed at the Plataforma Solar de Almeria in Spain (Photo: D. Bockelmann) (Bahnemann, 2004).	44
Figure 7: X-ray for TiO ₂ Pellet from BASF, this analysis is performed in the laboratory of RASCO (Ras Lanuf Oil and Gas Processing Company) Ras Lanuf-Libya.	52
Figure 8: Glass spiral reactor	52
Figure 9: Coating procedure of the spiral reactor	53
Figure 10: Spiral packed reactor experimental set up	55
Figure 11: Polypropylene pan filled with 400 g of 5 mm . 5 mm of pellet type photocatalyst	57
Figure 12: Flat packed reactor, BASF Pellet catalyst size of 5 mm . 5 mm	58
Figure 13: Flat packed reactor setup experiment with circulation, irradiated area is 0.0924m ² .	58
Figure 14: Tubular packed reactor setup	59

Figure 15: Plot of TOC versus irradiation time during UV-A irradiation of a homogeneous DCA solution circulating through the spiral glass reactor. *Experimental conditions:* $c_{\text{DCA},0} = 1 \text{ mM}$, pH 3.0, $V = 500 \text{ mL}$, $F = 105 \pm 2 \text{ L h}^{-1}$, $I_{\text{hv}} = 28 \text{ W m}^{-2}$, $T = 21 \pm 1^\circ\text{C}$. 62

Figure 16: Plot of TOC versus time during recirculation of a DCA containing TiO_2 suspension through the spiral glass reactor in the dark. *Experimental conditions:* $c_{\text{DCA},0} = 1 \text{ mM}$, Sachtleben Hombikat UV 100, $c_{\text{cat}} = 3.0 \text{ g L}^{-1}$, pH 3.0, $V = 500 \text{ mL}$, $F = 105 \pm 2 \text{ L h}^{-1}$, $I_{\text{hv}} = 0 \text{ W m}^{-2}$, $T = 21 \pm 1^\circ\text{C}$. 62

Figure 17: Plot of TOC versus irradiation time during recirculation of a DCA containing TiO_2 suspension through the spiral glass reactor. *Experimental conditions:* $c_{\text{DCA},0} = 1 \text{ mM}$, Sachtleben Hombikat UV 100, $c_{\text{cat}} = 3.0 \text{ g L}^{-1}$, pH 3.0, $V = 500 \text{ mL}$, $F = 105 \pm 2 \text{ L h}^{-1}$, $I_{\text{hv}} = 28 \text{ W m}^{-2}$, $T = 21 \pm 1^\circ\text{C}$. 64

Figure 18: Plot of TOC versus irradiation time during recirculation of a DCA containing TiO_2 suspension through the spiral glass reactor. *Experimental conditions:* $c_{\text{DCA},0} = 1 \text{ mM}$, Sachtleben Hombikat UV 100, $c_{\text{cat}} = 3.0 \text{ g L}^{-1}$, pH 3.0, $V = 1000 \text{ mL}$, $F = 105 \pm 2 \text{ L h}^{-1}$, $I_{\text{hv}} = 28 \text{ W m}^{-2}$, $T = 21 \pm 1^\circ\text{C}$. 64

Figure 19: Plot of the oxygen concentration versus irradiation time during recirculation of a DCA containing TiO_2 suspension through the spiral glass reactor. *Experimental conditions:* as given in the legend of Fig. 17. 65

Figure 20: Plot of TOC versus irradiation time during recirculation of a DCA containing TiO_2 suspension through the spiral glass reactor. *Experimental conditions:* $c_{\text{DCA},0} = 1 \text{ mM}$, Evonik Aeroxide P25, $c_{\text{cat}} = 3.0 \text{ g L}^{-1}$, pH 3.0, $V = 500 \text{ mL}$, $F = 105 \pm 2 \text{ L h}^{-1}$, $I_{\text{hv}} = 28 \text{ W m}^{-2}$, $T = 21 \pm 1^\circ\text{C}$. 66

Figure 21: Plot of the oxygen concentration versus irradiation time during recirculation of a DCA containing TiO_2 suspension through the spiral glass reactor. *Experimental conditions:* as given in the legend of Fig. 20. 66

Figure 22: Plot of TOC versus irradiation time during recirculation of a DCA containing TiO_2 suspension through the spiral glass reactor. *Experimental conditions:* $c_{\text{DCA},0} = 1 \text{ mM}$, Evonik Aeroxide P25, $c_{\text{cat}} = 3.0 \text{ g L}^{-1}$, pH 3.0, $V = 1000 \text{ mL}$, $F = 105 \pm 2 \text{ L h}^{-1}$, $I_{\text{hv}} = 28 \text{ W m}^{-2}$, $T = 21 \pm 1^\circ\text{C}$. 67

Figure 23: Plot of the oxygen concentration versus irradiation time during recirculation of a DCA containing TiO_2 suspension through the spiral glass reactor. *Experimental conditions:* as given in the legend of Fig. 22. 67

Figure 24: Logarithmic plot of the normalized DCA concentration versus irradiation time during recirculation of 500 mL DCA-containing Hombikat UV100 suspension through the spiral glass reactor. Correlation coefficient of the regression line: $R^2 = 0.9856$. *Experimental conditions*: as given in the legend of Fig. 17. 68

Figure 25: Logarithmic plot of the normalized DCA concentration versus irradiation time during circulation of 1000 mL DCA-containing Hombikat UV100 suspension through the spiral glass reactor. Correlation coefficient of the regression line: $R^2 = 0.9955$. *Experimental conditions*: as given in the legend of Fig. 18. 68

Figure 26: Logarithmic plot of the normalized DCA concentration versus irradiation time during recirculation of 500 mL DCA-containing Evonik Aeroxide P25 suspension in the spiral glass reactor. Correlation coefficient of the regression line: $R^2 = 0.9983$. *Experimental conditions*: as given in the legend of Fig. 20. 69

Figure 27: Logarithmic plot of the normalized DCA concentration versus irradiation time during recirculation of 1000 mL DCA-containing Evonik Aeroxide P25 suspension in the spiral glass reactor. Correlation coefficient of the regression line: $R^2 = 0.9950$. *Experimental conditions*: as given in the legend of Fig. 22. 69

Figure 28: Plot of TOC versus irradiation time during circulation of a wastewater (Solvay) containing Evonik Aeroxide P25 through the spiral glass reactor. *Experimental conditions*: $c_{\text{cat}} = 4.0 \text{ g L}^{-1}$, natural pH, $V = 250 \text{ mL}$, $F = 105 \pm 2 \text{ L h}^{-1}$, $I_{\text{hv}} = 28 \text{ W m}^{-2}$, $T = 21 \pm 1^\circ\text{C}$. 72

Figure 29: Plot of COD versus irradiation time during circulation of a wastewater (Solvay) containing Evonik Aeroxide P25 through the spiral glass reactor. *Experimental conditions*: as given in the legend of Fig. 28. 72

Figure 30: Plot of TOC versus irradiation time during recirculation of a DCA solution through the TiO_2 coated spiral glass reactor. *Experimental conditions*: $c_{\text{DCA},0} = 1 \text{ mM}$, pH 3.0, $V = 1000 \text{ mL}$, $F = 105 \text{ L h}^{-1}$, $I_{\text{hv}} = 30 \text{ W m}^{-2}$, $T = 21 \pm 1^\circ\text{C}$. 74

Figure 31: Logarithmic plot of the normalized DCA concentration versus irradiation time during recirculation of a DCA solution through the TiO_2 coated spiral glass reactor. Correlation coefficient of the regression line: $R^2 = 0.9784$. *Experimental conditions*: as given in the legend of Fig. 30. 74

Figure 32: Plot of TOC versus irradiation time during recirculation of a DCA solution through the spiral glass reactor containing catalyst pellets. *Experimental conditions*: $c_{\text{DCA},0} = 1 \text{ mM}$, BASF catalyst pellets $3 \text{ mm} \cdot 3 \text{ mm}$, pH 3.0, $V = 500 \text{ mL}$, $F = 8 \pm 2 \text{ L h}^{-1}$, $I_{\text{hv}} = 28 \text{ W m}^{-2}$, $T = 21 \pm 1^\circ\text{C}$. 76

Figure 33: Logarithmic plot of the normalized DCA concentration versus irradiation time during recirculation of a DCA solution through the spiral glass reactor containing catalyst pellets. Correlation coefficient of the regression line: $R^2=0.999$.
Experimental conditions: as given in the legend of Fig. 32. 77

Figure 34: Plot of TOC versus irradiation time during recirculation of a wastewater (Solvay) through the spiral glass packed reactor containing catalyst pellets.
Experimental conditions: BASF catalyst pellets 3 mm · 3 mm, pH 3.0, V = 400 mL, F = 6 L h⁻¹, I_{hv} = 28 W m⁻², T = 21±1°C 78

Figure 35: Plot of TOC versus irradiation time during treatment of a DCA solution in the pan reactor containing catalyst pellets. *Experimental conditions:* a) TOC₀ = 34 mg L⁻¹, V = 500 mL (◆), and b) TOC₀ = 64 mg L⁻¹, V = 1000 mL (▲); BASF catalyst pellets 5 mm · 5 mm, pH 3.0, I_{hv} = 23 W m⁻², ambient T. 80

Figure 36: Logarithmic plot of the normalized DCA concentration versus irradiation time during treatment of a DCA in the pan reactor containing catalyst pellets. Correlation coefficient of the regression line: $R^2=0.9944$. *Experimental conditions:* TOC₀ = 34 mg L⁻¹, BASF catalyst pellets 5 mm · 5 mm, pH 3.0, V = 500 mL, I_{hv} = 23 W m⁻², ambient T. 80

Figure 37: Plot of TOC versus irradiation time during recirculation of a DCA solution through the flat packed reactor containing catalyst pellets. *Experimental conditions:* c_{DCA,0} = 1 mM, BASF catalyst pellets 5 mm · 5 mm, pH 3.0, V = 2000 mL, F = 30 (◆), 60 (■), and 120 L h⁻¹ (▲), I_{hv} = 33.6 W m⁻², no control of T. 82

Figure 38: Logarithmic plot of the normalized DCA concentration versus irradiation time during recirculation of a DCA solution through the flat packed reactor containing catalyst pellets. Correlation coefficient of the regression line: $R^2=0.999$. *Experimental conditions:* as given in the legend of Fig. 36. 82

Figure 39: Plot of TOC versus irradiation time during recirculation of a DCA solution through the tubular reactor containing catalyst pellets. *Experimental conditions:* c_{DCA,0} = 1 mM, BASF catalyst pellets 3 mm · 3 mm, pH 3.0, V = 1000 mL, F = 18 L h⁻¹, I_{hv} = 33.6 W m⁻², no control of T (start: T = 21±1°C). 84

Figure 40: Logarithmic plot of the normalized DCA concentration versus irradiation time during recirculation of a DCA solution through the tubular reactor containing catalyst pellets. Correlation coefficient of the regression line: $R^2=0.986$.
Experimental conditions: as given in the legend of Fig. 39. 85

Figure 41: Plot of TOC versus irradiation time during recirculation of a DCA solution through the tubular reactor containing catalyst pellets. *Experimental conditions:*

$c_{\text{DCA},0} = 1 \text{ mM}$, BASF catalyst pellets $3 \text{ mm} \cdot 3 \text{ mm}$, pH 3.0, $V = 1000 \text{ mL}$, $F = 18 \text{ L h}^{-1}$, direct solar light, ambient T. 86

8.2 list of tables

Table 1: Sources and uses of water in Libya.....	9
Table 2: Band positions of some common semiconductor photocatalysts in aqueous solution at pH=1.	22
Table 3: Main advantages and drawback of concentrating and non-concentrating solar photocatalytic reactors	45
Table 4: Advantages and disadvantages of slurry reactors and immobilized reactors.....	49
Table 5: Main characteristics of two different commercial titania powders.....	50
Table 6: Calculated reaction rate constants k , initial degradation rates r_0 , and initial photonic efficiencies ζ_0 of the photocatalytic DCA degradation in TiO_2 suspensions employing the spiral glass reactor.....	71
Table 7: Calculated reaction rate constants k , initial degradation rates r_0 , and initial photonic efficiencies ζ_0 of the photocatalytic DCA degradation employing the spiral glass reactor with a photocatalytic coating.	73
Table 8: Calculated reaction rate constants k , initial degradation rates r_0 , and initial photonic efficiencies ζ_0 of the photocatalytic DCA degradation employing the spiral glass reactor packed with photocatalyst pellets.	76
Table 9: Calculated reaction rate constants k , initial degradation rates r_0 , and initial photonic efficiencies ζ_0 of the photocatalytic DCA degradation employing the pan reactor filled with photocatalyst pellets.	79
Table 10: Calculated reaction rate constants k , initial degradation rates r_0 , and initial photonic efficiencies ζ_0 of the photocatalytic DCA degradation employing the flat packed reactor containing photocatalyst pellets.	83
Table 11: Calculated reaction rate constants k , initial degradation rates r_0 , and initial photonic efficiencies ζ_0 of the photocatalytic DCA degradation employing the tubular reactor containing photocatalyst pellets.	86
Table 12: Overview over the combinations of photocatalyst type and phototocatalytic reactor studied in this thesis.	87

Table 13: Experimental data of the laboratory experiments of the photocatalytic degradation of DCA..... 89

Table 14: Experimental data and the kinetic parameter k_m^3 (average value) of the laboratory experiments of the photocatalytic degradation of DCA 103

8.3 Curriculum Vitae (CV)

Muftah Alghazali Omer

Institut für Technische Chemie,

Gottfried Wilhelm Leibniz Universität Hannover

Tel.: +49 (0511) 762 2773

Fax: +49 (0511) 762 2774

Mobile: 004917624066325

e-mail omer@iftc.uni-hannover.de

mofthah_omer@yahoo.com

PERSONAL DETAILS:

Date of Birth: 14/04/1963

Place of Birth: Darna / Libya

Marital Status: Married

EDUCATION:

1996 – 1997 MSc. (Environmental Science and Technology) at IHE Delft Netherlands. International institute for Infrastructural, Hydraulic and Environmental Engineering, Delft, The Netherlands

Subjects studied: Solar detoxification of Petrochemical wastewater in aqueous suspension of a titanium dioxide photo catalyst.

1991 – 1992 Postgraduate Diploma in Environmental Science and Technology.
International Course Held in IHE Delft, The Netherlands.

1981 – 1984 B.Sc. (Environmental Studies) at Higher institute of Technology ,
Brack, Libya.

EXPERIENCE:

2009 – 2011 Empolyer with Libyan Emirates oil refining company, Libya.

1985 – 2003 Employer with Raslanuf Oil and Gas Processing company, Libya.

COMPUTER SKILLS:

IBM Compatible PCs running Microsoft Windows, MS-DOS, Microsoft office.

Conferences:

Fifth International Symposium on “*Environment, Catalysis and Process Engineering*” 24-26 April 2006 Fez Morocco. Oral presentation titled “Development of a photocatalytic reactor for water purification using fixed photocatalyst”.

Training:

French-German Summer School of Research, September 28th –October 1st, 2004, Saarbrueken, Germany“ [New Devolopments in Catalysis](#)” [NDCat](#) 2004.

Publications :

Gamil Alhakimi, Lisa H. Studnicki, **Muftah Al-Ghazali** (Photocatalytic destruction of potassium hydrogen phthalate using TiO₂ and sunlight: application for the treatment of industrial wastewater), Journal of Photochemistry and Photobiology A: Chemistry 154 (2003) 219–228.

Gamil Alhakimi, Lisa H. Studnicki, Saleh Gebril and **Muftah Al-Ghazali** (Photocatalytic destruction of organic pollutants in refinery wastewater: Direct comparison of artificial UV – light and natural sunlight) Recent res. Devel. Photochem. Photobiol., 7(2004) ISBN : 81-7895-129-0.